ECOLOGICAL STOICHIOMETRY OF BACTERIAL ASSEMBLAGES

A DISSERTATION
SUBMITTED TO THE FACULTY OF THE GRADUATE SCHOOL
OF THE UNIVERSITY OF MINNESOTA
BY

Casey Michael Godwin

IN PARTIAL FULFILLMENT OF THE REQUIREMENTS
FOR THE DEGREE OF
DOCTOR OF PHILOSOPHY

James Bryan Cotner, Adviser

December 2013

Acknowledgments

I am indebted to the many people who helped me to pursue this research. I wish to give thanks to all of them for their patience, support, and instruction and to acknowledge the efforts of my collaborators.

Thanks to Jim Cotner for being a patient mentor and enthusiastic collaborator over the past five years and for not flinching when I uttered 'hundreds of chemostats'. Thanks to the members of my committee, Jeff Gralnick, Tim LaPara, and Bob Sterner for their guidance in planning experiments and their feedback throughout this research. Thanks to Andrea Little and Sandy Brovold for helping me find my way through the lab, and for troubleshooting methods and equipment. Thanks to a great team of talented student collaborators: Alex Daniels, Emily Ellingson, James Lawton, Emily Whitaker, Kayla Wolfe, and Rachel Womack. Thanks to my cohorts in the Cotner lab: Leah Domine, Meghan Jacobson, Sean Marczewski, Kate Phillips, and Seth Thompson. Thanks to Tucker Burch for help with PCR-ARISA. Thanks to my IGERT collaborators: Patrick McNamara and Corey Markfort. Thanks to all of my previous mentors, especially Jeff Cardon, Andy McCollum, and Diana Wang. Thanks to Stuart Jones for sharing his bacterial isolates and for identifying several of our strains.

This research was made possible through support from NSF IGERT grant DGE-0504195 and the Itasca Director's Graduate Research Fellowship.

I am particularly indebted to my family for their love, support, and patience. Although I provided them with ample reasons for doubt, my parents provided me with endless encouragement and support.

Dedication

I dedicate this dissertation to my wife, Amy. Your love, support, and patience make anything possible. *Vous et nul autre*. I also dedicate this work to our daughter, Madeleine. May you grow to experience the opportunity, love, and joy that your arrival brought to our family.

Abstract

All organisms are faced with a chemical imbalance between their internal environment (cells, tissues, or body) and their external environment. Homeostasis is the ability to maintain an internal state that is different from the external environment and at least some degree of elemental homeostasis is required for metabolism and growth. Homeostasis is related to fitness since the degree of elemental imbalance between an organism's biomass and its resources controls the growth of populations, predicts the outcome of competition, and determines the relative rates of resource consumption, assimilation, and excretion of elements and energy. Since all organisms are composed of molecules that are comprised mainly of a common set of elements (carbon (C), hydrogen, oxygen, nitrogen (N), phosphorus (P), etc.), stoichiometric ratios of these elements in biomass (e.g. $C:P_{biomass}$) and resources ($C:P_{resources}$) can be used to diagnose the strength of imbalance and to assess the nutritional state of organisms. The strength of elemental homeostasis is variable within and among groups of taxa; some species and groups maintain strong homeostasis, but others adjust their chemical composition in response to their environment. Since ecosystems seldom contain only a single species, assemblages and communities can respond to elemental imbalance both through changes in the relative abundance of species and through simultaneous changes in the elemental content of the component species.

The goals of this dissertation are to evaluate the role of resource competition and species shifts in the stoichiometry of assemblages and to understand the ranges of stoichiometric regulation and biomass chemistry within the bacterial assemblages of lakes. In chapter 1, I introduce the conceptual framework of 'stoichiometric strategies' to align the gradient of stoichiometric regulation with physiological tradeoffs. Data from previously published studies on planktonic organisms show that the strength of homeostasis in a species is inversely proportional to the ratio of the two elements in its biomass when the denominator element is limiting. Under nutrient limitation, homeostatic species have lower biomass C:N, C:P, and N:P ratios than do species with flexible biomass stoichiometry. I show how a consumer-resource model with tradeoffs

related to competitive ability for C and P couples homeostatic regulation to competitive ability. The result is a conceptual model in which assemblages are dominated by homeostatic species under low resource imbalance and by species with flexible stoichiometry when nutrients are strongly limiting.

I test the stoichiometric strategies concept in chapter 2 by culturing assemblages of heterotrophic bacteria at a range of resource ratios and examining the strength of homeostasis in the dominant species. I found that low resource C:P ratios could select for homeostatic strains of bacteria and that higher resource C:P ratios yielded assemblages with flexible composition. In chapter 3, I use bacteria isolated from lakes to describe how homeostatic strains and flexible strains respond to imbalance in C and P. The strains exhibited substantial variation in stoichiometric regulation, but strong homeostasis was associated with higher C and P content and flexible stoichiometry was present only in strains with low P content. These experiments support the hypothesis that flexible biomass composition is competitively superior under P limitation. In the final chapter, I seek to characterize the range of cellular P content attainable by heterotrophic bacteria and determine how bacteria minimize their P content in response to P limitation. I show that bacteria can exhibit greater flexibility in P content than was known previously (< 0.01 to 3% of dry mass as P, biomass C:P of 30:1 to > 10,000:1) and that this flexibility is explained by a simultaneous increase in C content (13 to > 70 fmoles cell^{-1}) and decrease in P content (0.62 to < 0.06 fmoles cell^{-1}) under P limitation.

These studies highlight the importance of physiological constraints and assemblage-level interactions to understanding the impact of stoichiometry on biogeochemical cycles. Additionally, the results of these experiments show that strains of bacteria differ dramatically in their elemental composition, stoichiometric regulation, and resource demands and that the assumptions of strong homeostasis and high nutrient content are not representative of bacteria in aquatic environments. Although aquatic heterotrophic bacteria serve as a useful system to address these questions, the constraints appear to be fundamental and these results are likely applicable to other groups of organisms.

Table of Contents

Acknowledgments i

Dedication ii

Abstract iii

List of Tables vii

List of Figures viii

Chapter 1: Ecological Stoichiometry of Assemblages – Physiological Tradeoffs Couple Competitive Ability and Homeostasis 1

Summary 1

Introduction 1

Stoichiometric Homeostasis 5

Model of Competitive Ability and Stoichiometric Regulation 15

Stoichiometric Strategies 19

Conclusions 25

Figures and Tables 26

Chapter 2: Phosphorus Stoichiometry of Bacterial Assemblages – Do Shifts in Composition Mediate Homeostasis? 32

Summary 32

Introduction 33

Methods 35

Results 40

Discussion 44

Figures and Tables 50

Chapter 3: Diverse Responses of Aquatic Heterotrophic Bacteria to Elemental Imbalance: Stoichiometric Homeostasis is Determined by Phosphorus Quotas and Surplus Carbon Storage 61

Summary 61

Introduction 62

Methods 65
Results 71
Discussion 74
Figures and Tables 81

Chapter 4: Phosphorus Content of Aquatic Heterotrophic Bacteria: How Low Can They Go? 91

Summary 91
Introduction 91
Methods 94
Results 102
Discussion 106
Bibliography 122

Appendix A: Homeostasis and Stoichiometry Datasets 138

Zooplankton Homeostasis Datasets Summary 138
Phytoplankton Homeostasis Datasets Summary 140
Heterotrophic Bacteria Homeostasis Datasets Summary 142

Appendix B: Bootstrap Parameterization of Fulcrum Stoichiometry 145

Appendix C: Cell Quota Model and Equations 149

Appendix D: Cell Morphometry Equations and Figures 153

Appendix E: Photomicrographs of Bacterial Isolates 156

Appendix F: Literature Datasets for Bacterial Phosphorus Content 159

List of Tables

Table 1-1. Regression parameters for stoichiometric regulation in zooplankton, phytoplankton, and bacteria. 31
Table 2-1. Description of the source assemblage locations. 58
Table 2-2. Dissolved P concentrations and seston stoichiometry for the source assemblages. 59
Table 2-3. Biomass stoichiometry and results of ANOVA tests for selection experiments. 60
Table 3-1. Location and characteristics of the source lakes. 87
Table 3-2. Source and taxonomic affiliation of the strains used for this study. 88
Table 3-3. Growth rate, biomass stoichiometry, and strength of homeostasis for isolates. 89
Table 3-4. Elemental content of the isolates. 90

List of Figures

Figure 1-1. Schematic plot of biomass stoichiometry as a function of resource stoichiometry..... 26
Figure 1-2. Schematic plot of a gradient of stoichiometric regulation. 27
Figure 1-3. Parameter plots of the elevation versus slope for biomass-resource regressions..... 28
Figure 1-4. Equilibrium solutions for the consumer-resource model. 29
Figure 1-5. An example of tradeoffs in an assemblage leading to non-homeostasis of the assemblage. 30
Figure 2-1. Schematic plot of selection experiments and chemostats. 50
Figure 2-2. Assemblage C:$P_{biomass}$ ratios across C:P_{supply} treatments. 51
Figure 2-3. Slopes of log C:$P_{biomass}$ versus log C:$P_{resources}$ for selection experiments. 52
Figure 2-4. Assemblage N:$P_{biomass}$ ratios across C:P_{supply} treatments..... 53
Figure 2-5. Cellular P content of assemblages across C:P_{supply} treatments. 54
Figure 2-6. Assemblage length: width ratios across C:P_{supply} treatments. 55
Figure 2-7. Assemblage surface area: volume ratios across C:P_{supply} treatments. 56
Figure 2-8. Non-metric multidimensional scaling ordinations of assemblage ARISA profiles. 57
Figure 3-1. Yields of bacteria from Long Lake and Lake Itasca on rich and poor medium formulations. 81
Figure 3-2. Biomass C:P stoichiometry across C:P_{supply} for isolates in each category. 82
Figure 3-3. Biomass stoichiometry of isolates by stoichiometric category. 83
Figure 3-4. Carbon and phosphorus yields of isolates by stoichiometric category. 84
Figure 3-5. Carbon and phosphorus quotas of isolates by stoichiometric category. 85
Figure 3-6. Morphometry of isolates by stoichiometric category..... 86
Figure 4-1. Cell dry mass, abundance, phosphorus quota, and phosphorus content of assemblages..... 116
Figure 4-2. Effect of C:P_{supply} ratio on biomass C:P, C:N, and N:P ratios..... 117

Figure 4-3. Effect of $C:P_{supply}$ on phosphorus allocation within biomass in Experiment 1. 118
Figure 4-4. Plots of cellular length : width and surface area : volume ratios across $C:P_{supply}$ ratios. 119
Figure 4-5. Histograms of $C:P_{biomass}$ and $N:P_{biomass}$ for bacteria. 120
Figure 4-6. Model solutions for heterotrophic bacteria interacting with dissolved P and C. 121

Chapter 1: Ecological Stoichiometry of Assemblages – Physiological Tradeoffs Couple Competitive Ability and Homeostasis

Summary

The imbalance between the chemical composition of organisms and their resources is central to consumer-resource ecology and is the foundation of ecological stoichiometry. Stoichiometric regulation of biomass element content is coupled to competitive ability and resource requirements through constraints in physiology. In this chapter, I use these physiological constraints to scale single-species stoichiometric regulation to the stoichiometry of assemblages. Within broad phylogenetic and functional categories (zooplankton, phytoplankton, and heterotrophic bacteria), the strength of regulation (or homeostasis) is inversely proportional to the nutrient content of individuals when the denominator element is limiting: homeostatic species have lower biomass carbon: nitrogen (C:N), nitrogen: phosphorus (N:P), and carbon: phosphorus (C:P) ratios than species with flexible biomass stoichiometry. The same physiological constraints that produce the strong dependence between elemental content and stoichiometric regulation also determine the competitive ability of species. I introduce the conceptual framework of 'stoichiometric strategies' to align the gradient of stoichiometric regulation to generalized life history strategies. The stoichiometric strategies are compatible with a consumer-resource model, and simple tradeoffs in physiological parameters (e.g. P affinity versus C efficiency) can lead to dynamic non-homeostasis of assemblages.

Introduction

How should an organism regulate its elemental composition in a world of unbalanced resources? All organisms regulate the elemental composition of their biomass despite unbalanced availability of elements in the environment, but the degree of regulation is widely variable among taxa. As the supply of an element drops below an

organism's requirements, the organism can either maintain its proportion of the element (homeostasis) or alter its biomass composition. Ecological stoichiometry uses ratios and fluxes of elements to describe the relationships among organisms and their chemical environment (Sterner and Elser 2002). Ratios of carbon, nitrogen, and phosphorus (C:N:P) are commonly used to characterize the nutritional state and biomass composition of organisms, although other vital elements (e.g. Ca, Fe, K, Mg, Mn) are also required for growth. The elemental composition of an organism and that of its resources determine the relative rates of element uptake (Rhee 1978), assimilation (Smalley et al. 2003), and regeneration (Frost et al. 2005). Additionally, ecological stoichiometry uses the principle of mass balance to incorporate multiple elemental constraints into models of biological interactions such as consumer-resource dynamics (Elser and Urabe 1999; Sterner 1997), trophic dynamics (Frost et al. 2006; Hillebrand et al. 2009; Sterner 1990) and ecosystem-level processes (Bradshaw et al. 2012; Elser et al. 1998; Sterner et al. 1997).

The stoichiometry of individual organisms is determined by their evolutionary history, developmental stage, and acclimation to local conditions. At the most general levels of comparison, differences in gross structure explain much of the observed variation in stoichiometry among phyla (Elser et al. 1996). For instance, terrestrial plants have higher biomass C:P and C:N ratios than phytoplankton due to C-rich structural materials (Elser et al. 2000a; Raven et al. 2004). At finer levels of comparison, differences in biomolecule allocation explain patterns in stoichiometry. Each class of biomolecules has a characteristic C:N:P signature (Elser et al. 1996), such that the overall stoichiometry of an organism is a function of its proportions of protein, nucleic acids, lipids, and other molecules. Differential investments in growth (Elser et al. 2003), reproduction (Ventura and Catalan 2005), metabolic mechanisms (Jeyasingh et al. 2009), structure (Hendrixson et al. 2007; Pilati and Vanni 2007), storage (Rhee 1973), resource acquisition (Güsewell 2004), or defense (Branco et al. 2010) will all affect the overall C:N:P content of an organism and also its demand for each element. Additionally, the biomass C:N:P of an organism can change during the ontogeny of individuals (Laspoumaderes et al. 2010; Villar-Argaiz et al. 2002a).

The elemental composition of organisms may be regulated, but it is not static.

Although a particular biomass composition may be characteristic for an organism growing under specific conditions, variation in the availability of those elements as resources leads to deviations in biomass C:N:P. Because allocation to some biomass components is more flexible (e.g. surplus storage compounds) than others (e.g. DNA), organisms can alter their biomass stoichiometry in response to imbalance in resource availability (Rhee 1973). Previous works summarize the strength of elemental regulation in a wide range of taxa (Elser et al. 2003; Persson et al. 2010) and show that the degree of non-homeostasis (i.e. plasticity) is variable within and among phyla. Weak homeostasis is commonly associated with autotrophic growth and is partly attributable to the storage of surplus resources within biomass (Rhee 1973). Strong homeostasis is more commonly associated with heterotrophs, which have lower $C:N_{biomass}$, $C:P_{biomass}$ and $N:P_{biomass}$ and show dampened change in nutrient content when faced with resource imbalance (Elser et al. 2000a; Makino et al. 2003; Persson et al. 2010). However, beneath these broad generalizations, the wide range of homeostatic regulation within each group has important implications for understanding the ecological stoichiometry of populations.

While single-species stoichiometry provides insights into species autecology and comparative physiology, most organisms live in assemblages of species competing for one or more shared resources. Thus, the stoichiometry of any assemblage is a function of the abundance of the component species and their elemental composition (Hall et al. 2011). Persistence of a population within an assemblage is determined by the species' ability to avoid predation, overcome diseases, and successfully acquire resources despite competition. Under equilibrium conditions, the outcome of competition for a single shared resource is determined by the lowest concentration of the limiting resource (R*) at which each species is able to maintain non-zero net growth (Tilman 1982). High-affinity acquisition, loss minimization, and efficient use of resources contribute to improved competitive ability in steady-state environments. However, the outcome of competition under non-equilibrium conditions can be more complex (Huisman and Weissing 1999; Sommer 1985). Under non-equilibrium conditions, the traits that are beneficial under equilibrium competition remain beneficial (Grover 1991a), but other traits such as colonization rate (Tilman 1994), growth rate (Grime 1977), or flexible resource demands

(Hood and Sterner 2010) are also important. In both equilibrium and non-equilibrium environments, investments in acquisition and efficiency come at a cost and organisms face trade-offs in competitive ability for multiple resources (Tilman 1990). Since the elemental regulation and competitive ability of all organisms are determined by their physiology, it follows that competitive ability and stoichiometric regulation should be related.

While resource competition theory predicts that the best competitors are species with high resource acquisition affinity and low biomass content for the limiting resource, the framework does not explicitly predict how organisms might regulate their elemental ratios (and thereby their relative requirements) when faced with unbalanced resources. Similarly, ecological stoichiometry offers predictions regarding the interaction between pools of elements in resources and those in biomass, but it is challenging to scale these interactions to assemblages of multiple species. Expansion to assemblage- or community-level stoichiometry requires us to integrate concepts of these disciplines to predict how resource availability simultaneously affects both the relative abundance of species and their aggregate elemental content. Recognizing this coupling will improve our understanding of fluxes and feedbacks between assemblages and their resources. For instance, fertilizing an autotroph community with one or more nutrients alters the relative abundance of its component species (Gough et al. 2000; Hillebrand et al. 2007). Since the species that dominate under low- and high- nutrient conditions differ in their resource utilization, allocation, and regeneration (Tilman and Wedin 1991), it follows that the stoichiometric behavior of the community may differ from that of any single member species.

In this chapter I describe generalized strategies that couple stoichiometric regulation and resource competition within assemblages. This framework is an attempt to integrate aspects of ecological stoichiometry and competition theory by reviewing their related principles, outlining generalized strategies, and refining a combined model of stoichiometry and competition. I use the constraints that couple competitive ability and stoichiometric regulation to hypothesize a generalized response of assemblages to resource imbalance.

Stoichiometric Homeostasis

Strict homeostasis in biomass composition is theoretically possible at a wide range of biomass elemental ratios. However, any specific ratio in biomass is constrained by the macromolecular composition of an organism and the relative availability of the elements as resources. For C, N, and P, perfect homeostasis most likely represents an invariant allocation to nearly every major class of biomolecules within biomass. When the ratio of two elements in biomass is closely matched to the ratio of elements as resources, the organism experiences little imbalance and can potentially attain high yields for both elements, depending upon assimilation efficiency and metabolic losses. In contrast, strong imbalance between the ratio of two elements in biomass and the ratio of those elements as resources limits growth rates and potential yields. Here, the numerator element (X) is required at higher concentrations in biomass than the denominator element (Y). Maintaining a low X:Y ratio in biomass ($X:Y_{biomass}$) would minimize imbalance if the availability of X and Y ($X:Y_{resources}$) is similar to the ratio required in biomass (e.g. low $X:Y_{resources}$), but strict homeostasis at a low $X:Y_{biomass}$ would make an organism susceptible to resource limitation when $X:Y_{resources}$ is relatively higher (Figure 1-1). In contrast, strict homeostasis at low $X:Y_{biomass}$ could be favorable where $X:Y_{resources}$ is low and environmental variability is moderate. Similarly, perfect homeostasis at high $X:Y_{biomass}$ would minimize imbalance in environments where Y is persistently scarce relative to X (high $X:Y_{resources}$). The drawback of this strategy is that when Y becomes more abundant, due to spatial patchiness or temporal variability, the organism is unable to increase its quota of Y (i.e. lower its $X:Y_{biomass}$) and will experience low yield and a reduced growth rate. In the case of phosphorus, because the specific growth rate or production rate of many organisms is often correlated with their tissue P content (Elser et al. 2003; Elser et al. 2000b), homeostasis at high $C:P_{biomass}$ or $N:P_{biomass}$ would seem an unfavorable strategy. In environments where the $X:Y_{resources}$ is variable, organisms that exhibit reduced N or P quotas under nutrient-depleted conditions (high $X:Y_{biomass}$) and increased quotas under nutrient-replete conditions (non-homeostasis in $X:Y_{biomass}$) should experience an advantage relative to organisms exhibiting strict homeostasis. However,

costs associated with flexible biomass composition could make homeostasis at low $X:Y_{biomass}$ favorable under conditions where $X:Y_{resources}$ is low. This suggests a continuum of stoichiometric regulation bounded by strong homeostasis at a low or intermediate $X:Y_{biomass}$ and non-homeostasis (Figure 1-2).

The relationship between biomass stoichiometry and resource imbalance is commonly depicted using a $\log_{10}$-$\log_{10}$ plot of $X:Y_{biomass}$ versus $X:Y_{resources}$ (Sterner and Elser 2002). The slope of the log-log regression can be used to describe the strength of regulation and Sterner and Elser (2002) introduced the inverse of the slope (H') to quantify the strength of homeostatic regulation. The log-log regression equation relating biomass stoichiometry to resource stoichiometry is shown as Equation 1-1, where β is the slope and α is the elevation (intercept) of the regression.

$$log_{10}(X:Y_{biomass}) = \beta \cdot log_{10}(X:Y_{resources}) + \alpha \qquad \text{(Equation 1-1)}$$

This equation can be rearranged to form a power function (Equation 1-2), in which the first term on the right hand side defines the ratio about which the organism maintains its stoichiometry and the second term defines how the organism adjusts its biomass stoichiometry in response to resource imbalance.

$$X:Y_{biomass} = 10^{\alpha} \cdot X:Y_{resources}{}^{\beta} \qquad \text{(Equation 1-2)}$$

Theoretically, the strength of homeostasis is bounded by a slope equal to one (no homeostatic regulation of $X:Y_{biomass}$) and a slope equal to zero (perfect homeostasis in $X:Y_{biomass}$). When the slope is equal to zero, the biomass ratio is determined solely by the elevation. Although the slope (or strength of homeostasis) is indicative of how an organism regulates its biomass stoichiometry and the scaling of X and Y within biomass, this parameter does not reflect the absolute ratio of elements in biomass.

Patterns of Stoichiometric Regulation

Each organism possesses a suite of mechanisms, i.e. a stoichiometric strategy, to cope with unbalanced resource availability. Strong homeostasis and non-homeostasis

represent the extremes in a continuum of possible stoichiometric strategies. General characteristics such as structural tissues explain the large differences observed in C:N:P across phyla (Elser et al. 2000a), but there is also evidence for diverse strategies within these groups. Here I review the patterns of stoichiometric regulation in three broad functional groups and identify generalized patterns in stoichiometric regulation.

Data Sources. For each class of organisms that I consider in this chapter (zooplankton, phytoplankton, and heterotrophic bacteria), I collected data from studies that characterized the response of C:N, N:P, or C:P in biomass to changes in resource ratios. I obtained data from studies published prior to 2012, identified using Web of Science citation index (Thomson Reuters). I used all meaningful permutations of the search terms (stoichiom*, homeosta*, carbon, nitrogen, phosphorus) to identify the studies, and also included the references therein. Several criteria were applied to the datasets. First, each organism or assemblage must have been grown in at least three discrete levels of a resource ratio. This constraint was intended to minimize under-estimation of the slope since many species exhibit a breakpoint type regression. The second criterion was that the resource ratios must have been the result of manipulation or experimentation (i.e. no observational data from natural systems). Natural systems contain non-living organic material (i.e. detritus) and may contain organisms in various states of senescence or dormancy, both of which would obscure patterns in stoichiometric regulation. The third criterion was that the resource and biomass ratios must have been explicitly stated or simply calculated from provided information. Although many datasets contained data expressed as quotas (e.g. moles per cell) or mass content (e.g. moles per kg), converting these data to elemental ratios could conceivably obscure patterns in regulation. Multiple studies using the same organism were treated as separate observations. Similarly, when a third parameter was manipulated (e.g. temperature), the levels of this parameter were treated as separate observations. The number of datasets was comparable to other syntheses (Persson et al. 2010): 22 species of phytoplankton from 27 experiments, 14 species of zooplankton from 16 experiments, and 30 strains or assemblages of bacteria from 36 experiments.

The elevation of the log-log regression of $X:Y_{biomass}$ versus $X:Y_{resources}$ has

received comparatively little attention, but this parameter is indicative of the biomass ratio about which an organism regulates its composition. An organism hypothetically can maintain a specific degree of homeostasis (slope, β) around any biomass ratio (elevation, α). Clearly, both of these parameters are required to describe the biomass composition of an organism in response to resource availability. For each dataset, I performed linear regressions of $\log_{10}$ $X:Y_{biomass}$ versus $\log_{10}$ $X:Y_{resources}$. These regressions are referred to as biomass-resource regressions. The biomass-resource regression parameters for each dataset are listed in Appendix A.

Fulcrum Stoichiometry

Within each class of organisms considered in this chapter, I summarized the regulation of C:N, N:P, or C:P in biomass for each organism by plotting the elevations (α) of the biomass-resource regression versus the slopes (β) (Figure 1-3). The slopes and elevations of the biomass-resource regressions are not independent, but instead show a strong negative relationship (Figure 1-3). These plots are referred to as parameter plots. For each parameter plot, I performed a standardized major axis regression (Warton et al. 2006) of the elevations versus the slopes (Table 1-1). I used the regressions from the parameter plots to describe the constraint in stoichiometric regulation for each class of organisms. The strength of the negative relationship between the elevation and slope of the parameter plots indicates that the biomass-resource regressions for each class of organisms converge in a region of similar $X:Y_{biomass}$ and $X:Y_{resources}$ (Figure 1-2). Although the negative relationship between the elevation and slope is expected for regressions of points sampled from a defined region, the strength of this relationship suggests a constraint in how species adjust their biomass stoichiometry.

I propose the term 'fulcrum resource ratio' to describe the resource ratio at which the functions for the taxa approach convergence. I solved for these ratios using the major axis regressions for each dataset, where $\hat{\alpha}$ is the intercept of the major axis regression and $\hat{\beta}$ is the slope. The major axis regression (Equation 1-3) can be substituted for the elevation in Equation 1-2 to give a generic form where the elevation is determined by the slope using the major axis regression (Equation 1-4).

$$\alpha = \hat{\alpha} - \hat{\beta} \cdot \beta \qquad \text{(Equation 1-3)}$$

$$X{:}Y_{biomass} = 10^{\hat{\alpha}-\hat{\beta}\cdot\beta} \cdot X{:}Y_{resources}{}^{\beta} \qquad \text{(Equation 1-4)}$$

By solving Equation 1-4 for any two values of β, the resource ratio at the fulcrum is equal to $10^{-\hat{\beta}}$ and the corresponding biomass ratio is equal to $10^{\hat{\alpha}}$. This fulcrum resource ratio is depicted as the 'pivot' point in Figure 1-2.

The fulcrum stoichiometry is the point at which the biomass-resource plots for all of the species approach convergence. Under low resource imbalance, all of the species in each group have relatively similar biomass stoichiometry, but when resources are strongly unbalanced, species have different stoichiometry depending upon their physiology. The apparent constraint in stoichiometric regulation relates to a fundamental hypothesis regarding ecological stoichiometry: organisms with a common phylogeny, physiology, and ecological role should have a similar biomass composition under some set of conditions. The fulcrum stoichiometry concept does not predict how the biomass composition of species will differ when factors such as temperature (Chrzanowski and Grover 2008), energy availability (Glibert et al. 2013), body size (Allen and Gillooly 2009), or growth rate independently influence biomass composition. However, the strong negative relationship between the slope and elevation suggests a constraint in how organisms regulate their biomass stoichiometry. This relationship allows us to simplify the responses of a group of taxa to a set of related equations.

Uncertainties in the fulcrum resource ratio and fulcrum biomass ratio were calculated using the variance estimates for the slope and elevation of the parameter plot regressions (Warton et al. 2006). To determine the sensitivity of the parametric fulcrum estimates to the quantity of data available, I performed bootstrap resampling of the datasets used for the parameter plots following Crowley (1992). For each dataset (e.g. zooplankton C:N), I resampled the parameter plot data at least 20,000 times with replacement. For each of the iterations, I performed SMA regression of the elevation versus the slope and computed the fulcrum resource stoichiometry and biomass stoichiometry following Equation 1-4. Due to positive skewness in the output distributions, I compared the median value of the bootstrap output to the parametric estimate obtained using the complete dataset (Table 1-1). The 95% confidence intervals

for the bootstrap estimates were obtained directly from the output distributions (Appendix Figures B-1, B-2, and B-3). The median bootstrap values were similar to the fulcrum estimates obtained using the complete datasets (Appendix Table B-1). The lower confidence levels from the bootstrap method were similar to the parametric estimates, but positive skewness in the bootstrap output increased the upper confidence levels in several cases.

Zooplankton. Zooplankton and invertebrate consumers generally have lower $C:N_{biomass}$ and $C:P_{biomass}$ ratios than phytoplankton and plants at the base of the food web (Elser et al. 2000a). Previous syntheses have shown than zooplankton species regulate their N:P stoichiometry more tightly than algae (Persson et al. 2010) and that there is a range of regulation for zooplankton instead of uniformly strong homeostasis. Zooplankton species show a range of stoichiometric regulation in $C:N:P_{biomass}$, but this regulation is confined to a narrow region of the possible types of regulation (Figure 1-3), as shown by the robust R^2 for the regressions (Table 1-1). The strength of regulation can be represented as a continuum between strong homeostasis at low to moderate biomass ratios (C:N:P = 78:21:1) and varying degrees of non-homeostasis that pivot around the fulcrum stoichiometry.

Although more data are available for zooplankton C:N and $C:P_{biomass}$ stoichiometry (Table 1-1), the limited data for N:P stoichiometry also show a negative relationship between the slopes and elevations (Figure 1-3). The fulcrum resource ratio for zooplankton ($C:N:P_{resources}$ = 74:29:1) is not significantly different than estimates of phytoplankton $C:N:P_{biomass}$ including: the Redfield ratio of $C:N:P_{biomass}$ = 106:16:1 for marine phytoplankton (Redfield 1958), the mean C:N:P of lake seston (149:17:1, Cotner et al. 2010), and the median $C:N:P_{biomass}$ for phytoplankton species (256:26.5:1, Elser et al. 2000a). The fulcrum $N:P_{biomass}$ ratio for zooplankton (21:1) is higher than the median for freshwater invertebrate consumers (18.5:1, Elser et al. 2000a) and the fulcrum $C:P_{biomass}$ ratio (77.6:1) is lower than the median from the same dataset of invertebrate consumers (114:1). However, the confidence intervals for fulcrum $C:N:P_{biomass}$ (Table 1-1) overlap the values from the literature and also the Redfield ratio for phytoplankton $C:N:P_{biomass}$.

Phytoplankton. Redfield (1958) noted the similarity between the C:N:$P_{biomass}$ stoichiometry of marine phytoplankton (106:16:1) and the ratio of changes in dissolved C, N, and P (105:15:1). Although the Redfield ratio is commonly associated with balanced growth of phytoplankton, the ratio is variable across habitats (Elser et al. 2000a; Hecky et al. 1993; Sterner et al. 2008) and within individual species of phytoplankton (Klausmeier et al. 2004a; Quigg et al. 2011; Rhee 1973). The biomass stoichiometry of phytoplankton is also dependent upon many factors including resource availability (Hall et al. 2005; Klausmeier et al. 2004b), light intensity (Diehl et al. 2005; Healey 1985; Leonardos and Geider 2004b), and growth rate (Ågren 2004; Tett et al. 1985).

Individual species of phytoplankton show a range of regulation in their N:P stoichiometry (Persson et al. 2010 and references therein), from strict homeostasis (slope ≈ 0) to non-homeostasis (slope ≈ 1). While many publications have assumed that stoichiometric plasticity is typical within phytoplankton, some species clearly maintain similar N:$P_{biomass}$ content in their biomass despite varied resource ratios. Also, algae in culture become increasingly homeostatic as the dilution rate (realized growth rate) increases (Klausmeier et al. 2004b). The continuum of N:P regulation in phytoplankton (Figure 1-3) is bounded by species that are homeostatic at a moderate N:$P_{biomass}$ (≈13.9:1) and species with highly flexible stoichiometry. The intermediate strengths of regulation are constrained to a subset of potential regulation. Interestingly, no species of phytoplankton in this dataset exhibits strict homeostasis at high N:$P_{biomass}$. In this way, the strategies appear to 'pivot' around a fulcrum stoichiometry of N:$P_{resources}$ = 27.1:1. At this fulcrum stoichiometry, the fulcrum biomass ratio is N:$P_{biomass}$ = 13.9:1 (Table 1-1). This fulcrum biomass ratio is close to the Redfield ratio (16:1) (Redfield 1958) but lower than the median N:$P_{biomass}$ for freshwater phytoplankton (26.5:1) (Elser et al. 2000a) and the seston of lakes (20 - 21:1) (Sterner et al. 2008). Despite variation in the stoichiometry of phytoplankton populations and communities due to local resource availability, phytoplankton as a group exhibit a more uniform N:$P_{biomass}$ when the N:$P_{resources}$ is low than when P is scarce relative to N.

Heterotrophic Bacteria. Heterotrophic bacteria have been used as a model for understanding consumer-resource dynamics in osmotrophic organisms (Tezuka 1990).

Makino et al. (2003) cultured *Escherichia coli* in continuous culture at a range of $C:P_{resources}$ ratios and found that *E. coli* was strongly homeostatic (slope = 0.045). Other strains of bacteria also show strong to moderate homeostasis in their $C:P_{biomass}$ stoichiometry (Figure 1-3). Similar to zooplankton and phytoplankton, there appears to be a continuum of $C:P_{biomass}$ and $N:P_{biomass}$ regulation in bacteria, ranging from strong homeostasis at $C:P_{biomass} \approx 114:1$ and $N:P_{biomass} \approx 16:1$ to varying degrees of non-homeostasis. From the relationships between the slopes and elevations for C:P and N:P, the fulcrum resource stoichiometry for heterotrophic bacteria is $C:N:P_{resources} = 352:73:1$ (Table 1-1). The fulcrum biomass stoichiometry for bacteria is 115:16:1. This biomass composition is close to the Redfield ratio and the mean $C:N:P_{biomass}$ content of the bacterial-sized fraction of seston in temperate lakes (102:12:1, Cotner et al. 2010).

Several studies have investigated the stoichiometry of mixed cultures of bacteria (Jürgens and Güde 1990; Makino and Cotner 2004; Tezuka 1990). Similar to populations of bacteria in axenic culture, assemblages of bacteria from lakes and the ocean show a range of stoichiometric regulation (Figure 1-3). The biomass-resource regression parameters for assemblages of bacteria fall along the same axis of the parameter plot as those for populations. Some of the variation along the axis is due to the effect of dilution rates in continuous cultures. Increasing dilution rates in continuous (chemostat) cultures increases the strength of homeostasis in bacteria (Chrzanowski and Kyle 1996; Makino and Cotner 2004; Makino et al. 2003) and algae (Klausmeier et al. 2004b). Indeed, the most homeostatic assemblage was grown at a higher dilution rate in continuous culture ($0.7\ h^{-1}$) than other mixed cultures (Makino and Cotner 2004). These data suggest that assemblages and populations of bacteria are subject to the same constraints in stoichiometric regulation.

Fulcrum Stoichiometry and Constraints in C:N:P Homeostasis

To understand the connection between stoichiometric regulation and competitive ability, we need to first consider the constraints in elemental regulation. Although phytoplankton, zooplankton, and heterotrophic bacteria differ markedly in their physiology, metabolism, and biomass composition, these three broad taxonomic groups are subject to a common constraint in how they regulate their stoichiometry. For each

pair of C, N, and P, there is a gradient of stoichiometric regulation between strong homeostasis at a low to moderate ratio and varying degrees of non-homeostasis that appear to pivot around a fulcrum stoichiometry (Figure 1-3, Table 1-1). At some resource composition, all of the species have similar biomass stoichiometry, but under unbalanced resource ratios, the species have divergent stoichiometry. This commonality may be explained by the fact that all of the species within a taxonomic grouping share a common set of macromolecules and gross physiological requirements and thus should have a similar biomass composition under balanced resource ratios.

The fulcrum $N:P_{biomass}$ ratios for phytoplankton and bacteria were close to the Redfield ratio (Table 1-1). Although studies have shown that this ratio does not necessarily represent the typical (Geider and La Roche 2002; Hall et al. 2005) or optimal (Klausmeier et al. 2004a) biomass stoichiometry of plankton, the Redfield ratio of N:P = 16:1 appears to represent a fundamental biomass composition for plankton when N and P in resources are not strongly unbalanced. However, other factors including light availability, temperature, and growth rate could lead to deviation from the predicted biomass composition. Despite differences in their resource acquisition and evolutionary history, these groups share a similar stoichiometry at a basic level. Indeed, much of this consistency in N:P is attributable to the stoichiometry of highly conserved biomolecules and tissues (Sterner and Elser 2002). Despite physiological differences among species, the taxa within each group share a macromolecular composition (e.g. nucleic acids, protein, and lipids). Group-specific physiologies such as lignin and cellulose in plants or bony tissues in vertebrates, would lead to differences in the fulcrum C:N, N:P, and C:P ratios. Among these groups of taxa, consistency in the fulcrum $N:P_{biomass}$ is partly attributable to the ratio of rRNA to protein in translation, which is shared by all organisms (Loladze and Elser 2011).

The fulcrum $N:P_{resources}$ for zooplankton was lower than those for phytoplankton and bacteria, although the confidence intervals overlap for the three groups. Also, despite both groups being heterotrophs, zooplankton and bacteria have different fulcrum $C:N_{resources}$ and $C:P_{resources}$. These patterns are attributable to a fundamental difference in the mode of nutrient acquisition by the consumer groups. Phagotrophic organisms such as

zooplankton consume multiple elements simultaneously as food particles with non-independent stoichiometry (Frost et al. 2006; Sterner and Elser 2002) and N and P incorporated in organic compounds. Furthermore, some zooplankton selectively feed upon nutrient-rich phytoplankton particles (Butler et al. 1989; Cowles et al. 1988; Schatz and McCauley 2007), which enables the animals to mediate resource imbalance. In contrast, phytoplankton species acquire inorganic N and P separately and heterotrophic bacteria consume elements independently (i.e. organic carbon and inorganic N and P) or as small biomolecules.

Comparatively little data are available for N:P stoichiometric regulation in vascular plants, but Yu et al. (2011) performed a comparison of the strength of $N:P_{biomass}$ regulation in grassland plant species. In their study, the plant species with low $N:P_{biomass}$ exhibited weaker stoichiometric homeostasis than species with higher $N:P_{biomass}$ and the mean biomass N and P contents of each species were positively correlated with the degree of flexibility in $N:P_{biomass}$. This result is contradictory alongside the fulcrum stoichiometry concept, but would be produced from the slope-elevation constraint if the mean $N:P_{resources}$ were less than the fulcrum resource ratio for the taxa (i.e. the plants were adapted to low P availability).

The fulcrum stoichiometry concept provides a framework for simplifying the stoichiometric regulation within assemblages or groups of taxa. Specifically, species that attain high C:P, N:P, or C:N under limitation by N or P are non-homeostatic and the homeostatic species share a similar biomass stoichiometry. Thus, the stoichiometric responses of all of the species in the group are apparently constrained as depicted in Figure 1-3 and described by Equation 1-4. However, there is important flexibility in this constraint. This is apparent in Figure 1-3 as the residuals of the regressions of elevations versus slopes. While this variability might be characteristic of multiple tradeoffs in physiology (Tilman 1990), some variation is attributable to differences in culture conditions, experimental design, and simple measurement error. These confounding effects are difficult to control when compiling data from multiple experiments. One factor with particular influence is the effect of realized growth rate (or chemostat dilution rate) on the strength of regulation in bacteria and phytoplankton. Increasing growth rate

leads to a more homeostatic response (Makino and Cotner 2004; Makino et al. 2003; Ribalet et al. 2009). The effect of realized growth rate on stoichiometric regulation is predicted by consumer-resource theory. As the realized growth rate approaches the maximum growth rate, the cell quotas necessarily approach their maximum, leading to diminished flexibility in biomass ratios at high growth rates (Droop 1974; Klausmeier et al. 2004b; Thingstad 1987; Vrede et al. 2004).

Model of Competitive Ability and Stoichiometric Regulation

Patterns In Homeostasis And Competitive Ability

Numerous models have been proposed to describe the dynamic relationship between consumers and their resources using the law of mass balance between elements in the resources and those in biomass (Cherif and Loreau 2010; Droop 1974; Klausmeier et al. 2004b; Tilman 1977). These models consider the rate of resource acquisition by an organism and the resource use efficiency or yield. Tilman and Kilham (1976) demonstrated that phytoplankton species differ in their ability to compete for limiting nutrients, and related this competitive ability to physiological parameters. Tilman (1977) proposed that competitive ability could be expressed as a function of the parameters in the internal stores model (Droop 1973b; Droop 1974). This approach explicitly relates competitive ability to physiological mechanisms related to nutrient acquisition and allocation (Klausmeier et al. 2004b; Tilman et al. 1982).

To investigate the mechanisms by which stoichiometric regulation is coupled to competitive ability, I employed a cell quota model of consumer-resource interaction (Droop 1973a). This model (Appendix C) describes a heterotrophic bacterium consuming dissolved organic C and inorganic N and P (Thingstad 1987). The assumptions of this model are: (1) growth rate is proportional to the quota of the element which is in lowest within biomass relative to the minimum and maximum quotas, (2) the uptake of resources is dependent upon both extracellular availability and internal concentration, (3) the environment is homogenous and all organisms are subject to a uniform loss rate, and (4) the organisms interact only through their shared resources and loss rates are equal (i.e. no allelopathy, mixotrophy, or cooperation). Within this model, I manipulated each

parameter within biologically feasible limits (e.g. minimum quota < maximum quota and maximum growth rate > loss rate) to explore the simultaneous effects on stoichiometric regulation and competitive ability. For each set of parameters, I manipulated the supply of P to obtain $C:P_{resources}$ ratios from 100:1 to 10,000:1 and solved for the analytical equilibrium conditions. Competitive ability was summarized as R* (Tilman 1977) for each set of physiological parameters and dilution rate. The strength of stoichiometric regulation (slope) was calculated from log-log plots of the biomass ratio at equilibrium versus the ratio of resource supply rates (Sterner and Elser 2002). To facilitate this calculation, I fitted an interpolating polynomial function to the output of $C:P_{biomass}$ versus $C:P_{resources}$ and used the first derivative of the function to determine the local maximum rate of change in $C:P_{biomass}$. The threshold element ratio (TER) is the ratio at which the bacterium switches from C limitation to P limitation (Sterner and Elser 2002) and was estimated by solving for the supply C:P ratio where the ambient carbon and phosphorus supplies approach C* and P*, respectively. All calculations were performed using Mathematica version 7 (Wolfram Research).

The effect of each parameter on competitive ability qualitatively matched the predictions of other consumer-resource models (Grover 1991b). Increases in the dilution rate, minimum P quota ($Q_{P\,min}$), half-saturation constant for P uptake (K_P), ratio of C incorporated to respired (ρ_g), and the proportion of surplus C respired (ρ_r) led to increases in P* (i.e. decreased the competitive ability for P, Figure 1-4). Similarly, increasing $Q_{P\,max}$ and $V_{P\,max}$ led to decreases in P* (i.e. improved the competitive ability for P). These simulations show how cell quota models can exhibit inherent stoichiometric behavior. Manipulating each physiological parameter alters the biomass C and P quotas at equilibrium, leading to different biomass C:P ratios at a given supply ratio. Inherent stoichiometric regulation has been observed in other models (Grover and Chrzanowski 2006; Klausmeier et al. 2008; Klausmeier et al. 2004b), but here I show that, for each physiological parameter, the strength of elemental regulation is negatively correlated to the competitive ability for the limiting element (Figure 1-4).

For each parameter related to P physiology, there is an inverse relationship between the strength of C:P homeostasis and competitive ability for P (i.e. P* and slope

are negatively related, Figure 1-4). Increasing the dilution rate relative to the maximum growth rate causes the bacteria to become more homeostatic and less competitive for phosphorus. The difference between the maximum and minimum phosphorus quotas is inversely related to competitive ability for phosphorus and strength of C:P homeostasis. Increasing the uptake affinity ($K_P/V_{P\ max}$) leads to a coupled decrease in the strength of C:P homeostasis and an increase in competitive ability for phosphorus (Figure 1-4). Both of the parameters for carbon use efficiency (ρ_g and ρ_r) show an inverse relationship between the strength of homeostasis and competitive ability for carbon (not shown). For each of the parameters manipulated, there is an inverse relationship between the strength of homeostasis and the threshold element ratio (data not shown). In the manipulated range of $Q_{p\ min}$, the $TER_{C:P}$ decreases from 446:1 to 148:1 as the minimum P quota increases.

Some of the parameters have strong effects on homeostasis (d/μ_{max}, $Q_{P\ min}$, and K_P) while other parameters show less effect upon $C:P_{biomass}$ than competitive ability (notably $Q_{P\ max}$ and $V_{P\ max}$). While there are numerous tradeoffs in parameters that could couple competitive ability and homeostasis, the most dramatic are between d/μ_{max} and $Q_{P\ min}$. This tradeoff is supported by strong correlations between maximum growth rate and minimum quota in algae (Droop 2003). Although species with high μ_{max} could be competitive under local or temporary conditions of abundant resources (Sommer 1985), the high biomass P content associated with rapid growth (Elser et al. 2003) implies strong homeostasis at low $C:P_{biomass}$ or $N:P_{biomass}$. The fitness cost of becoming more homeostatic comes from being more susceptible to P limitation. Resource imbalance leads to a decrease in fitness since the organism's growth is limited by the element that is most scarce relative to its biomass. However, species with flexible biomass stoichiometry mitigate the impact of imbalance by adjusting their composition and should have a fitness advantage when nutrients are limiting. This model does not consider differences in loss rates that are associated with carbon or nutrient content. Some zooplankton predators preferentially consume high-nutrient prey items (Schatz and McCauley 2007), which could lead to other important tradeoffs related to susceptibility to grazing losses (Branco et al. 2010). These results illustrate how tradeoffs between competitive strategies can

have implications for individual species stoichiometry as well as for assemblage-level stoichiometry.

Assemblage-Level Model

Since the physiological parameters in the model couple stoichiometric regulation and competitive ability, assemblages might exhibit non-homeostasis as the result of competition among species. To simulate how one tradeoff scenario could lead to non-homeostasis of an assemblage, I populated the equations for 10 species in the consumer-resource model using simple a linear tradeoff. To create differences in competitive ability for C and P, a species with low phosphorus demand ($Q_{P\ min}$= 0.002 fmol cell^{-1}, $Q_{P\ max}$ = 0.04 fmol cell^{-1}, ρ_g=1.0, C^*= 0.212 μM, P^*= 0.00013 μM, $TER_{C:P}$=1,112) and a species with high growth efficiency for carbon ($Q_{P\ min}$= 0.01 fmol cell^{-1}, $Q_{P\ max}$ = 0.018 fmol cell^{-1}, ρ_g= 0.8, C^*= 0.188 μM, P^*= 0.001 μM, $TER_{C:P}$=200.8) were used as the extremes of the tradeoff gradient. For each simulation, each species was 'inoculated' at equally low density and uniform biomass C:N:P content. I performed numerical simulations at a range of supply C:P ratios (100:1 to 10,000:1) by manipulating the supply of P. All of the simulations asymptotically approached a steady-state monoculture condition, so an endpoint of 10,000 turnovers was used as the equilibrium state. All numerical simulations were performed using the Runge-Kutta method with a variable step size (Mathematica version 7, Wolfram Research).

The tradeoff between phosphorus requirement and carbon-use efficiency resulted in shifts in species abundance across resource ratios. Such species replacements across a gradient of resource ratios are well-known in consumer-resource theory (Danger et al. 2008; Tilman 1980). The aggregate stoichiometry of the assemblage locally resembles that of the dominant species, leading to an overall pattern in which the assemblage is homeostatic at low resource C:P, non-homeostatic at higher $C:P_{resources}$, and homeostatic again at the highest range of $C:P_{resources}$ (Figure 1-5). The extent of non-homeostasis in the assemblage is dependent upon the range of $C:P_{biomass}$ attainable by the best competitors for C and P. The tradeoff example used here illustrates that assemblages can exhibit non-homeostasis that is different from any of the component species. Furthermore, the range of $C:P_{biomass}$ exhibited by the assemblage is necessarily less than that of the most flexible

species.

This assemblage-level model demonstrates that simple tradeoffs in physiological capabilities can result in stoichiometric regulation of assemblages that differs from any of the component species. Because the functional groups responsible for nutrient cycling contain a range of stoichiometric regulation, models of assemblage- and community-level stoichiometry could be improved by coupling stoichiometric regulation to competitive ability. Only equilibrium solutions were explored in this analysis, but other tradeoffs are important in non-equilibrium environments, including growth rate (Grime 1977) or flexible resource demands (Hood and Sterner 2010). In particular, a tradeoff between low resource demand and high growth rate would alter the outcome in a non-equilibrium environment. Such a tradeoff scenario could explain the persistence of homeostatic species if they are competitive under conditions of locally abundant resources.

Stoichiometric Strategies

Generalized Strategies. In the first section, I showed that within each group of taxa, there is a continuum of stoichiometric strategies that is bounded by species with strong homeostasis at a moderate $X:Y_{biomass}$ ratio and species with responses that 'pivot' around a similar biomass composition at the fulcrum stoichiometry. This pattern is indicative of an underlying constraint in stoichiometry and competitive ability. Homeostatic species maintain low C:P and N:P in biomass, leading to P limitation when the availability of P decreases. In the subsequent section, I showed how this tradeoff could be driven by differences in many different physiological parameters among organisms within assemblages. From these syntheses, I propose a continuum of hypothetical 'stoichiometric strategies' that couple biomass homeostasis and competitive ability. This continuum is analogous to other tradeoff axes and life history strategies within ecological theory.

I propose that the homeostatic strategy is analogous to r-selected species (Jannasch 1974; MacArthur and Wilson 1967), competitive specialists (Grime 1977), and the velocity strategy (Crowley 1975; Sommer 1985). This strategy is characterized by high potential growth rates, high nutrient content, comparatively low $C:P_{biomass}$ and

$N:P_{biomass}$ ratios, and high nutrient requirements. In contrast, the non-homeostatic strategy is similar to K-selected species (Jannasch 1974; MacArthur and Wilson 1967), stress-tolerant species (Grime 1977), or affinity-adapted species (Crowley 1975; Sommer 1985). This strategy is characterized by low potential growth rates, low nutrient requirements, and variable nutrient content. These broad strategies parallel the continuum of stoichiometric regulation described in the first section and are compatible with the cell quota model of consumer-resource interactions.

Plant physiological ecology and phytoplankton community ecology provide a thorough exploration of consumer-resource theory and growth strategies. Grime (1977; 1979) outlined two generalized patterns in plant life history that are relevant to this synthesis: the stress-tolerant strategy and the competitive specialty. A third strategy, specializing in habitats with high rates of disturbance, is less relevant to this review. Stress-tolerant species are most abundant in habitats with persistent environmental stress, particularly low nutrient availability. These species are characterized by low potential growth rates and low nutrient requirements. Species typifying this strategy have variable nutrient content due to the fact that they often store surplus nutrients when the supply exceeds their low demand (Kilham and Hecky 1988; Sommer 1985). In contrast, velocity-adapted species are adapted to exploit favorable conditions by growing quickly, but are less competitive when resources become limiting. Because stress-tolerant species have lower nutrient content and allocate surplus nutrients to storage, their biomass stoichiometry should be responsive to the nutrient supply. Conversely, velocity-adapted species have higher nutrient content and growth requirements, making their growth rate highly sensitive to resource availability while their biomass stoichiometry changes little. Güsewell (2004) provides evidence for the generalization that velocity-adapted species have higher N and P content and lower N:P compared to stress-tolerant plants.

I propose that the velocity-adapted and stress-tolerant strategies correspond to the homeostatic and non-homeostatic stoichiometric strategies. Under high resource availability, species of both strategies have high nutrient content, but these are allocated differently. The velocity-adapted species allocate the available nutrients to structures for immediate growth, including ribosomes, reproductive tissues, and seeds. In contrast, the

stress-tolerant species allocate some of the surplus nutrients to storage, increasing their nutrient content at the cost of lower nutrient use efficiency (Klausmeier et al. 2004a). Under low nutrient availability, the velocity-adapted species retain high biomass concentrations of the limiting nutrient (homeostasis), but incur lower realized growth rates or may become dormant. The stress-tolerant species reduce their quota of the limiting nutrient by minimizing storage and maintaining a slow growth rate. These differences are characteristic of the tradeoff between growth rate and nutrient economy (Aerts 1999). I examined the C:P stoichiometric regulation of 24 strains of bacteria and found that homeostatic strains had higher quotas of C and P than non-homeostatic strains (chapter 3). This finding is consistent with the hypothesis that strong homeostasis leads to reduced competitive ability for a limiting nutrient.

It is important to note that these generalized strategies are extremes along a continuum. Species might exhibit only some of the physiological mechanisms associated with a strategy, leading to intermediate phenotypes. Since multiple physiological traits couple stoichiometric regulation and competitive ability, this tradeoff continuum is likely composed of numerous physiological axes. This is supported by the constrained gradient of C:N:P regulation observed within groups of taxa (Figure 1-3). However, because the degree of elemental regulation is related to the ability to compete for nutrients, this continuum of strategies may be scaled to the level of assemblages.

Strategies Within Assemblages. Numerous factors control the distribution of species within assemblages including grazing and predation, disease, dispersal, light, temperature, and nutrient availability. Although consumer-resource dynamics are clearly insufficient to explain all of the patterns and processes observed in ecosystems, nutrient resources play a key role in determining how assemblages interact with their environments. Since assemblage function is determined by both species abundance and physiology, strategy classifications may be used to understand successional patterns as they relate to assemblage function (Tilman 1988).

The stoichiometric regulation of assemblages is dependent upon the stoichiometric regulation of their component species and the relative abundance of those species. Three scenarios could describe how population stoichiometry could be scaled to

assemblages. First, the stoichiometry of an assemblage may be representative of a common response for all component species. In this way, the biomass stoichiometry of the assemblage is independent of assemblage composition. However, given the range of regulation observed in single-species cultures (Figure 1-3, Persson et al. 2010), this scenario seems unlikely. In an alternative scenario, resource imbalance can cause shifts in the relative abundance of species within assemblages. In this second scenario, all species in an assemblage share a common strength of regulation but differ in the level at which they maintain their stoichiometry (i.e. they have the same slope but different elevations). Makino et al. (2003) speculated that assemblages of bacteria are non-homeostatic as the result of selection among multiple strains with different homeostatic 'set points' (elevations). Again, this scenario seems unlikely due to the range of homeostatic regulation observed within groups of taxa (Figure 1-3).

A third possibility is that species differ in the strength of homeostasis, but their relative nutrient content determines their competitive ability. In this case, the assemblage will exhibit varying degrees of non-homeostasis due to shifts in relative abundance. Danger et al. (2008) presented an assemblage-level model of C:P stoichiometry of heterotrophic bacteria in which the TER for resources and the $C:P_{biomass}$ at the TER were positively correlated among species. They demonstrated that the assemblage would undergo shifts in species composition and exhibit non-homeostasis as a result. Their model successfully couples competitive ability and stoichiometric regulation, but does not include an explicit constraint in how the strength of regulation differs among species. The constraint in regulation represented by the fulcrum stoichiometry suggests that species differ in both their strength of regulation (slopes) and their biomass ratios (elevations). If the dominant strains at low $C:P_{resources}$ exhibit stronger homeostasis than the strains that are dominant at high $C:P_{resources}$, the assemblage will exhibit non-homeostasis. Furthermore, because the local response to imbalance would be dependent upon the dominant species, the aggregate stoichiometry would show locally decreasing homeostasis at intermediate resource ratios.

The challenge of scaling ecological stoichiometry to the level of assemblages requires that we explore the apparent tradeoffs between homeostasis and competitive

ability and other traits that affect the success of organisms (e.g. predator avoidance). Unfortunately, few studies have done this. Jeyasingh et al. (2009) demonstrated the link between competitive ability and homeostatic regulation using *Daphnia* clones. In three separate competition experiments, the more homeostatic clones outcompeted the less homeostatic clones when the prey C:P was low, but the less homeostatic clones were dominant when prey C:P was increased. The authors attributed the coupling between competitive ability and homeostatic regulation to genetic variation at a single locus (phosphoglucose isomerase) that couples P and C metabolism. Although other genes and physiologies could explain part of this coupling, their study demonstrates how physiology couples stoichiometric homeostasis and competitive ability.

Although there has not been a study that explicitly investigates the simultaneous effects of resource availability on species abundance and stoichiometric strategies within assemblages, there are several examples of experiments in which the nutrient demand of the dominant species correlated with nutrient availability (Güsewell et al. 2003; Mamolos et al. 1995). Mamolos et al. (1995) manipulated the N and P supply in a grassland community and found that species with higher relative N or P content increased in abundance when N or P was added. Selection for stoichiometric strategies might influence the outcome of fertilization experiments or nutrient enrichment bioassays performed in assemblages. Strongly homeostatic species should respond to addition of a limiting nutrient only by increasing their growth rate, but non-homeostatic species could respond to addition of a limiting resource by increasing their biomass content with little or no change in growth rate.

Strategies and Tradeoffs Within Assemblages. The consumer-resource model predicts that assemblages should be inherently non-homeostatic due to physiological tradeoffs that couple stoichiometric regulation and competitive ability. Field surveys show some support for this prediction, especially over large scales (Hall et al. 2005). However, these observations may be confounded by numerous factors that are specific to each location (e.g. light, temperature, or predation). Using phytoplankton communities grown in mesocosms, Sterner and Hessen (1994) demonstrated that $N:P_{biomass}$ increases with increasing $N:P_{resources}$ as expected, but also showed that nitrogen fixation can lead to

elevated $N:P_{biomass}$ at low $N:P_{resources}$. Hall et al. (2005) manipulated the $N:P_{resources}$ in mesocosms and showed non-homeostasis in phytoplankton $N:P_{biomass}$. However, the phytoplankton assemblage became more homeostatic in $N:P_{biomass}$ when the total supply of N and P was reduced or grazers and predators were present in the mesocosms.

In addition to tradeoffs related to resource acquisition and allocation, assemblages are subject to grazing losses. Grazing may indirectly affect the stoichiometry of producers through nutrient regeneration (Frost et al. 2002; Hillebrand and Kahlert 2001; Sterner 1990). Susceptibility to grazing is determined by conspicuousness, defenses, and palatability of the prey. Tradeoffs between competitive ability and susceptibility to grazing are tied to nutrient acquisition and allocation (Branco et al. 2010; Sunda and Hardison 2010). Branco et al. (2010) identified a tradeoff between phytoplankton species with high nutrient affinity and species that are comparatively poor competitors but are resistant to grazing by zooplankton. Such a tradeoff allows for persistence of poor nutrient competitors and selective grazing may affect the abundance of species within assemblages. Multiple studies have demonstrated zooplankton preference for algae with high nutrient content (Cowles et al. 1988; Price 1988; Schatz and McCauley 2007). If biomass nutrient content is determined by the stoichiometric strategy, producer assemblages subject to strong grazing pressure should be dominated by non-homeostatic species.

Stoichiometric Strategies and Variable Resource Environments. Resource concentrations and ratios are variable across space and time. This means that competitive ability under steady-state conditions may not indicate the outcome of competition in fluctuating environments (Grover 1989; Sommer 1984; Sommer 1985). Sommer (1984) demonstrated that variable nutrient supply rates (i.e. pulsed supply) enabled persistence of velocity-adapted species. This finding illustrates how r-selected (or homeostatic) species could persist within assemblages despite their susceptibility to exclusion through nutrient limitation. Hood and Sterner (2010) characterized homeostatic zooplankton species as ‘growth integrators’ that capitalize on periods of abundant resources and non-homeostatic species as ‘resource integrators’ that utilize flexible stoichiometry to buffer changes in resource availability and quality. The resource integrators have an advantage

in environments where the resource ratio is variable in spatial or temporal patches. Their classification parallels the generalized strategies described here, but also highlights the circumstances under which homeostasis may be favored over non-homeostasis.

Conclusions

Stoichiometric regulation and competitive ability are coupled by their dependence on a common set of physiological parameters. This constraint leads to a tradeoff between homeostasis and competitive ability within assemblages of species. Dynamic $C:N:P_{biomass}$ regulation in assemblages has implications for understanding the stoichiometry of nutrient recycling. In general, overall non-homeostasis in assemblages will diminish the stoichiometric imbalance between biomass composition and resource availability. Specifically, aggregate non-homeostasis in the assemblage serves to decouple the stoichiometry of nutrient availability and that of nutrient regeneration (Elser and Urabe 1999). By assuming strict homeostasis or a universal degree of homeostasis for assemblages (Tambi et al. 2009; Tanaka et al. 2009) we overlook the effect of species shifts and non-homeostasis within assemblages. For example, assuming strong $C:P_{biomass}$ homeostasis for an assemblage of consumers would lead to an overestimation of regeneration of C relative to P when the $C:P_{resources}$ is low. Similarly, assuming non-homeostasis in $N:P_{biomass}$ would result in an underestimation of regeneration of N relative to P when the $N:P_{resources}$ is low. Predicting the stoichiometric behavior of an assemblage from the physiology of each of the component species is a daunting task, even in well-studied groups such as zooplankton and phytoplankton. However, the continuum of stoichiometric strategies within a functional group effectively describes the patterns of regulation for all of the component species, but requires far less parameterization.

Figures and Tables

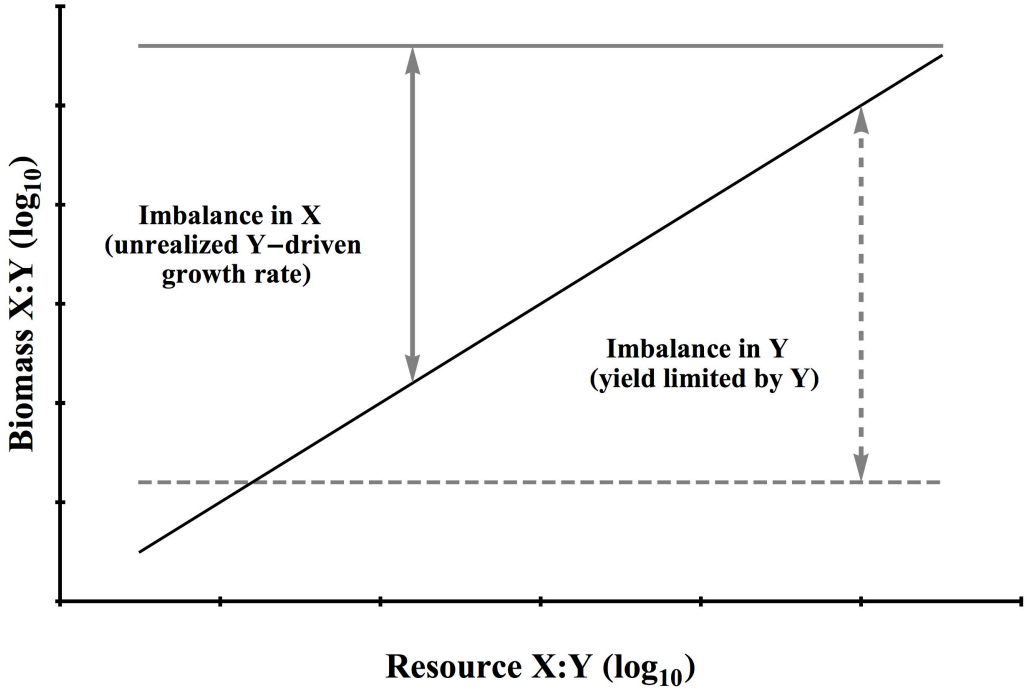

Figure 1-1. Schematic plot of biomass stoichiometry as a function of resource stoichiometry.

The solid black line represents the 1:1 relationship between $X:Y_{biomass}$ and $X:Y_{resource}$. The solid gray line represents strict homeostasis at a high $X:Y_{biomass}$ and the dashed gray line represents strict homeostasis at a low $X:Y_{biomass}$.

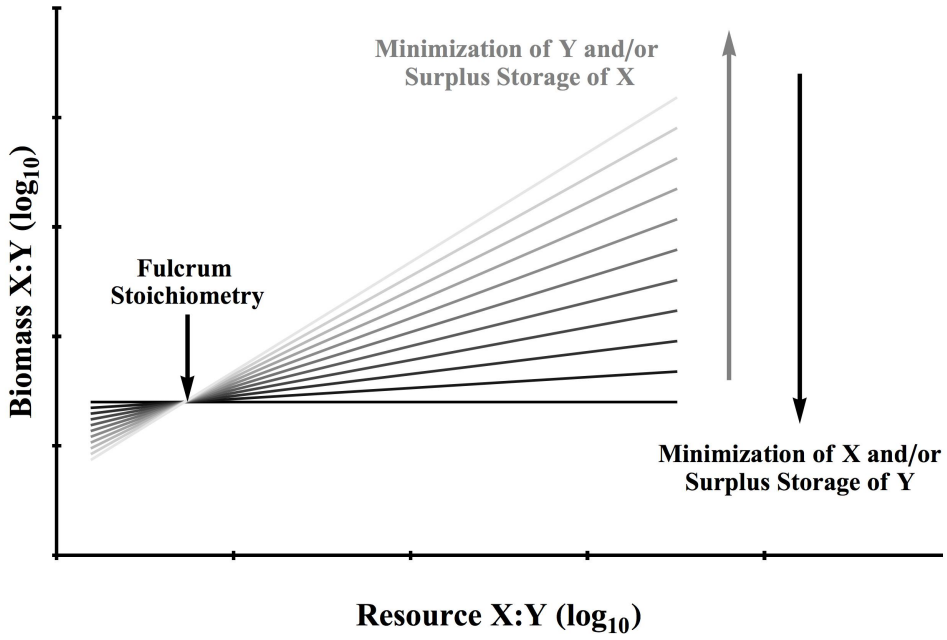

Figure 1-2. Schematic plot of a gradient of stoichiometric regulation.

Lines represent stoichiometric strategies ranging from strict homeostasis at intermediate X:Y (dark gray lines) and non-homeostasis (light gray line).

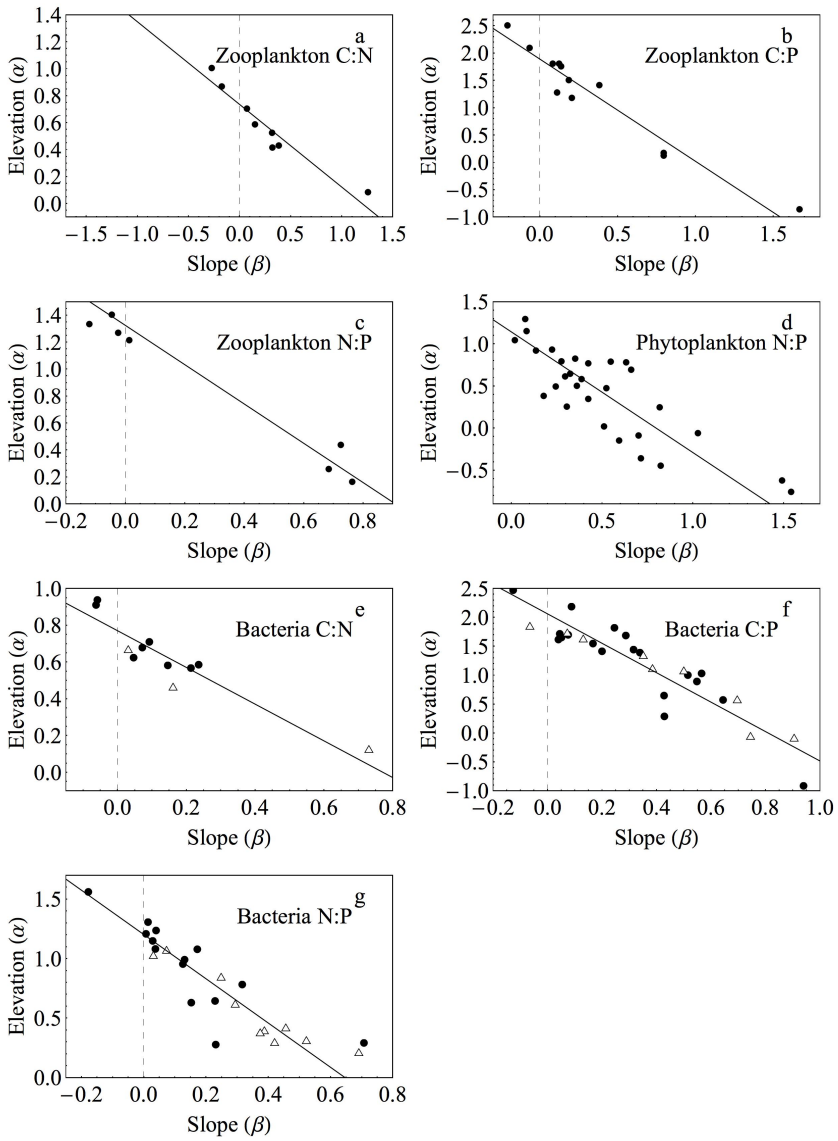

Figure 1-3. Parameter plots of the elevation versus slope for biomass-resource regressions.

Separate plots are for zooplankton C:N (a), C:P (b), and N:P (c); phytoplankton N:P (d); bacteria C:N (e), bacteria C:P (f), and bacteria N:P (g). Solid lines represent the standardized major axis regression for each dataset. Dashed lines represent the slope of zero (strict homeostasis). In panels e-g, populations of bacteria are denoted by solid circles and assemblages are represented open triangles. Regression parameters for each dataset are in Table 1.

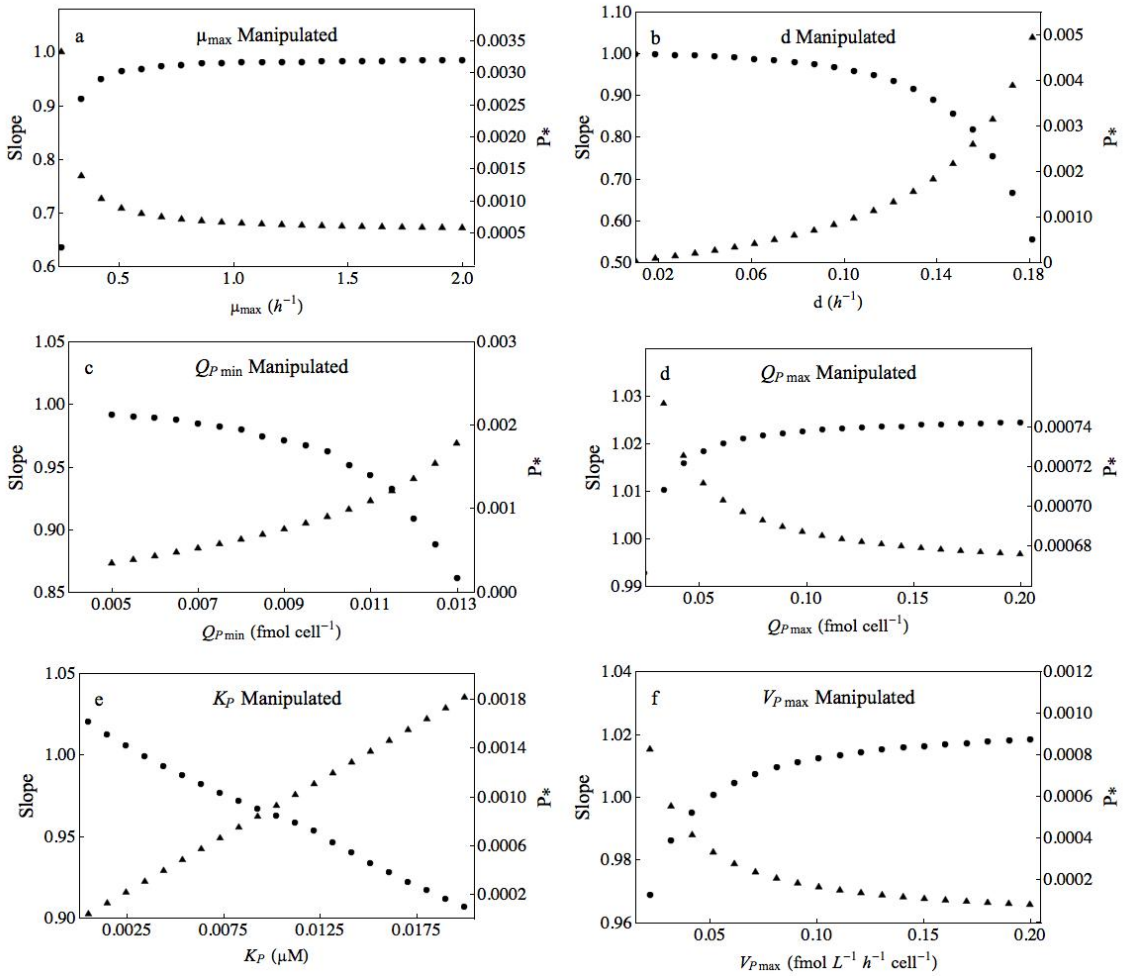

Figure 1-4. Equilibrium solutions for the consumer-resource model.

Separate panels show the results of manipulation of μ_{max} (a), dilution rate (b), $Q_{P\,min}$ (c), $Q_{P\,max}$ (d), K_P (e), and $V_{P\,max}$ (f). Triangles denote P* (indicator of competitive ability for P, see text) and circles denote the strength of C:P homeostasis (slope). As P* increases the strength of homeostasis increases and when P* decreases the strength of homeostasis decreases. Values for all other parameters were fixed and given in Appendix C.

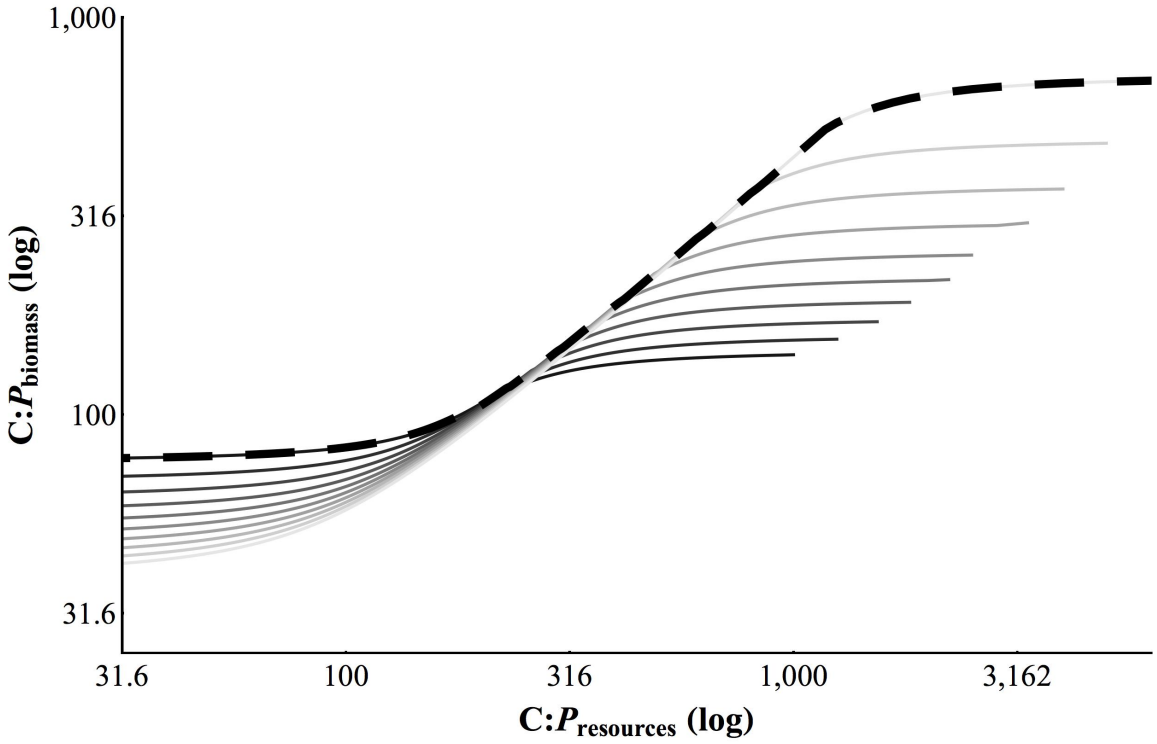

Figure 1-5. An example of tradeoffs in an assemblage leading to non-homeostasis of the assemblage.

The single-species data are represented by a gradient from the superior P competitor (light grey line) to the superior C competitor (dark grey line). The dashed black line represents the co-culture assemblage biomass. The fulcrum stoichiometry occurs at $C:P_{resources}$ of approximately 250:1. See text for physiological parameters.

Table 1-1. Regression parameters for stoichiometric regulation in zooplankton, phytoplankton, and bacteria.

The fulcrum resource ratio is the ratio in resources at the coalescence point for all of the individual regressions. The biomass ratio at the fulcrum resource ratio is equal to the biomass ratio at perfect homeostasis.

Taxa	Ratio	N (data sets)	N (species or assemblages)	Elevation Equation (R^2)	Biomass ratio at fulcrum (95% confidence interval)	Fulcrum resource ratio (95% confidence interval)
Zooplankton	C:N	8	7	0.74-0.61*Slope (0.92)	5.43 (4.46, 6.62)	4.10 (2.89, 6.54)
Zooplankton	C:P	12	6	1.89-1.87*Slope (0.93)	77.61 (48.84, 123.33)	74.21 (36.30, 174.94)
Zooplankton	N:P	8	7	1.32-1.46*Slope (0.93)	21.08 (14.55, 30.54)	28.67 (13.42, 76.44)
Phytoplankton	N:P	29	19	1.14-1.43*Slope (0.69)	13.85 (8.75, 21.91)	27.08 (14.16, 60.67)
Bacteria	C:N	13	10	0.77-1.00*Slope (0.86)	5.89 (5.15, 6.74)	9.97 (6.07, 18.78)
Bacteria	C:P	36	27	2.06-2.55*Slope (0.87)	114.83 (82.69, 159.47)	352.17 (176.81, 768.85)
Bacteria	N:P	28	20	1.20-1.86*Slope (0.83)	15.94 (12.50, 20.31)	72.60 (37.98, 155.75)

Chapter 2: Phosphorus Stoichiometry of Bacterial Assemblages – Do Shifts in Composition Mediate Homeostasis?

Summary

Several studies have noted a disparity between the stoichiometric regulation of bacterial assemblages and populations. Many bacterial populations of a single strain exhibit less flexibility in their biomass carbon (C) to phosphorus (P) ratios (C:P) than assemblages, which are often non-homeostatic. Assemblages could be inherently non-homeostatic as the result of simultaneous changes in relative abundance and stoichiometric flexibility of some strains. The experiments presented in this chapter are a test of the hypothesis that non-homeostasis commonly observed in assemblages is the result of shifts in assemblage composition. I cultured six assemblages of heterotrophic bacteria from four lakes in chemostats with varying C:P supply ratios and measured their biomass C:P ratios. As expected, the assemblages exhibited non-homeostasis when cultured at varying C:P supply ratios. There was no effect of lake trophic state on the degree of homeostasis, which suggests that the non-homeostatic strategy was present in all of the assemblages. Using the chemostat cultures as an assemblage composition filter, I subsequently cultured the high-P and low-P selected fractions at varying C:P supply ratios and found that all of the low-P selected fractions were less homeostatic than the high-P selected fractions. In contrast, the high-P selected fractions were homeostatic in three of the lake assemblages, demonstrating that a range of stoichiometric regulation is present within a single assemblage and that stoichiometric homeostasis can be selected at low supply ratios. The divergent stoichiometry was coupled with changes in the assemblage composition, which highlights the role of ecological selection in stoichiometric homeostasis.

Introduction

A fundamental feature of biology is homeostasis, or the ability of an organism to maintain a consistent physiological state despite variability in the environment. For example, birds and mammals exhibit homeostasis in body temperature whereas other vertebrates show weaker regulation of temperature. In the case of homeostasis of elements, many organisms are confronted with a fundamental imbalance between the chemical composition of their resources and their biomass stoichiometry. Plants and phytoplankton encounter stoichiometric imbalance when the availability of individual nutrients is variable across space and time (Hall et al. 2005; Yu et al. 2011) and consumers are subject to imbalance due to variability in the nutrient and energy content of their prey (Elser and Hassett 1994; Hood and Sterner 2010). In response to nutrient imbalance, many primary producers exhibit weak homeostasis and alter their biomass chemistry to reduce their nutrient demands (Klausmeier et al. 2004b; Rhee 1973), whereas many heterotrophs exhibit homeostasis (Persson et al. 2010; Sterner and Elser 2002). The stoichiometry of single species has been examined for a diverse suite of organisms (Elser et al. 2003; Persson et al. 2010; Sterner and Elser 2002), but comparatively few studies have examined the response of whole assemblages to resource imbalance (Fanin et al. 2013; Makino and Cotner 2004; Tezuka 1990). Because resource availability influences both species abundance and biomass stoichiometry, the elemental composition of assemblages may respond to imbalance differently than populations of single species.

Heterotrophic bacteria are responsible for most of the remineralization of organic carbon (C) in aquatic ecosystems (Biddanda et al. 2001; Cotner and Biddanda 2002) and affect the availability of dissolved nitrogen (N) and phosphorus (P) (Danger et al. 2007; Kirchman 1994). As consumers of multiple independent resources (e.g. dissolved organic C and inorganic nutrients), heterotrophic bacteria are subject to elemental imbalance, particularly in unproductive ecosystems (Cotner and Biddanda 2002). The biomass C:N:P stoichiometry ($C:N:P_{biomass}$) and strength of homeostasis determine how bacteria respond to limitation by multiple nutrients and the rates at which they can assimilate or regenerate

these elements (Hall et al. 2011). Specifically, strongly homeostatic bacteria with low $C:P_{biomass}$ should regenerate inorganic P at low $C:P_{resources}$ and remineralize C at high $C:P_{resources}$. To date, there is no evidence of strains that exhibit strong homeostasis at high $C:P_{biomass}$ (Scott et al. 2012, chapter 1, chapter 3). In contrast, non-homeostatic bacteria can assimilate excess C and P, serving to mediate imbalance between biomass and resources.

Studies investigating the ecological stoichiometry of heterotrophic bacteria show an apparent discrepancy between the C:P homeostasis of single strains and that of assemblages. Several strains of heterotrophic bacteria from the class γ-Proteobacteria (*Escherichia coli*, *Pseudomonas sp.*, and *Vibrio sp.*) are homeostatic and have low $C:P_{biomass}$ (Bratbak 1985; Løvdal et al. 2008; Makino et al. 2003). In contrast to the viewpoint that bacteria are P-rich and strongly homeostatic, assemblages of bacteria from lakes adjust their $C:P_{biomass}$ ratios in response to resource imbalance and often have higher $C:P_{biomass}$ than single strains (Makino and Cotner 2004; Tezuka 1990). Recent work with bacterial strains isolated from lakes has shown that $C:P_{biomass}$ can be higher than previously assumed and that some strains are weakly homeostatic in their $C:P_{biomass}$ (Phillips et al. in preparation; Scott et al. 2012). Although stoichiometric regulation has been characterized for few assemblages, the available data suggest that assemblages could be inherently non-homeostatic (Danger et al. 2008; Fanin et al. 2013).

Makino et al. (2003) demonstrated strong C:P homeostasis in *E. coli* and hypothesized that if assemblages were composed of homeostatic strains with different $C:P_{biomass}$, resource-dependent shifts in the relative abundance of strains would lead to non-homeostasis in the assemblage. This hypothesis has been implicated in numerous studies demonstrating non-homeostasis of assemblages (Danger et al. 2008; Fanin et al. 2013), but previous studies have not attempted to quantify the impact of assemblage composition on assemblage stoichiometry. In assemblages where a gradient of homeostatic regulation is present, both physiological acclimation and resource-dependent changes in assemblage composition could affect the stoichiometry of assemblages. This dynamic seems probable since phosphorus availability causes shifts in microbial community composition (Allison and Martiny 2008; Haukka et al. 2006) and that isolates

from lakes exhibit a range of stoichiometric regulation (Phillips et al. in preparation; Scott et al. 2012).

In chapter 1, I show that when strains differ in both the absolute C:P ratio of their biomass and their strength of stoichiometric homeostasis, simple physiological tradeoffs can lead to flexible stoichiometric regulation of the assemblage. If the dominant strains at low $C:P_{resources}$ exhibit stronger homeostasis and lower $C:P_{biomass}$ than the strains that are dominant at high $C:P_{resources}$, the assemblage will exhibit non-homeostasis (chapter 1). This chapter is an experimental test of my hypothesis that within a single assemblage of bacteria, the strains that are dominant at high P availability are more homeostatic than the strains that are dominant at low P availability. I predicted that a tradeoff between phosphorus homeostasis and competitive ability for phosphorus should be evident in bacterial assemblages when enrichment cultures are performed at high and low $C:P_{resources}$. I sought to answer three questions in this chapter: 1) Does the strength of homeostasis in an assemblage depend upon ecosystem productivity? 2) Are homeostatic strains dominant under low resource supply ratios? And 3) Do shifts in assemblage composition explain non-homeostasis observed in assemblages? I addressed these questions using 'selection experiments' in which I enriched natural assemblages of bacteria at a range of $C:P_{resources}$ in continuous cultures, and subsequently characterized the degrees of homeostasis in the high- and low-P selected fractions. If multiple stoichiometric strategies are present within assemblages, and the strength of homeostasis is linked to competitive ability for C and P, then the high-P and low-P selected fractions should exhibit divergent strength of homeostasis. The experiments described in this chapter show that assemblages from different trophic environments contain bacteria with a range of stoichiometric regulation and that homeostasis can be dominant under high P availability.

Methods

Inoculum Assemblages. The four source lakes for this study spanned a gradient of productivity within Minnesota, USA (Table 2-1). Lake Superior is a large, deep, oligotrophic lake with low productivity (Biddanda et al. 2001) and very low

concentrations of dissolved and particulate phosphorus (Sterner 2011). Christmas Lake is a mesotrophic lake and Lake Owasso is a eutrophic lake (Biddanda et al. 2001; Stets and Cotner 2008) and both are located in southeastern Minnesota. Lake Leverson is a highly productive shallow lake in western Minnesota (Theissen et al. 2012). Samples of water were collected from the surface layer of the lakes and transported to the laboratory in sterilized acid-washed polyethylene bottles. Within 24 hours of collection, the samples were filtered through a sterilized Whatman GF/B filter (nominal retention size 1.0 μm) to exclude protist grazers and most phytoplankton. Samples from each lake were filtered through a 0.2 μm polycarbonate filter for measurements of total dissolved phosphorus and soluble reactive phosphorus (APHA 1995). Particulate C, N, and P in the bacterial-sized fraction were measured for samples collected on Whatman GF/F filters, using methods described below for cultures.

Growth Media. Basal Microbiological Medium was prepared following Tanner (2002) using 18.2 MΩ deionized water (Milli-Q Nanopure System). All glassware was soaked in 10% hydrochloric acid and rinsed with deionized water to remove trace contamination of phosphate. All chemical stocks were ACS grade or equivalent. Glucose was supplied at 23.88 mmoles-C L^{-1} as the sole source of carbon and energy and ammonium chloride was supplied at 18.69 mmoles-N L^{-1} to ensure nitrogen sufficiency. Additional minerals, vitamins, and trace metals were supplied at concentrations described in Tanner (2002). Phosphorus was added as potassium phosphate at four levels (three levels in Lake Owasso summer and fall), to create molar C:P ($C:P_{supply}$) from 100:1 (239 μmoles-P L^{-1}) to 3,162:1 (7.55 μmoles-P L^{-1}). The medium was buffered between pH 7.2 and 7.4 using 11 mmoles L^{-1} N-(tris(hydroxymethyl)methyl)-2-aminoethanesulfonic acid (Lake Owasso summer and fall) or 11 mmoles L^{-1} 3-(N-Morpholino)propanesulfonic acid (MOPS).

Chemostat Cultures. The bacterial-sized fraction of lake water for each experiment was used to inoculate triplicate batch cultures at each level of $C:P_{supply}$. Five milliliters of filtered lake water were added to 100 mL of medium and the cultures were incubated at 22-24ºC on a rotary shaker until turbid growth developed in all flasks (optical density at 600 nm > 0.05 cm^{-1}). Ten to twenty milliliters of each batch culture

were used to inoculate triplicate chemostats at each level of $C:P_{supply}$. Chemostats, medium reservoirs, and tubing were acid-soaked, rinsed with deionized water, and sterilized by autoclave prior to use. Polypropylene 100 mL chemostats were continually aerated and mixed with 0.2-µm filtered air. The chemostats were maintained in a dark incubator at the same temperature as the source lake (Table 2-1). For each lake, the chemostats were diluted at a uniform rate of 1 d^{-1} (0.218 d^{-1} for Lake Superior) for 9 complete turnovers prior to harvesting samples for analyses.

Chemostat Selection and Re-Inoculation. Following the initial assemblage chemostat cultures, samples were collected for biomass analyses, as described below. The assemblages grown at the highest $C:P_{supply}$ are referred to as low-P selected assemblages and the cultures grown at the lowest $C:P_{supply}$ are referred to as high-P selected assemblages. The bacterial abundance in the high- and low-P selected assemblages was determined as described below. To isolate the strains that were abundant at high or low P availability, samples from the high-P and low-P selected assemblages were diluted in sterile medium to approximately 100 cells. These bottlenecked assemblages became the inoculums for the second phase of batch cultures at each level of $C:P_{supply}$ (Figure 2-1). As in the first phase of the experiments, the batch cultures were used to inoculate triplicate chemostats at each level of $C:P_{supply}$. The second phase of chemostats was maintained as before and sampled after 9 complete turnovers.

Cellular Phosphorus, Carbon and Nitrogen Analyses. Triplicate samples from each culture were filtered onto acid-rinsed Whatman GF/F filters using low vacuum pressure (<100 mm Hg). The filtered samples were rinsed with deionized water and frozen at -20ºC until analysis. Filters were digested with 25 g L^{-1} potassium persulfate at 121ºC for 30 minutes (APHA 1995) to liberate organic phosphate. Following digestion, the phosphorus content was determined using the ascorbic acid molybdenum blue method using potassium phosphate as a standard. Filter blanks were included in each run of analyses and used to correct the phosphorus content of the samples. Triplicate samples from each chemostat were collected onto pre-combusted Whatman GF/F filters as described for phosphorus. The filters were frozen at -20ºC and then dried at 60ºC for 7 days prior to measuring the carbon and nitrogen content using a CHN analyzer (Perkin-

Elmer 2400CHN) with combustion at 925ºC. Acetanilide was used as the primary standard (Elemental Microanalysis Ltd.) and an internal zooplankton standard was used to assess complete recovery of organic C and N. Filter blanks were used to correct the carbon and nitrogen content for each run of filters.

Bacterial Abundance and Morphometry. Samples from each chemostat were preserved for microscopy with formaldehyde (final concentration 3.7%, w/v) and were stored at 4ºC until analysis. Samples were diluted in 188 mmoles L^{-1} sodium pyrophosphate (0.2 μm filtered) and sonicated to disperse clumps of cells (Velji and Albright 1993). Duplicate samples from each chemostat were stained with acridine orange (Sigma Aldrich), filtered onto black polycarbonate membrane filters (Millipore Nucleopore, 0.2 μm pore size), and mounted to slides for microscopy (Hobbie et al. 1977). Cell counts were performed manually at 1000x magnification using an Olympus BX40 epifluorescence microscope and the ocular grid. At least 10 fields and 300 cells were enumerated on each filter.

A digital camera (Spot 2, Diagnostic Instruments) was used to obtain photomicrographs of the prepared slides at 1000x magnification. Cell dimensions (length, width, planar area, and planar perimeter) were determined for at least 100 cells (50 cells in Lake Owasso summer and fall) in each chemostat using image analysis software (Image Pro Plus, Media Cybernetics). Cell shape was modeled as cylinders capped with two hemispheres (Hillebrand et al. 1999). Cell dimensions were determined using the planar area and perimeter, rather than the box length and width method, which overestimates width and underestimate length of curved cells (Appendix Figure D-1). The equations used for estimating cell length, width, surface area, and volume are given in Appendix D.

Bacterial Assemblage Composition. To examine shifts in assemblage composition as the result of the selection treatments, the chemostat cultures were analyzed by automated ribosomal intergenic spacer analysis (ARISA, Fisher and Triplett 1999). Samples of the chemostat assemblages from Lake Owasso (spring), Lake Superior, Lake Leverson, and Christmas Lake were preserved for fingerprinting by suspending the pelleted cultures (1 mL) in lysis buffer (5% sodium dodecyl sulfate in 120 mmoles L^{-1}

phosphate buffer, pH 8.0) and freezing at -20ºC (Ghosh and LaPara 2007). The samples were further lysed by three cycles of freezing (-20ºC) and thawing (22ºC) and digestion with proteinase K at 56ºC. The nucleic acids were isolated and purified using the DNeasy Blood and Tissue Kit (Qiagen). The intergenic region was amplified following Nelson et al. (2010) using the primers ITSf (labeled with HEX) and ITSreub (Cardinale et al. 2004), using GoTaq polymerase and buffer (Promega).

Sample fragment lengths were resolved by capillary electrophoresis using a 3730xl sequencer (Applied Biosystems) with the size standard Map Marker 1000 (Bioventures) at the University of Minnesota Genomics Center. Sizing was performed using the PeakScanner software version 1.0 (Applied Biosystems). The fragment peak areas were manually checked for each sample to ensure that the peak fluorescence was greater than the crossover fluorescence from the size standards. Fragment lengths below 156 and greater than 1000 base pairs were excluded prior to binning the fragment sizes from each experiment using the Interactive Binner source code for R statistical software (Ramette 2009). Peak sizes within ±1 base pairs were binned as a single peak and a manual check was performed for each experiment to ensure that the automated alignment was sufficient. Individual peaks representing at least 0.5% of the total peak area for a sample were used to perform non-metric multidimensional scaling (NMDS) using the package Vegan for R (Oksanen et al. 2011). Ordination was performed using the Bray-Curtis distance algorithm with two NMDS dimensions. Confidence ellipses (95%) were computed with the Vegan package. Due to low sample fluorescence, the following single replicate chemostats were excluded from analysis: Christmas Lake initial assemblage 316:1, Christmas Lake low-P selected assemblage 100:1, Lake Leverson high-P selected 1,000:1, Lake Owasso spring initial assemblage 100:1, Lake Superior high-P selected assemblage 316:1, and two replicates from Lake Superior low-P selected 3,162:1.

Statistical Analyses. The mean cellular C, N, and P measurements were used to calculate a single estimate of the molar $C:N:P_{biomass}$ for each chemostat culture. Samples that were below detection limits were excluded from figures and statistical analyses. Two samples from the Lake Superior assemblage cultures were below detection for P (low-P selected, $C:P_{supply}$ = 3,162:1) and one sample from Lake Owasso (fall) was below

detection for N (low-P selected, $C:P_{supply}$ = 316:1). Mean stoichiometry (C:P, N:P, and C:N) and cellular P content from the initial chemostats were compared within and among lake assemblages using analysis of variance (ANOVA) with the lake assemblages as a fixed effect and $\log_{10}$ $C:P_{supply}$ as the quantitative treatment. The initial assemblage and selected assemblage chemostats were not compared using inferential statistics due to nested dependence of the replicates. The biomass stoichiometry data ($\log_{10}$ transformed) and cell abundance were analyzed using a three-way ANOVA with lake assemblages and selection treatment as fixed effects and $C:P_{supply}$ ($\log_{10}$ transformed) as the quantitative treatment. Where the three-way tests revealed a significant interaction with lake assemblages, separate two-way ANOVA tests were performed for each lake assemblage. Morphometry data (length : width and surface area : volume) were $\log_{10}$ transformed to improve normality and homogenize variances (Box and Cox 1964). Morphometry data from the initial assemblages were analyzed by two-way ANOVA with lake assemblages and $C:P_{supply}$ as fixed effects, and chemostat replicates as a random effect, nested in lake assemblages and $C:P_{supply}$ level. Morphometry data from the selected assemblages were analyzed by three-way ANOVA with lake assemblages, selection treatment, and $C:P_{supply}$ as fixed effects and chemostat replicate as a random effect nested in selection treatment and lake assemblages. The degree of stoichiometric flexibility (1/H') (Sterner and Elser 2002) for each set of chemostats was calculated as the slope of the linear regression of $\log_{10}$ $C:P_{biomass}$ versus $\log_{10}$ $C:P_{supply}$.

Results

Initial Assemblage Cultures

The lakes exhibited a wide range of dissolved phosphorus concentrations and plankton stoichiometry (Table 2-2). Christmas Lake and Lake Superior had low concentrations of dissolved P and relatively high $C:P_{biomass}$ and $N:P_{biomass}$ in the bacterial-sized fraction. Lake Leverson had a high concentration of dissolved P and low $C:P_{biomass}$ and $N:P_{biomass}$. Across all of the lake assemblages, cell abundance in the initial

assemblages decreased in response to decreasing P supply (ANOVA, $p < 0.0001$) and there was no significant difference among lake assemblages.

Biomass Stoichiometry. The initial assemblages exhibited non-homeostasis in $C:P_{biomass}$ and the ANOVA indicated significant effects of lake assemblages and $C:P_{supply}$ (both $p < 0.0001$), but no significant interaction between lake assemblages and $C:P_{supply}$ (Figure 2-2, Figure 2-3). The lack of an interaction between lake assemblages and $C:P_{supply}$ indicates that there was no significant difference in the strength of homeostasis among lake assemblages. Across all levels of $C:P_{supply}$, the initial assemblage culture from Lake Superior had lower $C:P_{biomass}$ than the other lake assemblages. The Christmas Lake assemblage showed the highest $C:P_{biomass}$ under P limitation and also the greatest range of $C:P_{biomass}$, increasing from a mean of 82:1 at $C:P_{supply}$ =100:1 to a mean of 849:1 at $C:P_{supply}$ =3,162:1 (Figure 2-2). In the Lake Leverson assemblage, $C:P_{biomass}$ increased rapidly between $C:P_{supply}$ of 100:1 and 316:1, but showed little change from $C:P_{supply}$ of 316:1 to 3,162:1. The slope of stoichiometric flexibility (chapter 1) ranged from 0.338 to 0.697 (Table 2-3), with Lake Superior and Christmas Lake having the highest slope and Lake Leverson the lowest.

The $N:P_{biomass}$ of the initial assemblages behaved similarly to the $C:P_{biomass}$, exhibiting non-homeostasis (Figure 2-4), with significant effects of lake assemblages, $C:P_{supply}$, and an interaction between lake assemblages and $C:P_{supply}$ (all $p < 0.01$). The initial assemblages from Lake Leverson and Lake Owasso (summer) were more homeostatic in $N:P_{biomass}$ than the other assemblages. The assemblage from Christmas Lake showed the greatest range in $N:P_{biomass}$, increasing from a mean of 18:1 at $C:P_{supply}$ = 100:1 to a mean of 119:1 at $C:P_{supply}$ = 3,162:1 (Figure 2-4). The initial assemblage $C:N_{biomass}$ was less variable than $C:P_{biomass}$ and $N:P_{biomass}$, but increased with increasing $C:P_{supply}$ in all lake assemblages ($p < 0.0001$) and showed no interaction between lake assemblages and $C:P_{supply}$. $C:N_{biomass}$ differed significantly among the initial assemblages ($p < 0.0001$) and was lower in Lake Superior across all levels of $C:P_{supply}$ (3.0 - 10.5:1) compared to the other lakes (3.5 - 13.9:1).

Biomass Elemental Content. Cellular phosphorus quotas of the initial assemblages showed significant effects of lake assemblages, $C:P_{supply}$ and an interaction between lake

assemblages and $C:P_{supply}$ (all $p < 0.003$). In all lake assemblages except Lake Owasso (summer), the increase in $C:P_{biomass}$ under P limitation was accompanied by a decrease in P quota (Figure 2-5), and this was significant in Christmas Lake, Lake Leverson, and Lake Owasso (fall) (all $p < 0.05$). Among all of the initial assemblages, P quotas ranged from 0.02 to 1.23 fmoles $cell^{-1}$. In all assemblages except Lake Leverson, mean C quotas of the initial assemblages increased in response to increased $C:P_{supply}$, but this increase was significant only in Lake Owasso (spring) and Christmas Lake. Similar to the variability in cellular P, cellular C quotas ranged from 2.17 to 112 fmoles $cell^{-1}$.

Cell Morphometry. The initial assemblages showed substantial variability in cell morphometry (Figure 2-6, Figure 2-7). Cell length: width (L:W) in the initial assemblages increased with $C:P_{supply}$ and varied among lake assemblages (ANOVA all $p < 0.0001$). Cell L:W increased significantly in response to increasing $C:P_{supply}$ in Christmas Lake, Lake Leverson, and Lake Owasso (fall) (one-way ANOVA, all $p < 0.05$). Cell surface area: volume (SA:V) decreased in response to increased $C:P_{supply}$ ($p < 0.02$) and showed significant differences among lake assemblages ($p < 0.0001$).

High-P and Low-P Selected Assemblages

Biomass Stoichiometry. In the selected assemblages, the ANOVA for $C:P_{biomass}$ indicated significant effects of $C:P_{supply}$ (ANOVA, $p < 0.0001$), an interaction between selection treatment and lake assemblages ($p < 0.02$), an interaction between selection treatment and $C:P_{supply}$ ($p < 0.0001$), and a three-way interaction ($p < 0.003$). Three of the lake assemblages (Lake Owasso Summer, Lake Owasso Fall, and Christmas Lake) showed a significant difference in $C:P_{biomass}$ flexibility between the low-P and high-P selected fractions of the assemblage (Figure 2-3, Table 2-3). In these lake assemblages, the high-P selected fractions of the assemblage were more homeostatic and had a smaller range of $C:P_{biomass}$ than the low-P selected fraction. The homeostatic high-P selected assemblages from Lake Owasso (summer and fall) and Christmas Lake had mean $C:P_{biomass}$ of 138, 187, and 211:1, respectively. In the same lake assemblages, mean $C:P_{biomass}$ of the non-homeostatic, low-P selected fractions ranged from 73 to 1,823:1. The low-P selected assemblage from Christmas Lake showed the greatest range of mean $C:P_{biomass}$, ranging from 75:1 to 1,823:1 between $C:P_{supply}$ = 100:1 and 3,162:1. In the lake

assemblages without a significant interaction between $C:P_{supply}$ and selection treatment (Lake Owasso spring, Lake Superior, and Lake Leverson), both the high- and low-P selected fractions were non-homeostatic in $C:P_{biomass}$ and resembled the response of the initial assemblages (Figure 2-2).

In the selected assemblages, the response of $N:P_{biomass}$ to $C:P_{supply}$ was similar to the response described for $C:P_{biomass}$. Assemblage $N:P_{biomass}$ increased with increasing $C:P_{supply}$ (ANOVA, $p < 0.0001$) and showed significant interactions between lake assemblages and selection treatment ($p < 0.02$), selection treatment and $C:P_{supply}$ ($p < 0.0004$), and the three-way interaction ($p < 0.0001$). In three of the lake assemblages (Christmas Lake, Lake Owasso summer, and Lake Superior), $N:P_{biomass}$ exhibited a significant interaction between selection treatment and $C:P_{supply}$ (all $p < 0.05$). The low-P selected assemblage from Christmas Lake showed the greatest range in $N:P_{biomass}$, increasing from 16:1 to 205:1 between $C:P_{supply}$ = 100:1 and 3,162:1. Biomass C:N was less variable than $C:P_{biomass}$ and $N:P_{biomass}$, but increased significantly with $C:P_{supply}$ ($p < 0.0001$) and showed significant effects of lake assemblages ($p < 0.002$) and an interaction between selection treatment and $C:P_{supply}$ ($p < 0.03$).

Biomass Elemental Content. Across the second phase chemostats, increasing $C:P_{supply}$ led to a decrease in cellular phosphorus quotas (Figure 2-5). Phosphorus quotas showed significant effects of lake assemblages (ANOVA, $p < 0.0003$), $C:P_{supply}$ ($p < 0.0001$), and the three-way interaction ($p < 0.02$). Phosphorus quotas ranged from 0.017 to 0.366 fmoles $cell^{-1}$ and were most variable in the high-P selected assemblage from Lake Superior. Mean carbon quotas increased in response to increasing $C:P_{supply}$ in all of the low-P selected assemblages, although the increase was significant only in Christmas Lake, Lake Leverson, and Lake Owasso (fall) (ANOVA, $p < 0.05$). In the Christmas Lake assemblage, the mean carbon quota of the low-P selected fraction increased from 14 to 116 fmoles $cell^{-1}$ between $C:P_{supply}$ of 100:1 and 3,162:1. In contrast, the mean carbon quota of the high-P selected fraction for Christmas Lake ranged from 19 to 29 fmoles $cell^{-1}$. Lake Owasso (summer) also exhibited increased C quotas in the low-P selected fraction, but the range was modest (13-23 fmoles $cell^{-1}$).

Cell Morphometry. In all of the selected assemblages, cell L:W was significantly affected by $C:P_{supply}$ ($p < 0.0001$). In all of the selected assemblages except for Lake Superior, there was a significant interaction between selection treatment and $C:P_{supply}$ ($p < 0.0001$). All of the low-P selected assemblages except Lake Owasso (summer) exhibited a significant increase in cell L:W under P limitation ($p < 0.0001$). Three of the high-P selected assemblages increased cell L:W under P limitation (Lake Leverson, Lake Owasso summer, and Lake Superior, $p < 0.01$). Cell SA:V showed a significant effect of lake assemblage ($p < 0.001$), $C:P_{supply}$ ($p < 0.0001$), and an interaction between selection treatment and $C:P_{supply}$ within each lake assemblage ($p < 0.0001$). In all lake assemblages, there was a significant interaction between selection treatment and $C:P_{supply}$ for SA:V (all $p < 0.05$). Cell SA:V decreased in response to increasing $C:P_{supply}$ in all of the selected fractions ($p < 0.05$), except the high-P selected fraction from Christmas Lake, the high-P selected fraction from Lake Owasso (summer), and the low-P selected fraction from Lake Owasso (spring) which exhibited a significant increase in SA:V under P limitation.

Assemblage Composition. The assemblages exhibited divergent ARISA composition both within and among selection and $C:P_{supply}$ treatments (Figure 2-8). In three of the experiments (Lake Owasso spring, Lake Superior, and Lake Leverson), there was substantial overlap in assemblage composition among the initial, low-P selected and high-P selected treatments. In the Christmas Lake experiment, the initial, low-P selected, and high-P selected assemblages exhibited divergent composition (Figure 2-8). The confidence ellipses for the high-P and low-P selected assemblages in Christmas Lake were distinct.

Discussion

The selection experiments described in this chapter were designed to test my hypothesis that homeostatic strains of bacteria can be dominant under conditions where P is abundant relative to C. I used the data from these experiments to describe three aspects of the stoichiometry of assemblages. The first conclusion from this work is that although non-homeostasis was observed in each of the initial assemblages of bacteria, high P availability selects for homeostatic strains within these assemblages. The second

conclusion is that assemblages of bacteria cultured from different trophic environments have similar, though not identical, stoichiometric responses to imbalance in $C:P_{supply}$. The third conclusion from this work is that the stoichiometric behavior of assemblages is explained by shifts in assemblage composition, driven by resource availability. These conclusions are interrelated and provide insights to the stoichiometry of bacterial assemblages.

Selection for Stoichiometric Strategies. Three of the lake assemblages (Lake Owasso summer, fall, and Christmas Lake) exhibited divergent stoichiometric regulation in $C:P_{biomass}$ under high-P and low-P selection. In these assemblages, the high-P treatment effectively selected for more homeostatic strains. In contrast, the low-P selected fractions exhibited similar stoichiometric regulation, P quotas, and morphology to the initial assemblages. In the Christmas Lake experiment, the divergence in stoichiometric regulation between the selection treatments was matched by shifts in assemblage composition. This result supports my hypothesis that homeostatic strains can be dominant under high P availability. Several physiological tradeoffs could explain the apparent competitive advantage of strong homeostasis at low $C:P_{supply}$ (chapter 1). Although the high-P and low-P selected fractions exhibited divergent stoichiometric strategies, the two fractions had similar phosphorus quotas under P limitation (Figure 2-5). This suggests that aspects of P competition other than a low P quota might be relevant to the superior competitive ability of non-homeostatic strains under low P supply. Other relevant aspects of P physiology such as P affinity, acquisition, and P use efficiency may also be important. In Christmas Lake and Lake Owasso (summer) the low-P selected fractions had higher C quotas under P limitation than the high-P selected fractions, suggesting that C allocation and growth efficiency could be relevant physiological tradeoffs in homeostasis.

In three of the lake assemblages, the strength of homeostasis was not significantly different between the high-P and low-P selected fractions of the assemblages. Both of the selected fractions were non-homeostatic and resembled the initial assemblages, which shows that non-homeostatic strains were dominant in both the high- and low-P treatments and that high P availability did not select for more homeostatic strains or any particular

subset of strains. The ARISA results support this conclusion in that there were not substantial shifts in assemblage composition that were related to $C:P_{supply}$. This could be the result of weak selective pressure at low $C:P_{supply}$, insufficient time for competitive exclusion, or a low relative abundance of homeostatic strains in the initial cultured assemblage. Additionally, the uniformly low dilution rate used within each study could have enabled non-homeostatic strains to remain dominant despite lower maximum growth rates than homeostatic competitors.

Strength of Homeostasis in Assemblages from Different Environments. The initial assemblage cultures from each lake showed similar degrees of non-homeostasis, suggesting that local assemblage composition does not determine the stoichiometric response of the culturable assemblage. This result is surprising given the range of P availability and primary productivity among the lakes (Biddanda et al. 2001; Theissen et al. 2012). The lack of a significant difference in slopes among the initial assemblages, together with the fact that some strains isolated from lakes exhibit non-homeostasis (Scott et al. 2012) (chapter 3), suggests that the disparity between the stoichiometry of populations and assemblages could be attributable to the prevalence of non-homeostatic strains in natural assemblages. Microbes in plankton environments are likely to experience temporal variability in both C and P availability and imbalance, which should select for plasticity in biomass composition.

This study compared stoichiometric regulation in assemblages of bacteria from several environments using uniform culture conditions. Previous studies investigating the C:P stoichiometry of bacterial assemblages (Bratbak 1985; Goldman et al. 1987; Jürgens and Güde 1990; Makino and Cotner 2004; Tezuka 1990) have found widely varying degrees of non-homeostasis in $C:P_{biomass}$, with slopes from nearly 0 to 0.9 (reviewed in chapter 1). Unfortunately, these studies were not performed with the same experimental design, and some of this variation is attributable to differences in culture conditions. For example, Makino and Cotner (2004) cultured an assemblage from Lake Owasso at multiple chemostat dilution rates and found that a three-fold increase in dilution rate decreased the slope of $\log_{10} C:P_{biomass}$ versus $\log_{10} C:P_{resources}$ from 0.39 to 0.07. The effect of dilution rate on homeostasis is also observed in populations (Chrzanowski and

Kyle 1996; Makino et al. 2003), where increasing the dilution rate relative to the maximum growth rate of a microbe leads to stronger homeostasis in $C:P_{biomass}$ and increased P quotas. The uniform culture conditions and dilution rate used for the present study allowed for comparison of the strength of stoichiometric regulation among assemblages. The responses of the initial and selected assemblages ranged from strong homeostasis (slope = 0.014) to non-homeostasis (slope = 0.889, Table 2-3). Since the dilution rate was uniform (excluding Lake Superior), this shows that assemblage composition can be equally as important as the dilution rate if the strength of selection is sufficient.

The experiments presented in this chapter show no evidence that assemblage homeostasis is dependent upon ecosystem trophic state. Also, there was substantial variability in the strength of homeostasis within the assemblages cultured from a single lake (e.g. Christmas Lake experiments). Similarly, the inoculum from a moderately low-P environment (Christmas Lake) was less homeostatic and exhibited a greater range in $C:N:P_{biomass}$ than the assemblage from an environment where P is extremely scarce (Lake Superior). Factors other than the trophic state of the source lake likely affect the stoichiometric flexibility of the cultured assemblage. For instance, the rate of primary productivity and lability of dissolved substrates could shape the stoichiometric physiology of assemblages.

The Role of Assemblage Composition. The selection experiments described in this chapter illustrate how the stoichiometric behavior of bacterial assemblages is dependent upon assemblage composition. However, this effect is evident only under strong selective pressure. Specifically, there was no detectable difference in the strength of homeostasis in the initial assemblages, although the source environments differed substantially in terms of phosphorus availability and ecosystem productivity. This outcome is surprising and could indicate that the source environments represent weak selective pressure or that non-homeostatic strains are pervasive among the culturable strains in lakes, regardless of productivity. In contrast, the competitive environment of the chemostats was sufficient to alter the assemblage composition and select for homeostatic strains under high P availability in some lakes. Although these results

provide support for my hypothesis that homeostasis can be favorable under low resource imbalance, the incomplete selection in three of the experiments remains unresolved.

Morphological Change and Stoichiometry. In the initial and selected assemblages, cell morphology changed in response to $C:P_{supply}$. Under P limitation, cell L:W increased and SA:V changed little or decreased. This change in morphology is attributable to an increase in the length of cells without a substantial decrease in cell width. Although cell surface area increases as cells become elongated, these data show that the increase in surface area is outpaced by an increase in volume, often lowering SA:V ratios. Elongation in response to P limitation has been documented in multiple studies (Phillips et al. in preparation; Thingstad et al. 2005, chapter 3, chapter 4) and has been proposed as a strategy for cells to increase their surface area and thereby increase their P affinity (Thingstad et al. 2005). However increasing surface area of the cell in this manner requires a larger relative increase in volume, which leads to greater diffusion distances within the cytoplasm (Koch 1996), increased allocation to P-rich membrane and cell wall materials, and significant allocation of C to inclusion bodies (Thingstad et al. 2005). Although there is a clear morphological response to P limitation in assemblages, it is not apparent that this response is an adaptation to increase the uptake of P (chapter 3). Interestingly, cell elongation has been documented in response to limitation by nutrients other than phosphorus (Begg and Donachie 1978) and morphological responses can be dependent upon the specific nutrient limiting growth (Holmquist and Kjelleberg 1993).

Implications for Assemblage Stoichiometry. The experiments presented in this chapter show that assemblage P content and $C:N:P_{biomass}$ are flexible, in contrast to the common assumption that bacteria are homeostatic and rich in P. The non-homeostatic assemblages increased their $C:N:P_{biomass}$ in response to P limitation by decreasing their P quotas and simultaneously increasing their C and N quotas. Although the phosphorus quotas in the high-P and low-P selected fractions generally decreased under P limitation, these patterns showed only partial correspondence with changes observed in $C:P_{biomass}$ and $N:P_{biomass}$ (Figures 2-2, 2-3, and 2-4). This indicates that flexible C and N quotas are partially responsible for the plasticity observed in $C:P_{biomass}$ and $N:P_{biomass}$. The disparity between the stoichiometry of assemblages and populations was initially recognized in

bacterial assemblages, but the underlying processes should be relevant to assemblages at any trophic level. Tradeoffs in physiological parameters that couple competitive ability and stoichiometric regulation will lead to dynamic non-homeostasis of assemblages (chapter 1). Shifts in assemblage composition due to resource imbalance will cause assemblage biomass to exhibit homeostasis at low resource ratios and non-homeostasis under resource imbalance.

Figures and Tables

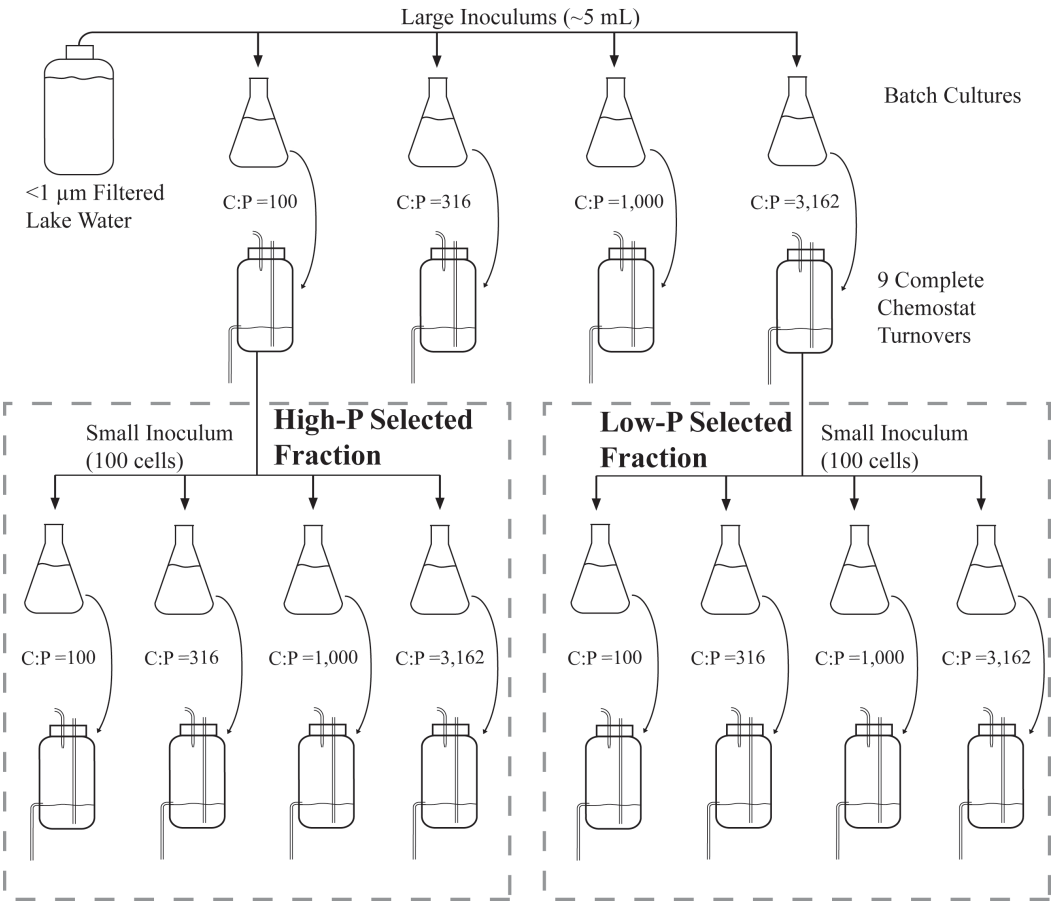

Figure 2-1. Schematic plot of selection experiments and chemostats.

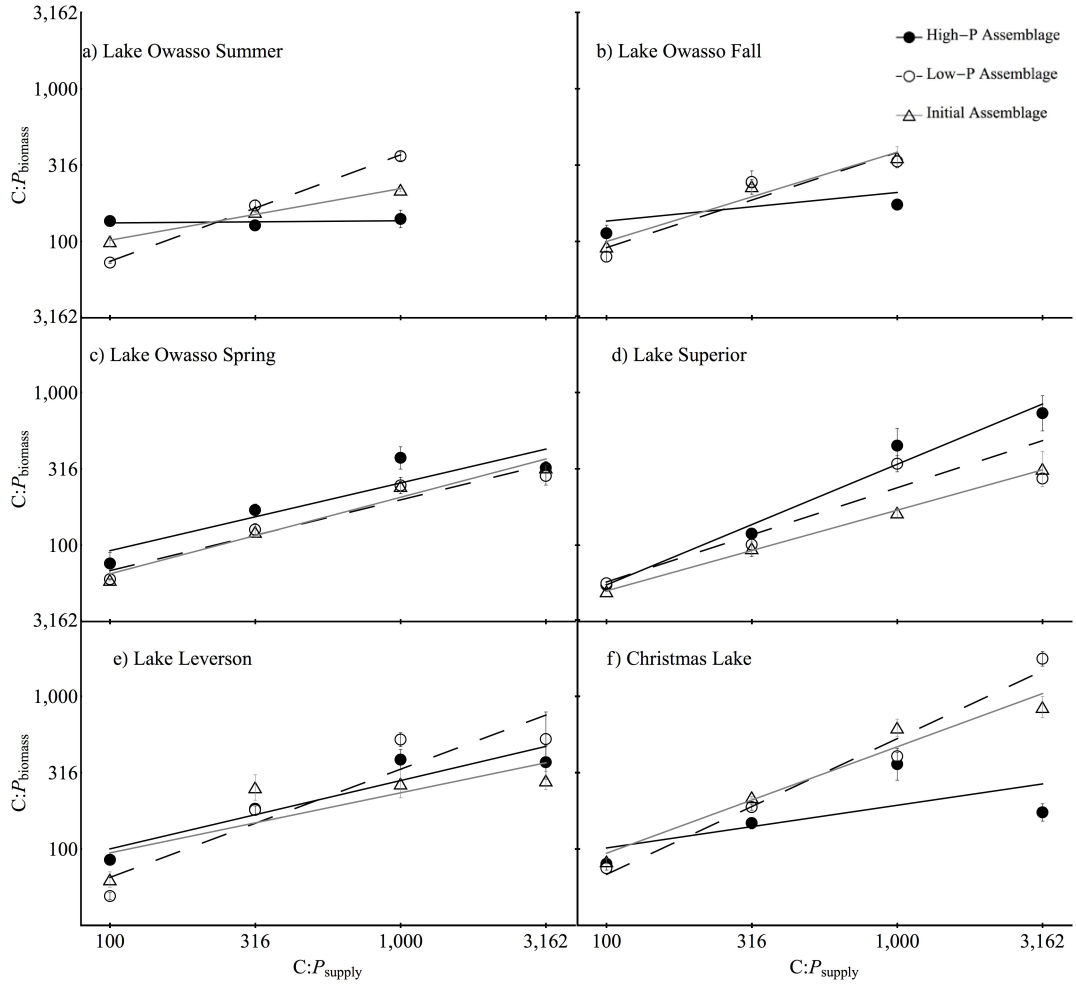

Figure 2-2. Assemblage C:P$_{biomass}$ ratios across C:P$_{supply}$ treatments.

Separate panels for a) Lake Owasso in summer, b) Lake Owasso in fall, c) Lake Owasso in spring, d) Lake Superior, e) Lake Leverson, and f) Christmas Lake. Error bars denote the standard error of the mean. Lines represent the linear regressions of $\log_{10}$ biomass ratio against $\log_{10}$ supply ratio. Both axes are log-scaled.

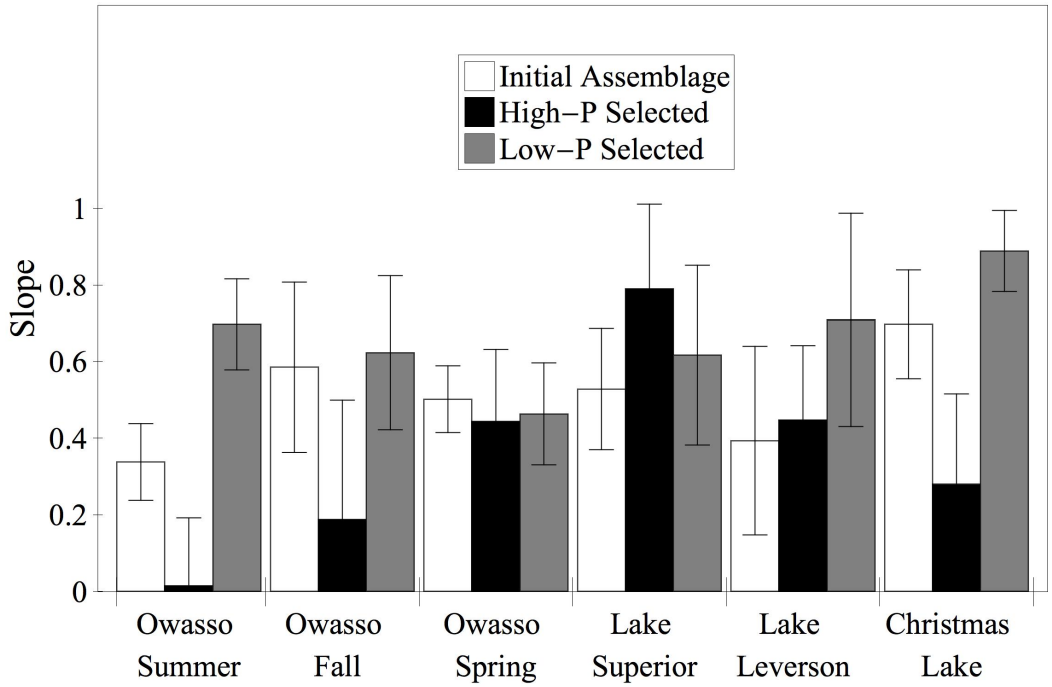

Figure 2-3. Slopes of log C:$P_{biomass}$ versus log C:$P_{resources}$ for selection experiments. Error bars represent the 90% confidence interval for the mean slope.

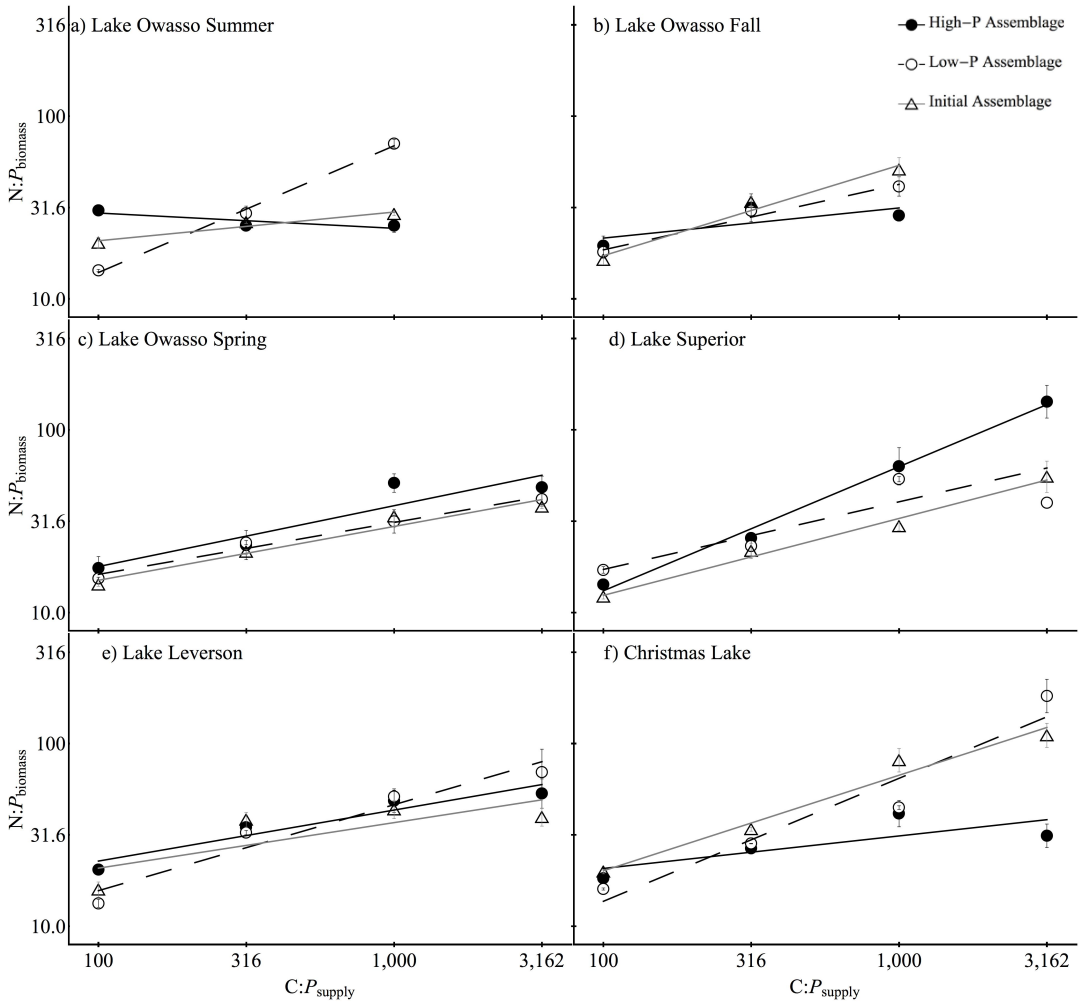

Figure 2-4. Assemblage N:P$_{biomass}$ ratios across C:P$_{supply}$ treatments.

Separate panels for a) Lake Owasso in summer, b) Lake Owasso in fall, c) Lake Owasso in spring, d) Lake Superior, e) Lake Leverson, and f) Christmas Lake. Error bars denote the standard error of the mean. Lines represent the linear regressions of $\log_{10}$ biomass ratio against $\log_{10}$ supply ratio. Both axes are log-scaled.

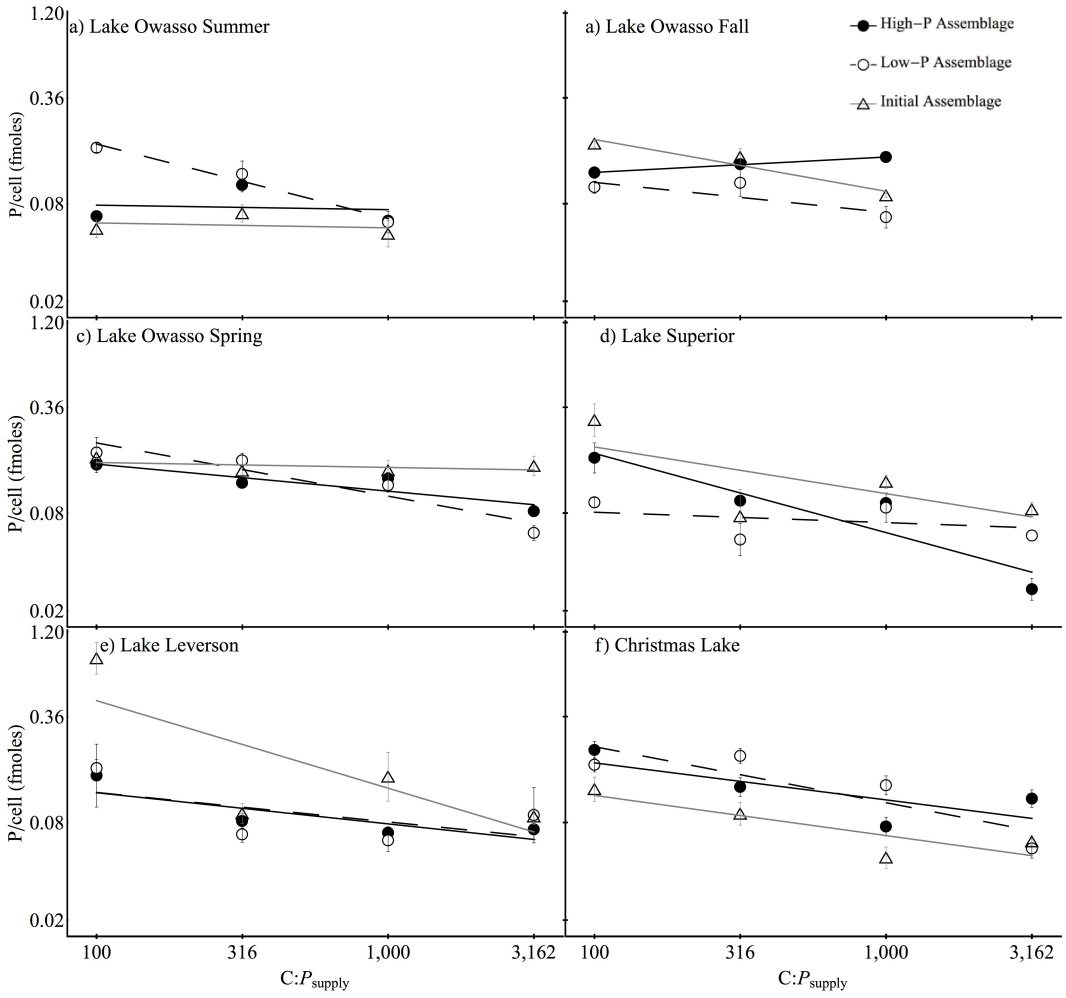

Figure 2-5. Cellular P content of assemblages across C:P_{supply} treatments.
Separate panels for a) Lake Owasso in summer, b) Lake Owasso in fall, c) Lake Owasso in spring, d) Lake Superior, e) Lake Leverson, and f) Christmas Lake. Error bars denote the standard error of the mean. Lines represent the linear regressions of $\log_{10}$ phosphorus quotas against $\log_{10}$ supply ratio. Both axes are log-scaled.

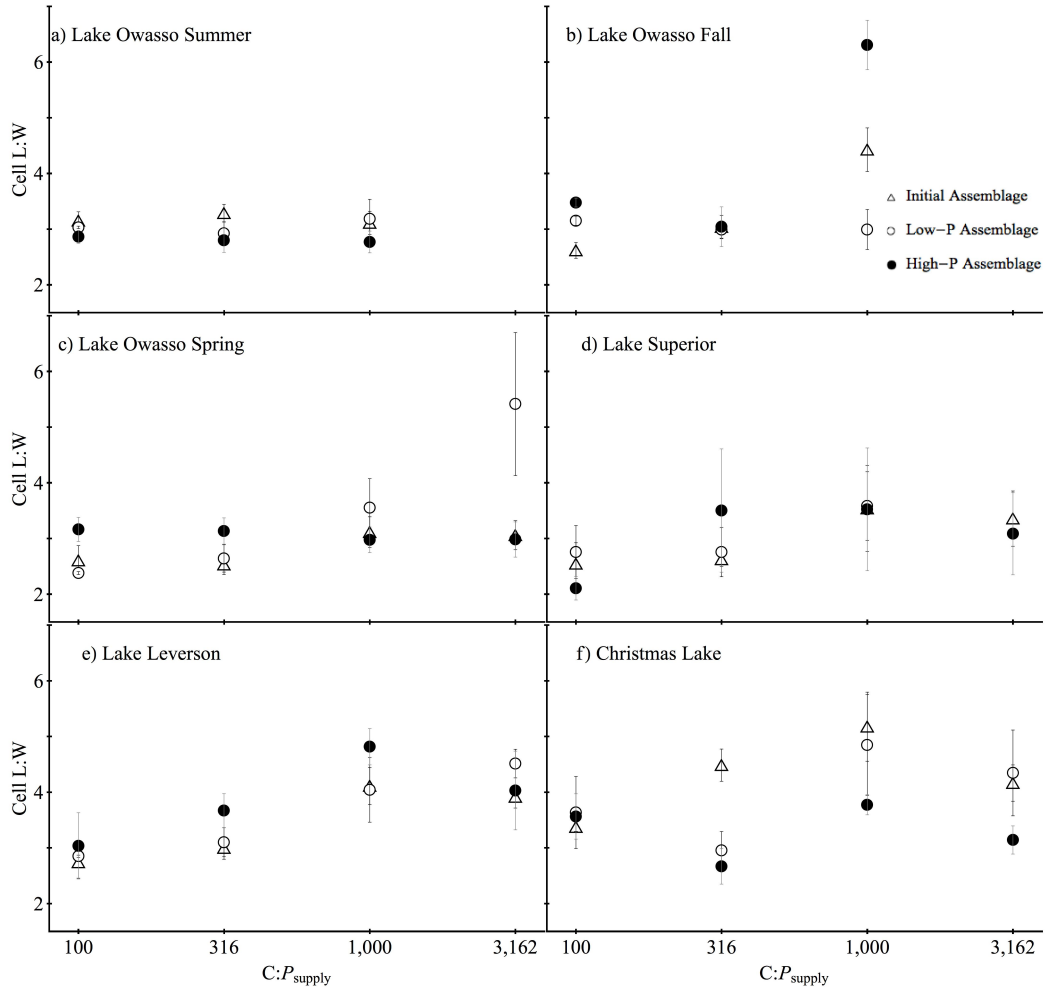

Figure 2-6. Assemblage length: width ratios across C:P$_{supply}$ treatments.

Separate panels for a) Lake Owasso in summer, b) Lake Owasso in fall, c) Lake Owasso in spring, d) Lake Superior, e) Lake Leverson, and f) Christmas Lake. Error bars denote the standard error of the mean.

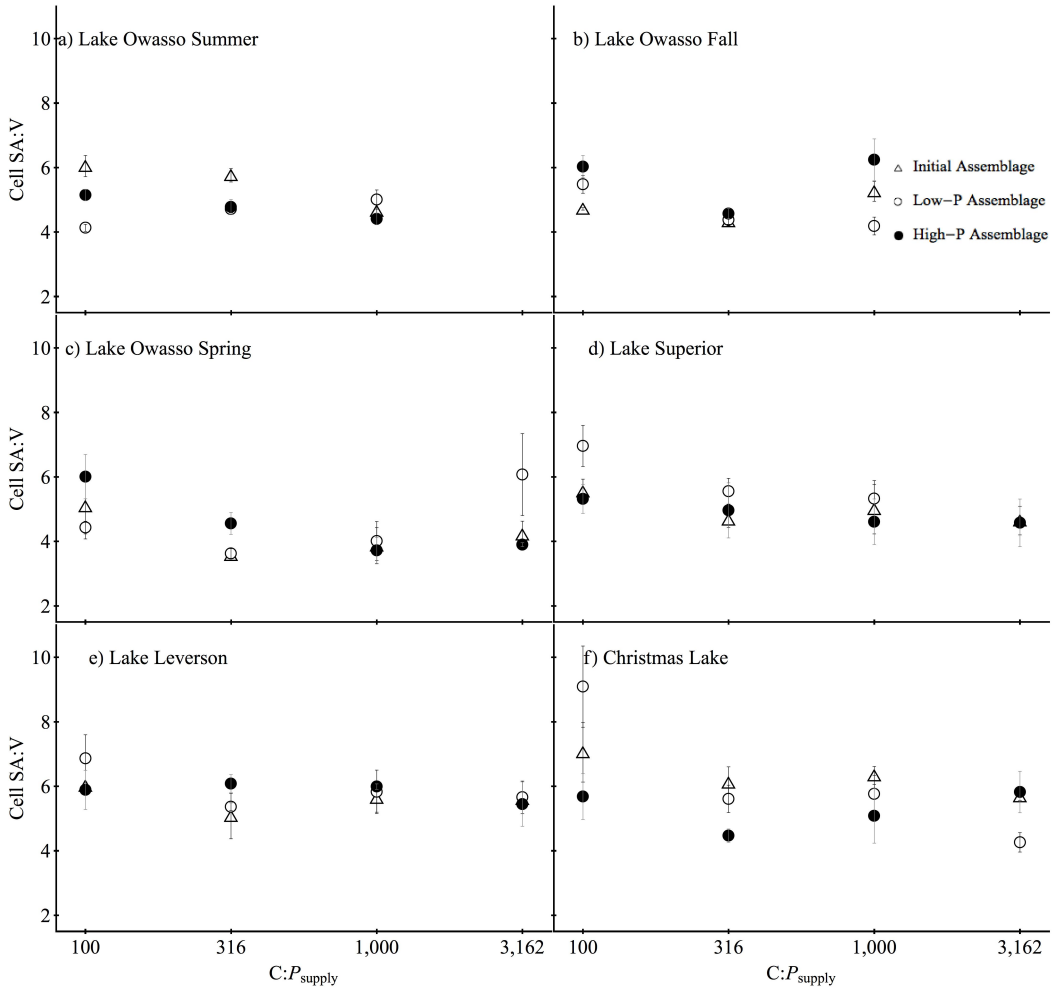

Figure 2-7. Assemblage surface area: volume ratios across C:P$_{supply}$ treatments. Separate panels for a) Lake Owasso is summer, b) Lake Owasso in fall, c) Lake Owasso in spring, d) Lake Superior, e) Lake Leverson, and f) Christmas Lake. Error bars denote the standard error of the mean.

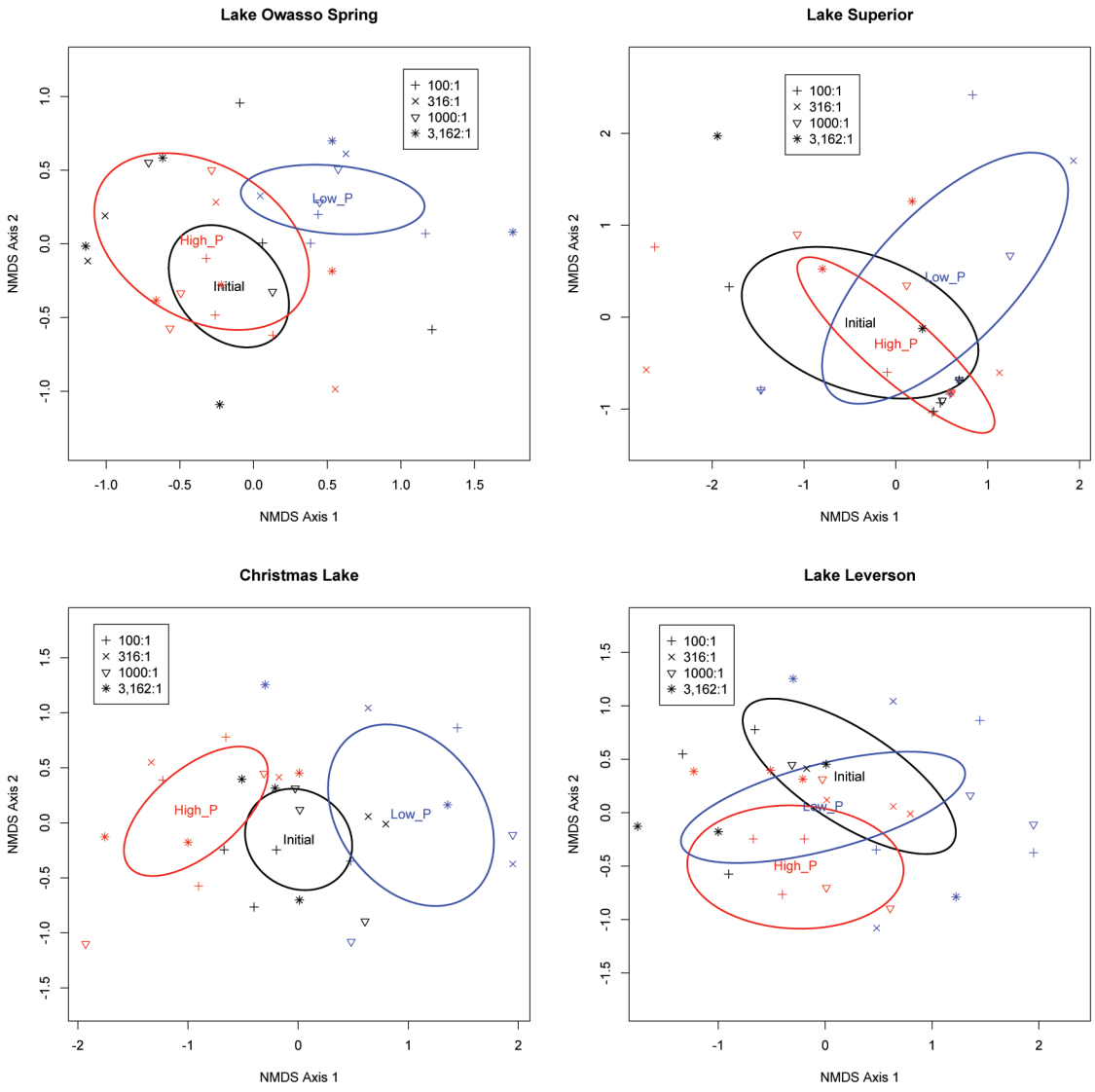

Figure 2-8. Non-metric multidimensional scaling ordinations of assemblage ARISA profiles.

Ellipses represent the 95% confidence region for the initial assemblages (black), high P selected assemblages (red), and low P selected assemblages (blue). Symbols represent C:P_{supply} levels as shown in the legend. In the experiments from Lake Owasso, Lake Superior, and Lake Leverson, there was not significant divergence in assemblage composition between the initial, high P selected, and low P selected fractions. In the experiments from Christmas Lake, the high P selected and low P assemblages had significantly different composition.

Table 2-1. Description of the source assemblage locations.

Lake	Date	Temperature (ºC)	Location (latitude, longitude)
Lake Owasso (summer)	9-01-2009	20	45° 2.356' N, 93° 6.798' W
Lake Owasso (fall)	11-08-2009	22	-
Lake Owasso (spring)	5-17-2010	16	-
Lake Superior	6-27-2010	16	46º 39.449’ N, 90º 30.239’ W
Lake Leverson	8-10-2010	27	45º 51.041’ N, 95º 53.707’ W
Christmas Lake	8-16-2010	26	44° 53.994' N, 93° 32.778' W

Table 2-2. Dissolved P concentrations and seston stoichiometry for the source assemblages.

Lake	Total Dissolved Phosphorus (µM-P)	Soluble Reactive Phosphorus (µM-P)	Seston Carbon (µM)	Seston Phosphorus (µM)	Seston C:N:P
Lake Owasso (summer)	-	-	15.18	0.181	84:29:1
Lake Owasso (fall)	-	-	-	-	-
Lake Owasso (spring)	0.49	0.28	-	0.104	-
Lake Superior	0.23	< 0.20	13.84	0.062	223:25:1
Lake Leverson	1.55	0.50	22.23	0.583	38:7:1
Christmas Lake	0.54	0.31	6.92	0.065	106:24:1

Table 2-3. Biomass stoichiometry and results of ANOVA tests for selection experiments.

Slope is for $\log_{10}$-$\log_{10}$ regressions of $C:P_{biomass}$ versus $C:P_{supply}$ and $C:N:P_{biomass}$ ranges are for individual chemostats.

Lake	ANOVA Selection x $C:P_{supply}$	Initial Assemblage C:P Slope (C:N:P range)	High-P Selected C:P Slope ($C:N:P_{biomass}$ range)	Low-P Selected C:P Slope ($C:N:P_{biomass}$ range)
Lake Owasso (summer)	$p < 0.0001$	0.338 (102:21:1 – 218:29:1)	0.014 (89:19:1 – 183:38:1)	0.697 (70:14:1 – 448:82:1)
Lake Owasso (fall)	$p < 0.05$	0.585 (93:17:1 – 381:54:1)	0.187 (80:16:1 – 399:54:1)	0.623 (63:14:1 – 430:61:1)
Lake Owasso (spring)	$p > 0.50$	0.502 (59:14:1 – 325:38:1)	0.443 (50:12:1 – 565:78:1)	0.463 (59:15:1 – 437:55:1)
Lake Superior	$p > 0.35$	0.528 (50:12:1 – 396:63:1)	0.789 (45:13:1 – 1,530:239:1)	0.617 (53:15:1 – 519:60:1)
Lake Leverson	$p > 0.15$	0.393 (66:16:1 – 306:45:1)	0.447 (67:17:1 – 862:101:1)	0.709 (42:11:1 – 1,396:166:1)
Christmas Lake	$p < 0.001$	0.697 (83:20:1 – 910:118:1)	0.280 (76:17:1 – 820:73:1)	0.889 (68:15:1 – 2,440:314:1)

Chapter 3: Diverse Responses of Aquatic Heterotrophic Bacteria to Elemental Imbalance: Stoichiometric Homeostasis is Determined by Phosphorus Quotas and Surplus Carbon Storage

Summary

Generalizations about the strength of elemental homeostasis within groups of taxa are common in the field of ecological stoichiometry and allow reduction of complex physiological mechanisms to a more tractable mass balance problem. Although such simplifications enable modeling of resource limitation, elemental imbalance, and nutrient regeneration, the biomass stoichiometry and strength of homeostatic regulation for entire trophic levels have been characterized using data from only a few species or strains and might not represent the variation present within natural assemblages. It is frequently presumed that heterotrophic bacteria in aquatic environments have low carbon (C) content, relatively high phosphorus (P) content, and maintain homeostasis at low C:P in biomass. To evaluate this assumption, I evaluated biomass C:P homeostasis in 24 strains of bacteria isolated from temperate lakes. Overall, the strains exhibited a range of homeostatic regulation from strong homeostasis to highly flexible biomass composition, but rich medium formulations isolated proportionally more homeostatic strains and fewer non-homeostatic strains compared to dilute media. Strains exhibiting homeostasis in biomass C:P had high cellular C and P content and showed little morphological change between C- and P limitation. In contrast, non-homeostatic strains had much lower P quotas and increased their C quotas and cell size under P limitation. Additionally, maximum growth rate was correlated with P content when cultured under P sufficiency at one third of the maximum growth rate. These results show that stoichiometric flexibility is closely related to C and P content, suggesting that selection for low P requirements could lead to dominance of non-homeostatic species.

Introduction

Most organisms experience imbalance between the chemical composition of their biomass and the chemical composition of their resources. Nutrient limitation is a form of imbalance in which the resources are lacking in at least one essential chemical component, which may be an element (e.g. nitrogen or iron) or a biomolecule that the organism is unable to synthesize (e.g. vitamins). Nutrient limitation may be manifest in reduced biomass production (Aerts and Chapin 2000), realized growth rate (Droop 1973a; Monod 1949), reproductive output (Færøvig and Hessen 2003), or other aspects of fitness. Elemental imbalance and nutrient limitation are not absolute, but rather they occur relative to the availability of a resource and the physiological requirements of the organism. For instance, species of phytoplankton differ in both the amount of nutrient resources required for growth (Tilman et al. 1982) and also the ratio in which they consume different resources (Klausmeier et al. 2004a). Adaptations for dealing with resource limitation include reducing growth rate, increasing consumption or uptake rates, minimizing loss rates, and minimizing the quantity of the resource required within biomass. Although all organisms exhibit at least one of these mechanisms, flexible biomass composition is particularly important because realized growth rate and resource acquisition rates are coupled indirectly by internal nutrient concentrations (Droop 1973a; van den Berg 2001).

Ecological stoichiometry uses the concept of elemental homeostasis to describe how organisms can alter their biomass composition in response to resource imbalance. The strength of stoichiometric homeostasis for carbon (C), nitrogen (N), and phosphorus (P) differs among major phylogenetic groups (Persson et al. 2010), but there is substantial variation within each group in both the strength of regulation and the range of biomass stoichiometry (chapter 1). For instance, autotrophs such as phytoplankton often have flexible biomass stoichiometry, whereas consumers such as zooplankton often exhibit stronger homeostasis (Persson et al. 2010; Sterner and Elser 2002). Just as the ratio of C:N:P within biomass has implications for competition and coexistence within local assemblages (Anderson et al. 2004; Moe et al. 2005), variability in the strength of

stoichiometric regulation among related taxa is key to understanding species-level interactions in environments where resource stoichiometry varies across space or time (Hood and Sterner 2010; Jeyasingh et al. 2009).

It is challenging to assess the variability in C:N:P regulation within a group of organisms because it requires measurements of biomass C:N:P at several resource ratios for each species or strain (Sterner and Elser 2002). Due to experimental constraints, such detailed characterizations are seldom performed for more than a few taxa in a single study. Furthermore, combining data on stoichiometric regulation from multiple studies may introduce unrecognized effects of experimental design and culture conditions, potentially masking important patterns. However, determining the ranges of elemental content and stoichiometric homeostasis within a functional or phylogenetic group is essential to understanding how communities respond to changes in their environment.

Heterotrophic bacteria couple multiple biogeochemical cycles within terrestrial and aquatic ecosystems (Azam 1998; Cole 1999; Schlesinger et al. 2011). In their role as 'gatekeepers' of nutrients within aquatic ecosystems (Kirchman 1994), the biomass nutrient content, stoichiometry, and homeostatic regulation of bacterial communities affect the rates at which bacterial communities can remineralize or sequester nutrients and carbon. Stoichiometric regulation in bacteria was initially examined using *Escherichia coli*, which grows more rapidly than most strains of bacteria, and exhibited strong homeostasis in biomass C:N:P across two orders of magnitude in P supply (Makino et al. 2003). In a subsequent study, an assemblage of bacteria cultured from a temperate freshwater lake was non-homeostatic, suggesting that assemblages could exhibit non-homeostasis as the result of shifts in relative abundance of strains driven by nutrient availability (Makino and Cotner 2004). Indeed, assemblages of bacteria from multiple lakes exhibit non-homeostasis and this is partly attributable to selection for different stoichiometric strategies (chapter 2). Recent work with bacterial isolates (Phillips et al. in preparation; Scott et al. 2012) has demonstrated that strains encompass a wider range of homeostatic regulation than was presumed, but none of the strains exhibited the strong homeostasis or high growth rates characteristic of *E. coli*. Also, assemblages of bacteria subject to ecological selection at high P availability (low C:P in

resources) can exhibit strong homeostasis (chapter 2), indicating that homeostatic strains are likely present within natural assemblages. Despite these recent advances, the strength of stoichiometric homeostasis present within assemblages remains poorly characterized.

One problem in studying stoichiometric homeostasis of strains from natural environments is that few strains are readily culturable (Colwell and Grimes 2000; Kaprelyants et al. 1993) and there may be an inherent bias due to coupling of stoichiometric strategies to the medium used for isolation. Specifically, studies of stoichiometric homeostasis in bacteria have been restricted to a small number of strains that were isolated using rich media. Bacteria that readily colonize rich media often exhibit higher growth rates than natural assemblages (Staley and Konopka 1985) and rapidly growing organisms have high P content and P requirements due to the abundance of P-rich ribosomes required at high growth rates (Elser et al. 2003; Elser et al. 2000b). Therefore, strains isolated using rich media could have different P physiology and stoichiometry than other strains in an assemblage. I hypothesize that rich medium formulations select for strains with higher nutrient content and more homeostatic physiology than bacteria isolated using dilute minimal media. I also propose that this bias due to isolation medium has contributed to an under-representation the range of stoichiometric strategies present in natural assemblages.

In this chapter, I sought to answer three questions: 1) Does the medium used for isolation select for different stoichiometric strategies? 2) How do quotas of C and P differ between homeostatic strains and those with flexible stoichiometry? And 3) How does the response to varying P availability differ among homeostatic strains, non-homeostatic strains, and assemblages? To address these questions, I characterized homeostatic regulation of C:N:$P_{biomass}$, cell quotas, and morphometry in 24 strains of bacteria isolated from lakes using multiple isolation methods and culture media. Both within and among assemblages, the isolates exhibited a range of element content and stoichiometric regulation, from non-homeostatic strains with low P quotas to strongly homeostatic strains with high P content.

Methods

Sample Collection and Processing. I isolated bacteria from Lake Itasca and Long Lake, both located in or adjacent to the Itasca State Park, Clearwater County, Minnesota, USA. Lake Itasca is moderately productive and Long Lake is oligotrophic (Hall and Cotner 2007). The location and ambient measurements for each lake are given in Table 3-1. Chlorophyll-a, total dissolved nitrogen, dissolved organic carbon, and total dissolved phosphorus were measured as described elsewhere (APHA 1995; Hall et al. 2009). Water samples were collected from the upper mixed layer of each lake during the spring using acid-soaked and sterilized polyethylene bottles. Samples were processed within one hour of collection. The bacteria-sized fraction was separated from the whole water by filtration through a sterile Whatman GF/B filter (Hall et al. 2009). Cell-free lake water was prepared by filtering the lake water twice using a 0.22 μm pore-size sterile filter (Fisher SteriTop).

Dilution Isolation and MPN Method. To quantify the number of culturable cells obtained using each medium treatment, I performed dilution to extinction isolation (Page et al. 2004; Schut et al. 1993) and most probable number (MPN) assays (Klee 1993) using the bacterial-sized fraction from each lake. To detect growth of cells, resazurin (Sigma Aldrich) was added to a final concentration of 20 μmoles L^{-1} in both the inoculum water and the sterile media. Resazurin becomes highly fluorescent when it is reduced by bacterial respiration (Haines et al. 1996; Nix and Daykin 1992). I diluted the inoculums into four medium treatments: cell-free lake water, a complex medium (Difco Nutrient Broth, 8 g L^{-1}), a defined medium with high phosphorus, and a defined medium with low phosphorus. The composition of the nutrient broth was 1.39 mmoles P L^{-1} (total phosphorus), 1.38 mmoles P L^{-1} soluble reactive phosphorus, and 274 mmoles C L^{-1}, resulting in a molar C:N:P of 198:67:1. The defined medium was Basal Microbiological Medium (BMM), prepared following Tanner (2002) using deionized water, with glucose (23.9 mmoles C L^{-1}) as the sole source of carbon. Additional minerals, vitamins, and trace metals were supplied at concentrations described in Tanner (2002) and the medium was buffered between pH 7.2 and 7.4 using 11 mmoles L^{-1} 3-(N-

Morpholino)propanesulfonic acid (MOPS). Phosphorus was added as potassium phosphate at two levels to create molar C:P of 100:1 (239 μmoles-P L^{-1}) and 100,000:1 (0.239 μmoles-P L^{-1}).

Dilution cultures were performed in black 96-well microtiter plates (Nunc) at 11 dilutions between 1 and 2.39×10^{-7} (total culture volumes of 170 μL). Sixty replicate dilution series were performed for each lake in the BMM 100:1 and BMM 100,000:1 treatments. One hundred and eighty replicate dilution series were performed for each lake in the cell-free lake water and nutrient broth treatments. Each microtiter plate contained 8 control wells of medium without any inoculum. The plates were sealed with sterile transparent film (Excel Scientific, ThinSeal) and incubated at 20ºC in the dark. Fluorescence of the dilution plates was monitored using a using a Fluoromax 3 spectrofluorometer with a MicroMax 384 plate reader (Horbia Jobin Yvon). Fluorescence was measured using excitation at 560 nm and emission at 585 nm, both with 5 nm slit widths. Fluorescence of each well was averaged for one second and the plates were returned to the dark incubator between readings. The fluorescence of the plates was measured seven times between 3 and 38 days after inoculation.

After eighteen and 38 days, I identified the wells with positive growth as those where the slope of fluorescence versus time and the absolute fluorescence were greater than the 90% upper confidence interval for the slope of the control wells for each plate. I computed the MPN estimates and 95% confidence intervals for each lake and medium type following Jarvis (2010), using Mathematica version 7 (Wolfram Research). To obtain cultures with a high probability of being axenic, I harvested wells at high dilutions where the next lowest dilution did not show detectable growth. The contents of these wells were diluted again into the same medium type with resazurin and the fluorescence was monitored for nineteen days. Following the second dilution of the potential isolates, I harvested the highest dilutions with detectable growth and plated the cultures onto agar made with the same medium. Distinct colony morphologies were preserved as described below.

Agar Plate Cultures. I diluted the bacterial-sized fraction from each lake into cell-free lake water (dilution 1 - 1000x) and plated 100 μL onto agar plates. The plates were

prepared using 15 g agar L^{-1} (Sigma Aldrich) and each of the following medium formulations: nutrient broth (prepared as above), BMM at C:P of 100:1, and BMM at C:P of 100,000:1. Five replicate plates were used for each dilution of nutrient broth and ten replicate plates were used for the BMM formulations. The plates were incubated at 22-24ºC and visible colonies were characterized, enumerated, and harvested after 6 days and 12 days. For each set of replicate plates, single colonies of each distinct morphology were harvested and streaked onto agar plates with the same media. Permanent cultures were established by adding glycerol to liquid cultures of each potential isolate (final concentration 15% v/v) and freezing the cultures at -70ºC (Morrison 1977).

Isolates Selection, Identity, and Growth Rates. Isolates for use in the experiments were randomly selected from the list of potential isolates in each combination of medium treatment and lake. Strains that did not exhibit sufficient growth in liquid batch culture were excluded and other candidates were evaluated until each combination was represented by at least one strain. The strains were assigned to taxonomic affiliation using partial 16S rRNA sequences derived using the primers 8F and 1492R, and subsequent alignment against sequence libraries using the Basic Local Alignment Search Tool (BLAST, National Institutes of Health). To ensure that the strains for this study were not biased toward the isolation methods described above or the biogeography of Long Lake and Lake Itasca, I included seven additional strains provided by Stuart Jones (University of Notre Dame). The strains were isolated from lakes in Indiana and Michigan using WC minimal medium (Stuart Jones, unpublished). A strain of *Polynucleobacter necessarius* (Pnec), was obtained from the DSMZ collection (Leibniz Institute, Germany). The source, isolation conditions, and taxonomic affiliation of all of the study strains are given in Table 3-2.

Batch cultures were prepared in BMM medium (C:P = 100:1) using replicate cultures with a volume of one milliliter. Duplicate batch cultures of each isolate were inoculated from permanent cultures and incubated at 22-24ºC. At each time point, the cultures were rapidly frozen using liquid nitrogen and were stored at -70ºC until analysis. The population of bacteria in each culture was determined from the change in the concentration of double-stranded DNA using the PicoGreen reagent (Invitrogen Quant-It

PicoGreen Kit) and fluorescence measurement (Tranvik 1997; Cotner et al 2001). Poor sensitivity was observed when the PicoGreen reagent was added directly to cells growing in artificial medium. Sensitivity was improved substantially by extracting the DNA prior to quantification. After thawing the cultures, 125 µL of extraction buffer (29.1 mmoles L^{-1} sodium lauryl sarcosine, 54 mmoles L^{-1} tris(hydroxymethyl) aminomethane, and 5.4 mmoles L^{-1} ethylene(diamine)tetraacetic acid at pH 8.0) was added to the samples (Gorokhova and Kyle 2002) and the samples were incubated at 22-24ºC on a rotary shaker for one hour. DNA standards (Invitrogen) were prepared by dilution into TE buffer (10 mmoles L^{-1} tris(hydroxymethyl) aminomethane and 1 mmoles L^{-1} ethylene(diamine)tetraacetic acid at pH 8.0). The PicoGreen reagent was diluted 1:470 in extraction buffer and 150 µL was added to each sample, followed by mixing. The samples were incubated in the dark for at least ten minutes and transferred to 1 cm polymethylmethacrylate cuvettes (VWR Scientific). The fluorescence was measured using excitation of 500 nm and emission at 523 nm (5 nm slit widths) using a Fluoromax 3 fluorometer (Horbia Jobin Yvon). Fluorescence values were averaged over one second. The working range of the assay was 0.1 to 200 ng DNA mL^{-1} with detection limits of 50 pg mL^{-1}. Growth rates were estimated from cultures where the DNA concentration increased exponentially (log-linear $R^2 > 0.9$) for at least three successive time points and the DNA concentration was less than 40 ng mL^{-1}. Based upon a range of 3-20 fg DNA $cell^{-1}$ in cultured cells (Cotner et al. 2001; Makino and Cotner 2004; chapter 4), the cell densities used for growth rates were between 3.3 $x10^4$ and $1x10^7$ mL^{-1}. The growth rate estimates from replicate cultures (μ_{max}) were within 10%.

Chemostat Cultures and Biomass Analyses. Each isolate was cultured in 100 mL polypropylene chemostats diluted at 33% of µmax. The P content of the BMM formulation was manipulated to achieve molar C:P ratios of 100, 316, 1,000, 3,162, and 10,000:1 (2.4 to 239 µmoles P L^{-1}). Batch cultures for each treatment were inoculated with aliquots of the permanent cultures. After the batch cultures reached visible turbidity (optical density at 600 nm > 0.05 cm^{-1}), 5 mL of the batch cultures was used to inoculate duplicate chemostats at each level of $C:P_{supply}$. Chemostats were maintained at 20 ºC in

darkness, aerated and mixed with 0.2 μm-filtered air, and harvested after 9 complete generations.

Dry Mass and Elemental Content. Samples of biomass were collected from each chemostat using Whatman GF/F filters that were combusted at 450ºC. Three replicate filters were stored in a desiccator until weighing to the nearest 0.1 μg for determination of dry mass. The filters were rinsed with 10 % hydrochloric acid and then with deionized water prior to harvesting the cells under low vacuum (<100 mm Hg). The filter samples were rinsed with deionized water to remove excess media, and stored at -20ºC until analysis. Filters for dry mass were dried at 60ºC for seven days and weighed again, and the blank-corrected difference was used as dry biomass. One filter from each chemostat was randomly selected for direct measurement of C and N content using a CHN analyzer (Perkin-Elmer 2400CHN) with acetanilide (Elemental Microanalysis Ltd.) as a reference standard and an internal zooplankton recovery standard. Three filter samples from each chemostat were analyzed for bacterial P. Following digestion in 25 g L^{-1} potassium persulfate at 121ºC for 30 minutes (APHA 1995), the phosphorus content was determined using the ascorbic acid molybdenum method. Spinach leaf reference material (NIST) was used as a recovery standard for all phosphorus analyses.

Cell Abundance and Morphometry. Aliquots of the chemostat cultures were preserved with 0.2 μm-filtered formaldehyde (3.7 % by volume) and stored at 4ºC. One sample from each chemostat was prepared for microscopic enumeration by dilution in sodium pyrophosphate and sonication (Velji and Albright 1993). Each sample was stained with acridine orange, filtered onto black polycarbonate membrane filters (Nucleopore, 0.2 μm pore size), and mounted to slides for microscopy (Hobbie et al. 1977). Cell counts and morphometry measurements were performed at 1,000x magnification using an Olympus BX40 microscope. For cell counts, at least 10 fields and 300 cells on each filter were enumerated manually. Photomicrographs were obtained using a digital camera (Spot 2, Diagnostic Instruments) at 1,000x magnification. Cell dimensions (length, width, planar area, and planar perimeter) were measured for at least 100 cells from each chemostat using image analysis software (Image Pro Plus, Media Cybernetics). Cell shape was measured as cylinders capped with two hemispheres

(Hillebrand et al. 1999). Due to the high proportion of curved cells, cell dimensions were calculated using the planar area and perimeter, rather than the box length and width. The equations used for estimating cell length, width, surface area, and volume are given in Appendix D.

Statistical Analyses. The mean blank-corrected measurements for each chemostat were used to calculate molar ratios of elements ($C:P_{biomass}$, $N:P_{biomass}$, and $C:N_{biomass}$) and the elemental content of the cells (P $cell^{-1}$ and P relative to dry mass). In strains where quotas of C, N, and P increased under P limitation, the C:N:P of the added biomass was calculated as the molar ratio of the increases between $C:P_{supply}$ of 100:1 and 10,000:1. For each strain, the strength of stoichiometric regulation was assessed using segmented linear regressions (Kim et al. 2004) of $\log_{10}$ $C:P_{biomass}$ against $\log_{10}$ $C:P_{supply}$ (Sterner and Elser 2002). The break point was selected by iteratively bisecting the data series at each level of $C:P_{supply}$ from 316:1 to 10,000:1 and performing standard linear regression on the lower (flexible) and upper (homeostatic) ranges. The breakpoint was chosen as the level of $C:P_{supply}$ that minimized the total sum of squares for both segments. Strains were separated into three arbitrary and even categories (stoichiometric categories) based upon the degree of flexibility in $C:P_{biomass}$ observed in the chemostat cultures.

Morphometric data were $\log_{10}$-transformed prior to analysis to meet assumptions of approximate normality and homogeneity of variances (Sokal and Rohlf 1995). Biomass elemental content and morphometric data were analyzed by two-way analysis of variance (ANOVA) tests, using stoichiometric category as a fixed effect and $C:P_{supply}$ as a quantitative treatment. When a significant interaction was observed, separate one-way tests were performed for each level of $C:P_{supply}$. Pairwise differences in the one-way ANOVA analyses were evaluated using Tukey's Honest Significant Difference tests, with a significance cutoff of $p < 0.05$. To determine the effect of isolation medium on homeostatic classification of the isolates, the strains from Lake Itasca and Long Lake were grouped into those isolated using rich media (nutrient broth and BMM 100:1) and poor media (sterile lake water and BMM 100,000:1). The proportions of isolates belonging to each stoichiometric category were compared for rich and poor media using a chi-squared test (Sokal and Rohlf 1995).

Results

Cultivation and Medium Formulations. The bacterial assemblages diluted into a defined medium (BMM) with C:P of 100:1 showed significantly higher most probable number (MPN) estimates than the samples diluted into cell-free lake water or nutrient broth (Figure 3-1). The MPN estimates for Long Lake were higher than those for Lake Itasca in all medium treatments except for the nutrient broth. Samples plated onto solid media showed a similar pattern of reduced counts for nutrient broth compared to the BMM treatments (Figure 3-1). The ANOVA of CFU mL^{-1} revealed significant effects of medium treatment ($p < 0.003$), and lake ($p < 0.03$), but no interaction ($p > 0.10$). Post-hoc tests indicated that the nutrient broth had significantly lower CFU mL^{-1} than the BMM medium formulations (Tukey HSD, $p < 0.05$). The growth rates of the isolates ranged from 0.07 h^{-1} to 0.43 h^{-1} (Table 3-3). For the isolates from Lake Itasca and Long Lake (MN), there was no effect of isolation medium on growth rate (Wilcoxon two-sample test, $p > 0.05$).

Biomass Stoichiometry. The strains exhibited dynamic stoichiometry in chemostat cultures, with $C:P_{biomass}$ ranging from 47:1 to 994:1 and $N:P_{biomass}$ ranging from 8.2:1 to 132:1 (Table 3-3). $C:N_{biomass}$ was less variable, ranging from 2.3:1 to 11:1. ANOVA tests on $C:P_{biomass}$, $N:P_{biomass}$, and $C:N_{biomass}$ indicated significant effects of strain, $C:P_{supply}$, and an interaction (all $p < 0.0001$). Separate one-way ANOVA tests for each strain indicated significant effects of $C:P_{supply}$ for a subset of the strains (Table 3-3). The regression slopes of log $C:P_{biomass}$ versus log $C:P_{supply}$ (chapter 1) below the breakpoint ranged from -0.09 to 0.93 (Table 3-3, Figure 3-2). The strains were assigned into three arbitrary categories using the lower, middle, and upper third of the range in $C:P_{biomass}$. Homeostoichs exhibited ranges of $C:P_{biomass}$ less than 83, mesostoichs had ranges of $C:P_{biomass}$ from 83 to 210, and heterostoichs had ranges of $C:P_{biomass}$ greater than 210 (Figure 3-2). For the isolates from Lake Itasca and Long Lake (MN), medium types produced significantly different proportions of homeostoich, mesostoich, and heterostoich strains (chi-squared test, $p < 0.018$). Rich media formulations produced 6

homeostoichs, 1 mesostoich, and 1 heterostoich and poor media yielded 1 homeostoich, 1 mesostoich, and 5 heterostoichs.

At $C:P_{supply}$ of 100:1, there was no significant difference in biomass stoichiometry among the stoichiometric categories (all $p > 0.05$), with $C:N:P_{biomass}$ ranging from 52:11:1 to 104:19:1 and a median ratio of 81:16:1. Under P limitation, mean $C:N:P_{biomass}$ for each isolate ranged from 116:21:1 to 869:124:1. By stoichiometric category (Figure 3-3), $C:P_{biomass}$ showed significant effects of $C:P_{supply}$, category, and an interaction (all $p < 0.0001$). Among all strains, $N:P_{biomass}$ was affected by $C:P_{supply}$, category, and an interaction (all $p < 0.0001$). All three categories of strains exhibited significantly increased $N:P_{biomass}$ under P limitation ($p < 0.05$). Mean cell $C:N_{biomass}$ was affected by $C:P_{supply}$ ($p < 0.0001$), category ($p < 0.0001$), and an interaction ($p < 0.05$). For heterostoichs and mesostoichs, $C:N_{biomass}$ increased significantly under P limitation ($p < 0.05$), but homeostoichs did not exhibit significant flexibility in $C:N_{biomass}$ (Figure 3-3). For the isolates from Lake Itasca and Long Lake (MN), rich media produced isolates with significantly lower ranges in $C:P_{biomass}$, $N:P_{biomass}$, and $C:N_{biomass}$ (Wilcoxon test, all $p < 0.01$). At $C:P_{supply}$ of 100:1, mean $C:P_{biomass}$ showed a weak negative correlation with μ_{max} ($r^2 = 0.16$, ANOVA $p > 0.05$), but minimum $C:P_{biomass}$ showed a significant negative correlation with μ_{max} ($r^2 = 0.24$, $p < 0.02$).

Abundance of the cells in the cultures decreased with increasing $C:P_{supply}$, was different among stoichiometric categories, and the strength of the decrease was proportionally different among the categories (ANOVA, all $p < 0.0001$). At all levels of $C:P_{supply}$, heterostoichs had higher cell abundance than mesostoichs or homeostoichs (data not shown). As a percentage of available C, biomass C yield was significantly higher in the heterostoich strains compared to the mesostoichs and homeostoichs at all levels of $C:P_{supply}$ above 100:1 (Figure 3-4). Heterostoichs also exhibited significantly higher P yield than the homeostoichs and mesostoichs at $C:P_{supply}$ of 316 to 1,000:1.

Cellular C and P Content. Phosphorus quotas in the isolates ranged from 0.007 to 1.57 fmoles $cell^{-1}$ and carbon quotas ranged from 1.04 to 143 fmoles $cell^{-1}$ (Table 3-4). The ANOVA tests on cell quotas indicated a significant effect of $C:P_{supply}$ and an interaction between $C:P_{supply}$ and strain (all $p < 0.0001$). One-way ANOVA tests on

carbon and phosphorus quotas indicated significant effects of $C:P_{supply}$ in only a subset of the strains (Table 3-4, Figure 3-5). Under phosphorus limitation, phosphorus quotas increased significantly in three strains (D1207, D304, and D611) and decreased significantly in four strains (UND-FW12, UND-L41A, UND-WG21, and UND-WG36). Relative to cell volume, phosphorus content ranged from 0.009 to 1.53 fmoles μm^{-3} and carbon content ranged from 2.9 to 126 fmoles μm^{-3}. Under P limitation, P quotas relative to cell volume increased significantly only in one strain, but decreased significantly in eight strains (Table 3-4). There was no significant effect of $C:P_{supply}$ on C and P quotas ($p > 0.05$), but relative to volume, P content showed significant effects of $C:P_{supply}$ and an interaction between category and $C:P_{supply}$ ($p < 0.05$).

For the isolates from Lake Itasca and Long Lake (MN), poor media produced isolates with lower minimum P quotas (by volume, Wilcoxon test, $p < 0.03$) and lower maximum P quotas (per cell, $p < 0.02$). Isolation medium type did not affect minimum C quotas, but poor media produced isolates with significantly lower maximum C quota (by volume, $p < 0.004$). At $C:P_{supply}$ of 100:1, μ_{max} was positively correlated with phosphorus quotas ($r^2 = 0.37$, $p < 0.003$) and carbon quotas ($r^2 = 0.30$, $p < 0.008$) of the isolates. Phosphorus content of the cells relative to dry mass ranged from 0.032 to 2.08%. Under phosphorus limitation, all of the strains exhibited decreased phosphorus content relative to dry mass, although this decrease was statistically significant in only 16 of the strains (Table 3-4). Relative to dry mass, P content of the isolates showed significant effects of category and $C:P_{supply}$ (ANOVA $p < 0.001$).

Of the 11 strains that increased both their absolute C quota and P quota under P limitation, the C:P of the added biomass between $C:P_{supply}$ of 100:1 and 10,000:1 ranged from 205:1 to 5,866:1. For the 7 heterostoich strains exhibiting increased quotas of C and P between $C:P_{supply}$ of 100:1 and 10,000:1, the mean C:P of the added biomass was 1,964:1. In 13 of the strains, both C and N quotas increased under P limitation and the C:N of added biomass ranged from 5:1 (P045) to 63:1 (UND-WG36). In the 10 strains where both N and P increased under P limitation, N:P of the added biomass ranged from 17:1 to 372:1.

Cell Morphometry. The isolates exhibited a range of morphological responses to P limitation (Figure 3-6, Figure 3-7). Eighteen strains exhibited significantly increased length:width (L:W) under P limitation (ANOVA, $p < 0.05$) (Appendix Figures E-1, E-2, and E-3). Only 8 strains significantly increased surface area:volume (SA:V) in response to P limitation (2-25% change). Changes in cell morphometry were related to stoichiometric category (Figure 3-6). Mean cell length was significantly affected by stoichiometric category, $C:P_{supply}$, and an interaction (all $p < 0.0001$). At high $C:P_{supply}$, homeostoich strains increased less in length, volume, surface area, and L:W than the mesostoich and heterostoich strains. Cell volume showed significant effects of category, $C:P_{supply}$, and an interaction (all $p < 0.05$), again with heterostoichs increasing most in volume under P limitation. Cell surface area showed significant effects of category, $C:P_{supply}$, and an interaction (all $p < 0.001$). Cell L:W was affected by category ($p < 0.0001$) and $C:P_{supply}$ ($p < 0.0001$) without a significant interaction ($p > 0.05$). Cell SA:V did not show significant effects of category or $C:P_{supply}$.

Discussion

The strains examined in this study showed more variability in their elemental content and stoichiometry than was previously known for heterotrophic bacteria. Data from these experiments will be used to provide insight into four areas. First, these chemostat cultures illuminate a gradient of stoichiometric strategies and show that isolates from a single assemblage may exhibit strong homeostasis or flexible stoichiometry depending upon the isolation conditions used. Second, heterostoich strains attained flexibility in their stoichiometry through low P quotas at all P supply levels and dynamic C content, whereas homeostatic strains had high quotas of both C and P. Third, cell morphology and stoichiometric flexibility are related in most strains, but existing hypotheses appear insufficient to explain this linkage. Last, I will explain how the stoichiometric non-homeostasis observed in some isolates differs from that observed in assemblages of multiple strains.

Isolation Conditions Select for Stoichiometric Regulation. The medium formulations employed in this study differed in their effectiveness for culturing strains

from the bacterial assemblages in Lake Itasca and Long Lake (MN). Notably, more strains were viable in the BMM formulations than in the nutrient broth media. Previous studies have demonstrated that only a small portion of the bacterial community can be easily cultured (Eilers et al. 2000; Staley and Konopka 1985) and that rich media are often poorly suited to isolate bacteria from aquatic environments (Barer and Harwood 1999). For the defined medium agar, there was no effect of P availability on the number of colony-forming units. In dilution culture, there was a decrease in apparent cultivability when the P availability was decreased by three orders of magnitude. Thus, there were distinct effects of C source (large effect) and P availability (smaller effect) on the number of culturable cells. Fewer bacteria were capable of utilizing the animal-derived carbon substrates in the nutrient broth compared to the defined medium, which could be attributed to inhibition of growth in some strains by high concentrations of substrates (Morita 1997).

The medium formulations used to isolate these strains from Long Lake and Lake Itasca effectively selected for strains with different types of stoichiometric regulation. Both the rich and poor medium formulations yielded isolates exhibiting a range of stoichiometric regulation, but the rich media produced disproportionately more homeostatic strains compared to poor media. Previous studies on the stoichiometry of bacterial isolates have examined only strains that were isolated on rich media, specifically animal- and yeast-derived LB medium (Phillips et al. in preparation; Scott et al. 2012). Although some isolates obtained using rich media have exhibited non-homeostasis with $C:P_{biomass}$ of 100 to 1000:1 (Scott et al. 2012), these studies have described a comparatively small portion of the stoichiometric strategies culturable from natural assemblages.

Gradient of Stoichiometric Regulation in Isolates. The isolates described in this chapter showed a range of stoichiometric regulation, from strong homeostasis to non-homeostasis. This finding unequivocally demonstrates that bacteria differ in their strength of stoichiometric regulation and that assemblages contain multiple stoichiometric strategies. The first systematic examination of stoichiometric homeostasis in heterotrophic bacteria was performed with *E. coli*, which was strongly homeostatic

(Makino et al. 2003). Other studies did not find such strong homeostasis as in *E. coli*, with most strains exhibiting only moderate homeostasis or non-homeostasis (Chrzanowski and Kyle 1996; Løvdal et al. 2008; Phillips et al. in preparation; Scott et al. 2012). From these experiments, it appears that *E. coli* could represent an aberrant observation due to its high relative growth rate relative to other bacteria or due the culture conditions used. However, the homeostoich strains characterized in this chapter exhibited modest growth rates that did not differ significantly from the mesostoich or heterostoich strains, suggesting that strong homeostasis is not simply a signature of a high growth rate. This is contrary to my predictions (chapter 1), but the defined medium used in this study might not reflect the actual maximum growth rate of the strains. Instead, the existence of strongly homeostatic strains could represent physiological adaptation to environments with high nutrient availability and low imbalance. Furthermore, homeostatic strains of bacteria can be dominant at low $C:P_{supply}$ (chapter 2), but heterostoich physiology is dominant at high $C:P_{supply}$, suggesting that homeostatic strains are adapted to high resource environments or are poorly adapted to dealing with resource imbalance.

The range of stoichiometric regulation present within these isolates (slopes from ≅0 to 0.93) is equivalent to the range of stoichiometric regulation measured in all previously published studies of bacterial isolates and assemblages (chapter 1, references therein). Furthermore, this range is comparable to the extent of stoichiometric flexibility typically associated with species of phytoplankton (chapter 1, references therein). Although it is often assumed that heterotrophic bacteria are strongly homeostatic (Fanin et al. 2013; Tambi et al. 2009; Tanaka et al. 2009), this study and other recent studies with environmental isolates demonstrate that non-homeostasis is common among culturable bacteria. Taken together, these results indicate that assemblages of bacteria contain strains with a range of stoichiometric regulation and suggest a flexible and diverse role in carbon and nutrient cycling.

The range of $C:N:P_{biomass}$ exhibited by the cultures was greater than observed in other studies using bacterial isolates (Makino et al. 2003; Phillips et al. in preparation; Scott et al. 2012), but was comparable to the range observed in assemblages of bacteria cultured from lakes (chapter 2). Under low $C:P_{supply}$, all of the isolates had similar

$C:N:P_{biomass}$. This is explained by the 'fulcrum stoichiometry' concept: under low resource imbalance the strains have similar stoichiometry, presumably due to shared macromolecular composition (i.e. DNA, RNA, protein, and lipids). At increased $C:P_{supply}$, the strains had divergent stoichiometry and quotas because of differential allocation of the elements within biomass. Since any elemental ratio is sensitive to both the numerator and denominator quotas, these stoichiometry data alone cannot definitively diagnose whether the increased $C:P_{biomass}$ and $N:P_{biomass}$ under P limitation are due to minimization of P or storage of C and N within biomass. However, the isolates had relatively constrained $C:N_{biomass}$ compared to $C:P_{biomass}$ or $N:P_{biomass}$, which suggests that any macromolecules used for surplus storage of C also contained a substantial amount of N. Heterostoich strains showed increased $C:N_{biomass}$ under P limitation, but the increase was modest and does not necessarily imply storage of C and glycogen or poly-β-hydroxybutyrate, which are rich in C relative to N (Preiss 1984; Sterner and Elser 2002; Wilkinson 1963). Although the biomass stoichiometry data suggest possible C and N storage, these responses can be inferred more accurately by analyzing changes in cell quotas under C and P limitation.

Stoichiometry and Cell Quotas. The strains achieved widely varying $C:N:P_{biomass}$ as the result of plasticity in their cellular C and P content. Although the strains differed in the extent of plasticity in C and P quotas, several key patterns are apparent at the level of the stoichiometric categories. The first pattern is that heterostoichs as a group had lower P content than the other categories at all levels of $C:P_{supply}$ and showed decreased P content (both absolute and by volume) under P limitation (Figure 3-5). However, heterostoichs did not achieve plasticity in $C:P_{biomass}$ solely through flexibility in cellular P, but rather accumulated C under P-stress. The P content of the homeostoich strains was higher and changed less compared to the heterostoichs, although the categories had similar $C:P_{biomass}$ when P was abundant. No single measure is sufficient to definitively diagnose P nutritional status or resource imbalance. In particular, neither $C:P_{biomass}$ nor P quotas could be used to reliably diagnose P limitation in homeostoich strains. Instead, alternative measures such as transcriptional profiling (Boer et al. 2010), phosphatase activity (Cotner and Wetzel 1991), or growth rate bioassays (Cotner et al. 1997; Sterner

et al. 2004) would be more informative. Since the P content of the heterostoichs was lower than the other categories even at high P availability, it seems likely that a lower overall P quota is required for highly flexible biomass stoichiometry. Reduced P content and flexible C quotas of the heterostoich strains can also explain higher cell abundance and higher apparent yields of C and P.

The second key pattern is that the strength of stoichiometric homeostasis was not correlated with maximum growth rate, but the P content of the isolates under P sufficient conditions was positively correlated with maximum growth rate. This can be explained by high variability in P content among the mesostoichs strains. The Growth Rate Hypothesis (GRH) predicts that the P content of an organism is proportional to its growth rate due to the role of P-rich ribosomes in growth (Elser et al. 2000b). This correlation also provides support for the hypothesis that strains with high maximum growth rates are poor competitors under P limitation (chapter 1, chapter 2).

The third key result is that many strains increased their C content under P limitation, but in the heterostoich strains, the increase was disproportionate to changes in cellular P content and contributed to the elevated $C:P_{biomass}$. This shows that the heterostoichs achieved stoichiometric flexibility through coupled decreases in cellular P and increases in cellular C under P limitation (per cell and by volume) and suggests that heterostoichs could alter their biomass stoichiometry via accumulation of C-rich molecules (e.g. glucose, glycogen, extracellular polymers). In addition, the C:P and N:P of the biomass accumulated under P limitation were much higher than the existing biomass, whereas the C:N of the added biomass was only modestly higher in most of the strains. Under P limitation, strains D301 and D304 accumulated biomass with high C:N (43-44), which is characteristic of accumulation of a C-rich material such as poly-B-hydroxybutyrate or glycogen.

In addition to lower P content and variable stoichiometry, the heterostoich strains had higher C and P yields than mesostoich and homeostoich strains. The higher C yield of P limited heterostoichs is likely due to surplus storage of C within biomass. At intermediate levels of $C:P_{supply}$, the heterostoichs utilized more of the available P due to low P quotas. Together with the observation that many of the heterostoichs had

regression breakpoints ($C:P_{TER}$, Sterner and Elser 2002) of 1,000:1 or greater (Figure 3-2), this pattern indicates that the heterostoichs became P limited at higher $C:P_{supply}$ than the mesostoichs or homeostoichs. An increased $C:P_{TER}$ supports the hypothesis that heterostoichs have superior competitive ability at intermediate $C:P_{supply}$. However, it is not apparent that the competitive ability of strains under C limitation is attributable to stoichiometry or cell quotas alone, since heterostoichs had lower cellular C and P content than the other categories at low $C:P_{supply}$.

Role of Morphometry in Stoichiometry. Several strains showed morphological responses to P limitation that were associated with changes in biomass element content and stoichiometry. The homeostoich strains showed less plasticity in their morphometry than the mesostoich and heterostoich strains, mimicking differences in cell quota and stoichiometry. Other studies have documented an increase in cell length to width ratios under P limitation (Phillips et al. in preparation; Thingstad et al. 2005; chapter 2, chapter 4) and this is a hypothesized adaptation to increase the surface area for uptake of P across the cell membrane. This hypothesis is partially supported by the present study: the mesostoich and heterostoich strains increased their surface are but there was no change relative to their cellular volume. The allometric scaling of cell size and surface area is dependent upon cell shape and also the absolute dimensions of the cells (Grover et al. 2004; Okie 2013). At the dimensions of these cells, increasing length effectively increases surface area of the cell, but also increases volume, leading to no change in SA:V. In contrast, decreases in cell width would lead to increased L:W and also increased SA:V. Because there was not a significant difference in width among the stoichiometric categories, the morphological change that did occur resulted in tight coupling of surface area and volume. Since the heterostoich strains increased their surface area by adding biomass that was deplete in P, the increase in cellular volume might not represent a significant cost, supporting the hypothesis that surplus C can be used to increase diffusive uptake of P (Thingstad et al. 2005).

Stoichiometry of Strains Versus Assemblages. Assemblages of bacteria achieve non-homeostasis in $C:P_{biomass}$ through coupled decreases in mean P quota and increases in C quotas under P limitation (chapter 2, chapter 4). Although coupled responses in C and

P quotas were observed in populations of a few strains, the range of quota flexibility in all of these strains is far less than that observed for the aggregate C and P quotas of assemblages (chapter 4). This disparity could be attributable to two non-exclusive explanations. First, assemblages could exhibit a greater range in aggregate C and P quota as the result of shifts in assemblage composition in response to resource availability (chapter 2). In this way, the aggregate flexibility could exceed that of any of the component strains. The second explanation is that the strains examined to date represent only a portion of the physiologies present within culturable assemblages. Given that isolation medium selected for stoichiometric strategies and that the resulting isolates exhibited substantial variability in C and P content, both explanations are supported.

The strains of bacteria examined in the current study exhibited a range of plasticity in stoichiometry and element quotas that is nearly equivalent to that observed in assemblages of bacteria (chapter 2, chapter 4). Unlike assemblages of bacteria, the plasticity observed in the present study is attributable only to physiological acclimation. Assemblages cultured under high $C:P_{supply}$ can attain $C:P_{biomass}$ ratios of more than 10,000:1 as the result of the simultaneous increases in C quotas and substantial decreases in cellular P (chapter 4). In contrast, only a few of the strains examined here showed this negative coupling, but instead the non-homeostatic strains maintained their P quotas at relatively low levels and accumulated substantial amounts of surplus C. The low P content of the heterostoich strains examined in this study suggests that the decrease in cellular P content within an assemblage is most likely due to shifts in the dominant strains from homeostoich strains with high P quotas at low $C:P_{supply}$ to heterostoich strains with lower P quotas at high $C:P_{supply}$. Such selection for low P content under P limitation, coupled with surplus C storage by strains with low P content, provides a mechanism by which assemblages can exhibit substantial flexibility in their stoichiometry.

Figures and Tables

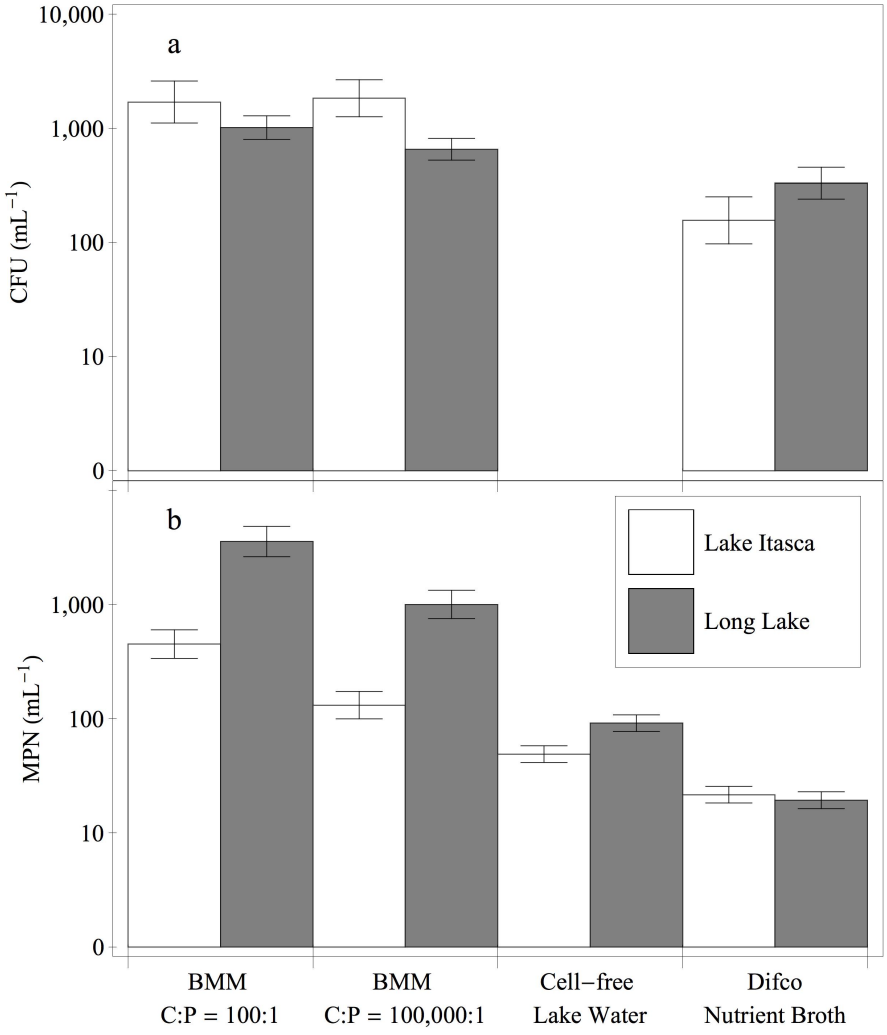

Figure 3-1. Yields of bacteria from Long Lake and Lake Itasca on rich and poor medium formulations.

Panels show colony-forming units (a) and most probable number estimates (b) for water samples inoculated into different medium treatments. Error bars denote the 95% confidence intervals for the estimates.

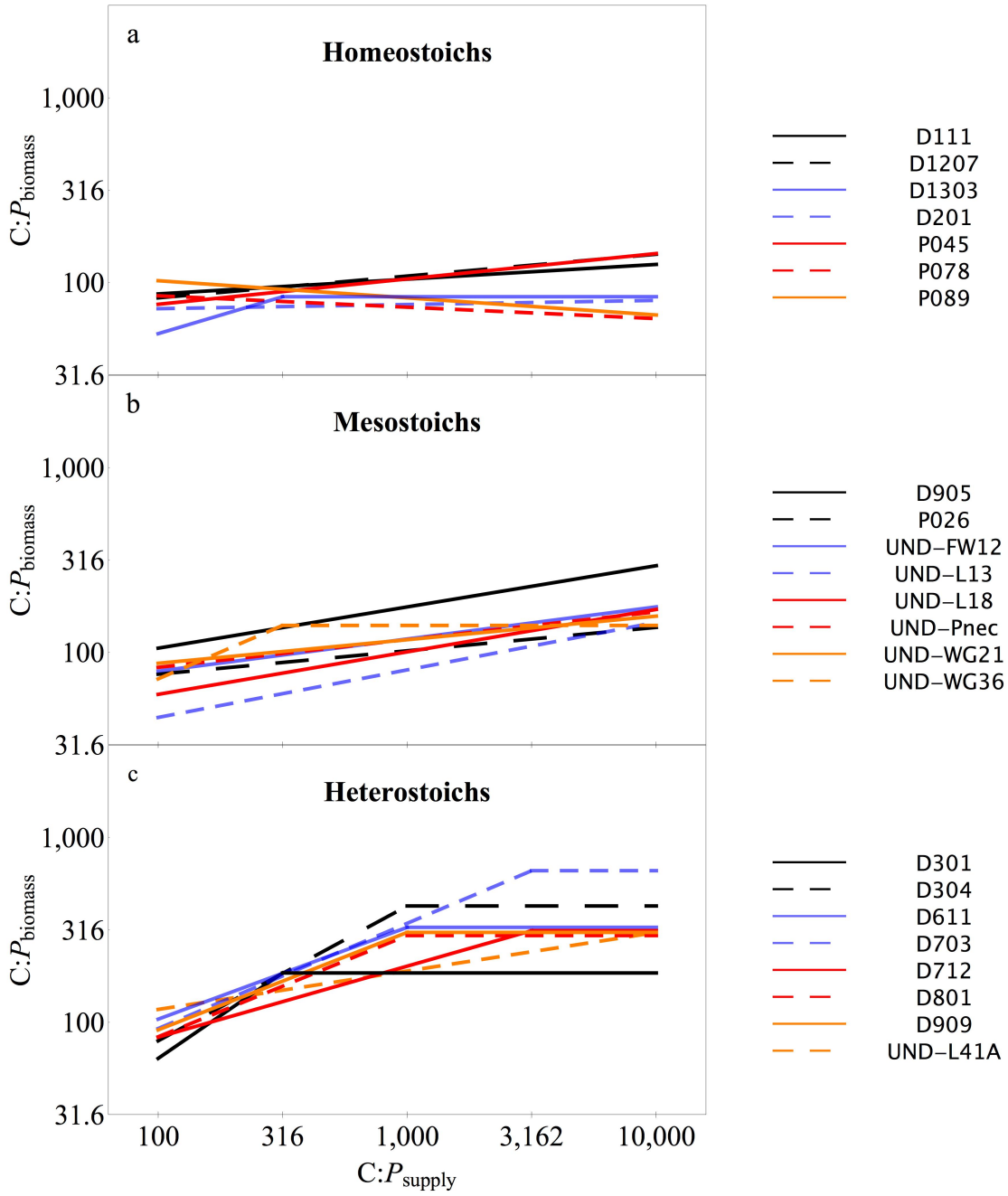

Figure 3-2. Biomass C:P stoichiometry across C:P$_{supply}$ for isolates in each category. Biomass C:P stoichiometry for the isolates in each category: homeostoichs (a), mesostoichs (b), and heterostoichs (c). Lines denote the segmented linear regression as described in the text.

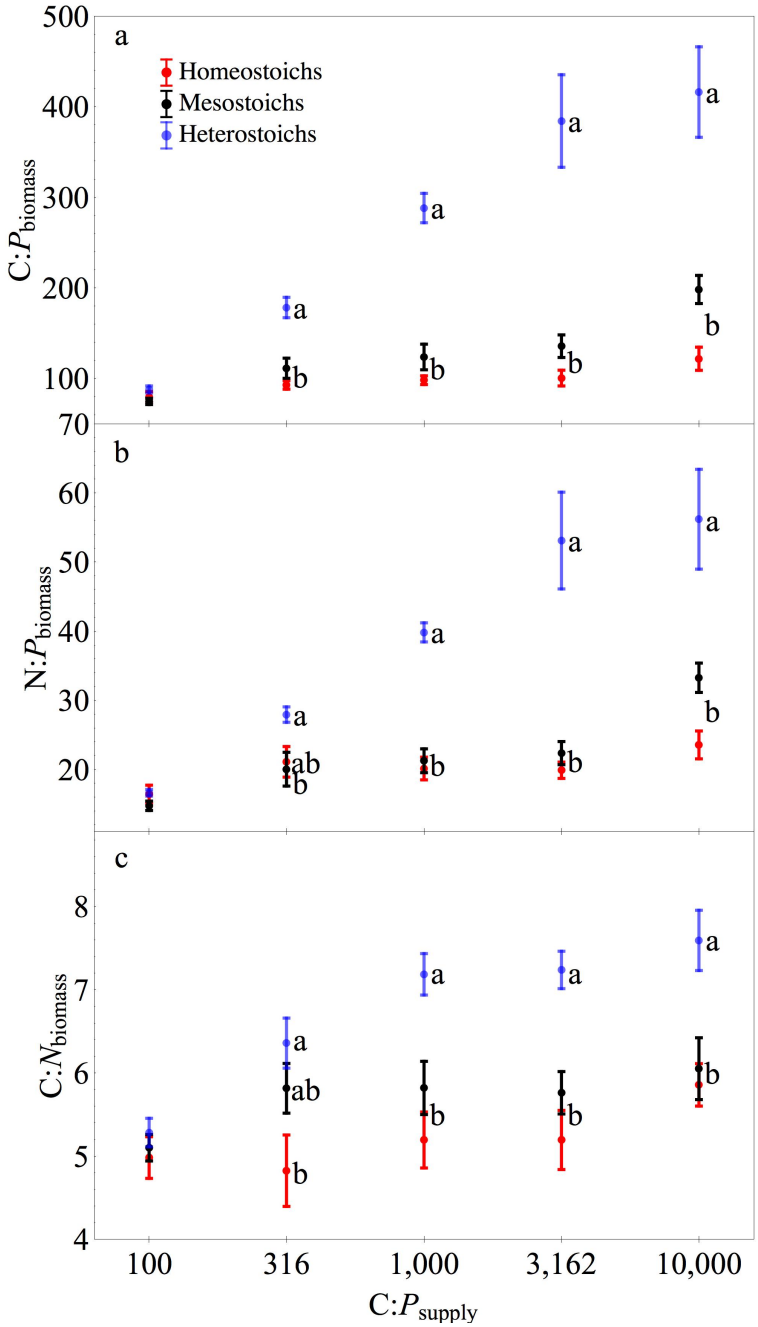

Figure 3-3. Biomass stoichiometry of isolates by stoichiometric category.

Separate panels for C:P (a), N:P (b), and C:N (c) stoichiometry across $C:P_{supply}$, with the mean and standard error by stoichiometric classification. Lower case letters denote significantly different subsets of the stoichiometric categories at each level of C:P supply (Tukey HSD, $p < 0.05$).

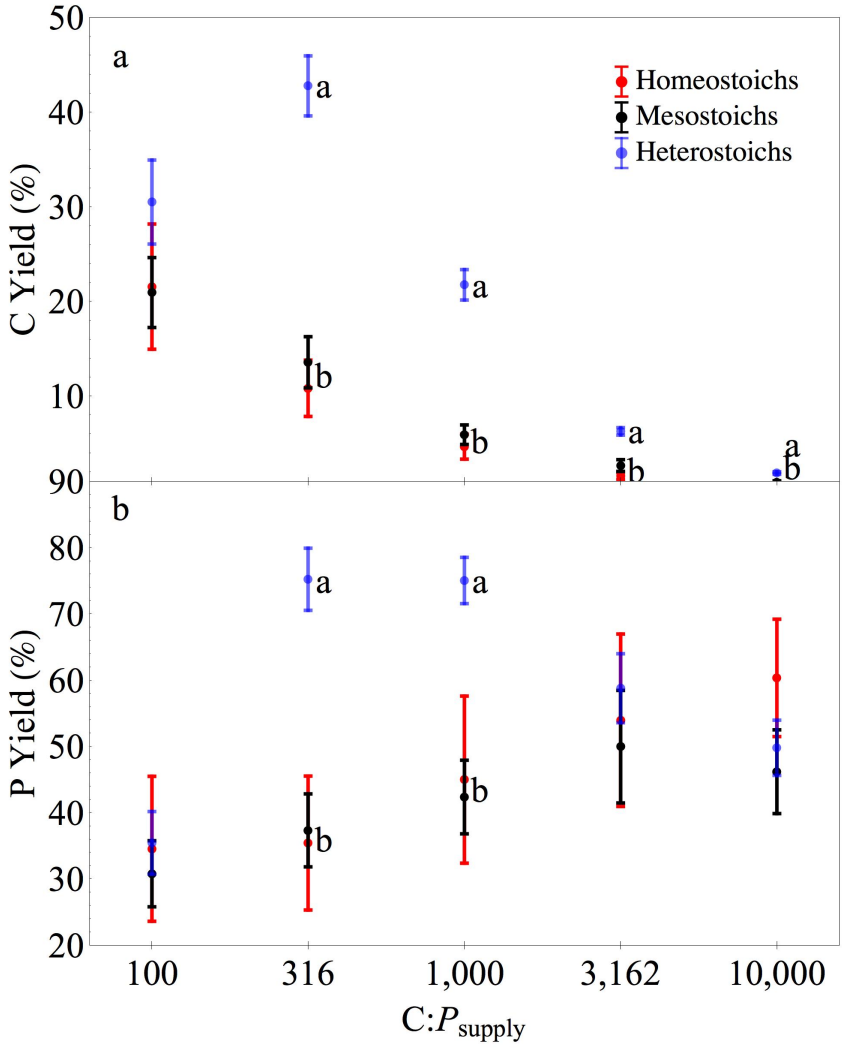

Figure 3-4. Carbon and phosphorus yields of isolates by stoichiometric category. Separate panels for carbon (a) and phosphorus (b) yields across C:P_{supply}, with the mean and standard error by stoichiometric classification. Yield is defined as the percentage of C or P supplied in the medium that is harvested as bacterial biomass. Lower case letters denote significantly different subsets of the categories at each level of C:P_{supply} (Tukey HSD, $p < 0.05$).

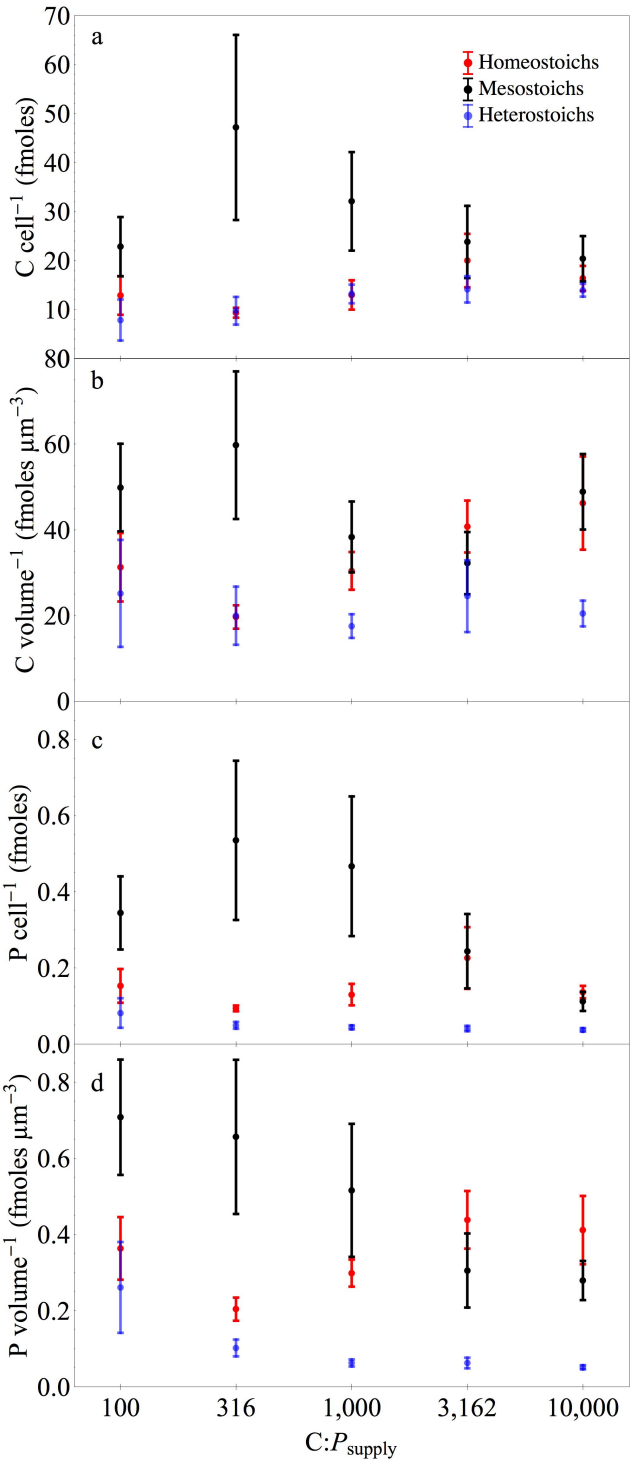

Figure 3-5. Carbon and phosphorus quotas of isolates by stoichiometric category. Separate panels for cellular carbon (a and b) and phosphorus (c, and d) quotas across C:P_{supply}, with the mean and standard error for each stoichiometric classification.

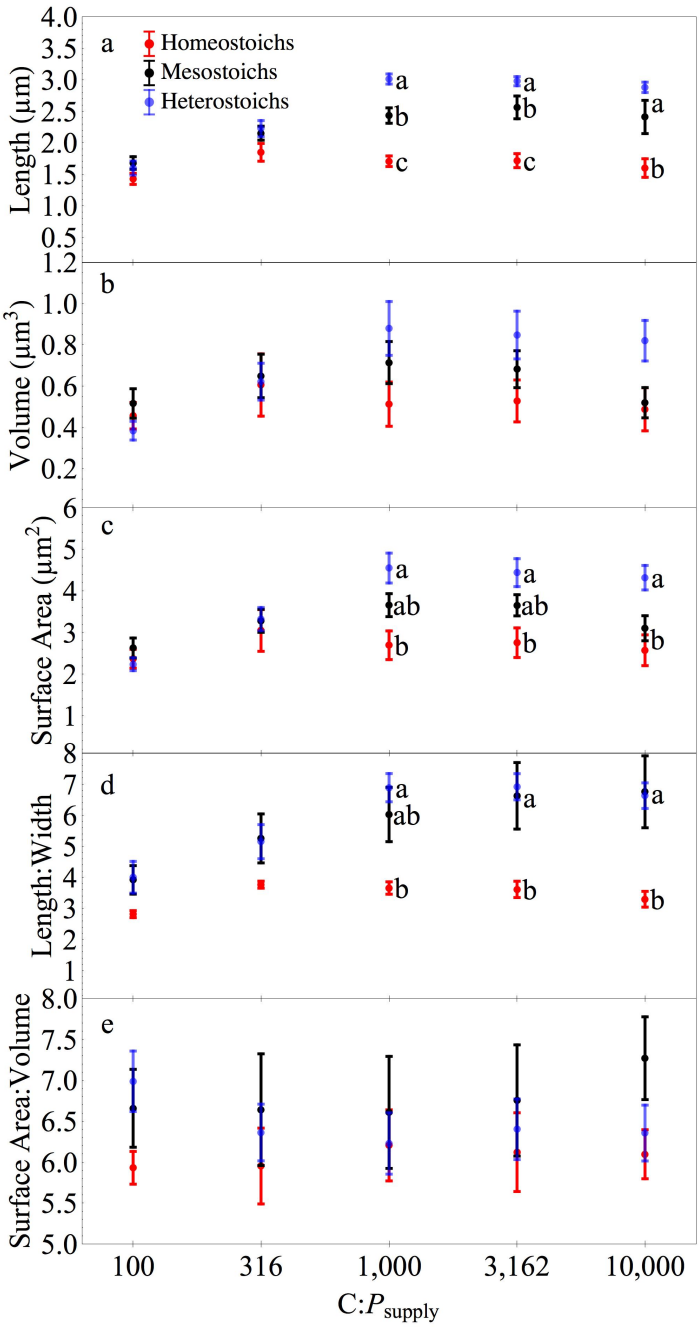

Figure 3-6. Morphometry of isolates by stoichiometric category.

Cell morphometry of the isolates across C:P supply with the means and standard error by stoichiometric classification. Panels for length (a), volume (b), surface area (c), length : width (d), and surface area : volume (e). Lower case letters denote significantly different subsets of the categories at each level of $C:P_{supply}$ (Tukey HSD, $p < 0.05$).

Table 3-1. Location and characteristics of the source lakes.

Lake	Location (Latitude, Longitude)	Temperature (ºC)	Chlorophyll-a ($\mu g\ L^{-1}$)	Dissolved Organic Carbon (mmoles C L^{-1})	Total Dissolved Nitrogen (mmoles N L^{-1})	Total Dissolved Phosphorus ($\mu moles\ L^{-1}$)
Lake Itasca	47.212ºN, 95.179ºW	17.0	7.0	0.416	0.191	1.07
Long Lake	47.276ºN, 95.297ºW	13.5	3.1	0.292	0.228	0.25

Table 3-2. Source and taxonomic affiliation of the strains used for this study.

Strain ID	Taxonomic affiliation	Source	Isolation method
D111	*Betaproteobacteria, Hylemonella*	Lake Itasca, MN	BMM 100:1
D201	*Betaproteobacteria, Hylemonella*	Long Lake, MN	BMM 100:1
D206	*Alphaproteobacteria, Brevundimonas*	Long Lake, MN	BMM 100:1
D301	*Alphaproteobacteria, Rhizobium*	Long Lake, MN	BMM 100,000:1
D304	*Alphaproteobacteria, Rhizobium*	Long Lake, MN	BMM 100,000:1
D611	*Alphaproteobacteria, Brevundimonas*	Long Lake, MN	Sterile Lake Water
D703	*Alphaproteobacteria, Brevundimonas*	Long Lake, MN	Sterile Lake Water
D712	*Alphaproteobacteria, Brevundimonas*	Long Lake, MN	Sterile Lake Water
D801	*Alphaproteobacteria, Brevundimonas*	Long Lake, MN	Sterile Lake Water
D905	*Alphaproteobacteria, Brevundimonas*	Long Lake, MN	Sterile Lake Water
D909	*Alphaproteobacteria, Brevundimonas*	Lake Itasca, MN	Nutrient Broth
D1207	*Betaproteobacteria, Achromobacter*	Long Lake, MN	Nutrient Broth
D1303	*Betaproteobacteria, Achromobacter*	Long Lake, MN	Nutrient Broth
P026	unique partial sequence	Long Lake, MN	BMM 100,000:1
P045	Alphaproteobacteria, Agrobacterium	Long Lake, MN	Nutrient Broth
P078	Actinobacteria, Microbacterium	Lake Itasca, MN	Nutrient Broth
P089	not sequenced	Lake Itasca, MN	Nutrient Broth
UND-FW12	*Betaproteobacteria, betII (Pnec)*	Pleasant Lake, IN	WC minimal medium
UND-L13	*Betaproteobacteria*	Little Long Lake, MI	WC minimal medium
UND-L18	*Gammaproteobacteria, gamIV gamIV-A Pseudo A1*	Little Long Lake, MI	WC minimal medium
UND-L41A	*Alphaproteobacteria, alfII Brev*	Little Long Lake, MI	WC minimal medium
UND-Pnec	*Polynucleobacter necessarius*	DSMZ culture collection	-
UND-WG21	*Bacteroidetes, Flavobacteria*	Wintergreen Lake, MI	WC minimal medium
UND-WG36	*Gammaproteobacteria, gamII gamII-A*	Wintergreen Lake, MI	WC minimal medium

Table 3-3. Growth rate, biomass stoichiometry, and strength of homeostasis for isolates.

Stoichiometry data are the ranges of mean values for each level of $C:P_{supply}$. The slope is the linear regression below the breakpoint in $C:P_{supply}$. The p-value associated with the one-way ANOVA of each parameter versus $C:P_{supply}$ is denoted by * ($p < 0.05$), ** ($p < 0.01$), and *** ($p < 0.001$). Underlining denotes samples with insufficient replication for ANOVA, italics denote strains where fewer than 10 chemostats were within detection limits for the parameter.

Isolate	μ_{max}	$C:P_{biomass}$	$N:P_{biomass}$	Slope
D111	0.116	88-132*	13-19	0.037
D201	0.153	*68-78*	*25-33*	0.036
D206	0.089	-	-	-
D301	0.142	64-280*	15-38*	0.926
D304	0.089	75-399**	16-43*	0.730
D611	0.091	103-374***	19-53***	0.497
D703	0.091	104-869***	19-124***	0.570
D712	0.124	87-297***	16-44**	0.384
D801	0.120	80-421***	15-67***	0.548
D905	0.112	90-287***	17-43**	0.480
D909	0.091	91-566**	17-78**	0.528
D1207	0.086	86-160*	19-28	0.079
D1303	0.138	53-116**	12-22*	0.400
P026	0.112	*62-160*	*9-22*	0.295
P045	0.219	67-146**	15-28*	0.464
P078	0.074	*66-85*	*15*	0
P089	0.222	*67-102*	*15-27*	-0.011
UND-FW12	0.078	80-179***	18-36***	0.146
UND-L13	0.342	50-241*	9-40*	-0.117
UND-L18	0.249	52-222*	11-25***	0.140
UND-L41A	0.144	100-372*	15-40***	0.158
UND-Pnec	0.204	*71-192*	*17-44*	-0.040
UND-WG21	0.097	79-162***	16-34***	0.350
UND-WG36	0.432	72-190**	13-32***	0.579

Table 3-4. Elemental content of the isolates.

Data are the ranges of mean values for each level of C:P_{supply}. The p-value associated with the one-way ANOVA of each parameter versus C:P_{supply} is denoted by * ($p < 0.05$), ** ($p < 0.01$), and *** ($p < 0.001$). Underlining denotes samples with insufficient replication for ANOVA, italics denote strains where fewer than 10 chemostats were within detection limits for the parameter.

Isolate	P/dry mass (%)	P cell^{-1} (fmoles)	C cell^{-1} (fmoles)	P volume^{-1} (fmoles µm^{-2})	C volume^{-1} (fmoles µm^{-2})
D111	0.57-1.09	0.191-0.245	17.7-31.1	0.726-0.960	67.7-121.61
D201	*0.17-0.38*	*0.015-0.074*	*1.03-5.79*	*0.054-0.341*	*3.68-26.7*
D206	-	*0.042-0.051*	-	*0.030-0.033*	-
D301	0.38-1.80**	0.062-0.075	4.4-17.5*	0.052-0.110*	7-14.5
D304	0.33-1.74	0.028-0.06*	2.1-22.0**	0.028-0.039	2.9-12.7**
D611	0.36-1.05***	0.019-0.031**	2.0-11.5***	0.042-0.062	6.3-18.8***
D703	0.03-0.76***	0.007-0.042	1.0-15.4**	0.009-0.059	3.6-24.8*
D712	0.06-1.25**	0.023-0.042	2.1-8.4***	0.041-0.09	6.8-14.8**
D801	0.11-1.20***	0.021-0.029	1.7-12.1***	0.037-0.096**	7.7-17.6**
D905	0.28-1.18***	0.026-0.038	2.9-9.6***	0.044-0.127*	9.2-15
D909	0.11-0.85***	0.033-0.084	3.1-37.5*	0.048-0.16	13.1-83.5
D1207	0.68-1.42*	0.032-0.13**	2.6-17.5***	0.106-0.493**	8.3-54.7***
D1303	1.01-2.08**	0.076-0.12	4.0-12.5***	0.155-0.259	8.2-25**
P026	0.32-1.35	*0.143-0.302*	*18.0-21.9*	*0.568-1.264*	*71.7-91.2*
P045	0.29-1.52***	0.11-0.23	11.7-27.8*	0.11-0.284	12.3-33.7
P078	*0.21-0.31*	*0.071-0.146*	*6.07-9.25*	*0.335-0.603*	*28.5-38.3*
P089	*0.27-1.03*	*0.440-0.768*	*41.19-50.96*	*0.756-0.888*	*58.9-71.8*
UND-FW12	0.24-0.84**	0.037-0.088*	5.4-9.2	0.124-0.38*	17.8-32.5
UND-L13	0.21-1.92*	*0.92-1.57*	*73.7-80.8*	*0.892-1.526*	*72.1-85.4*
UND-L18	*0.28-1.85***	0.28-1.18	27.6-142.6	0.29-1.031*	29.2-125.2
UND-L41A	0.28-1.13**	0.024-0.45**	4.7-46.5	0.06-1.238**	11.5-126.4*
UND-Pnec	*0.05-0.36*	*0.118-0.306*	*22.4-24.0*	*0.484-1.32*	*92.3-103.6*
UND-WG21	0.20-1.18**	*0.039-0.15**	*4.7-12.0*	*0.106-0.335**	*12.7-26.6*
UND-WG36	0.25-1.40***	0.10-0.17*	12.1-21.9	0.173-0.362*	25.9-36.5

Chapter 4: Phosphorus Content of Aquatic Heterotrophic Bacteria: How Low Can They Go?

Summary

The element content of bacteria is central to our understanding of microbial biogeochemical cycling. Bacteria with high biomass phosphorus (P) content have higher demands for P and are expected to function as net sinks for P within ecosystems. In contrast, bacteria with lower or more variable nutrient content are capable of growth at low P availability and can decouple rates of carbon (C), nitrogen (N) and P cycling. Recent studies have demonstrated that the P content of aquatic heterotrophic bacteria is variable and is sensitive to P availability. To determine the extent of flexibility in bacterial biomass composition and characterize how bacteria minimize their P content, I cultured assemblages of bacteria from a temperate lake using chemostats with varying P supply. These assemblage cultures were more flexible in biomass stoichiometry than almost all previously published measurements (C:P from < 30:1 to > 10,000:1 and N:P from 6.7:1 to > 1,600:1). The P content of bacteria ranged from 3.5% of dry mass under P-replete conditions to < 0.01% under P limitation. The assemblage cultures achieved this plasticity in biomass stoichiometry by both decreasing P quotas and increasing quotas of C and N in response to P limitation. The major pools of cellular P (nucleic acids, protein-P, lipid-P, and polyphosphate) all showed proportional increases as cell P quotas decreased. I use these new estimates of biomass composition to model the effect of non-homeostasis on C and P use by microbial assemblages in variable resource environments.

Introduction

Heterotrophic bacteria occupy a central role in the biogeochemistry of aquatic ecosystems. Despite their small biomass in comparison to other groups of plankton, bacteria have a disproportionate influence in nutrient uptake (Cotner and Wetzel 1992), nutrient regeneration (Azam et al. 1983), and respiration (Biddanda et al. 2001; Cole et

al. 1988) at the ecosystem-scale. As consumers of organic carbon (C) and dissolved nitrogen (N) and phosphorus (P), the elemental content of bacterial biomass affects the rates at which they remineralize C (Goldman et al. 1987) and their effect on the availability of nutrients. Heterotrophic bacteria are commonly assumed to have nutrient-rich biomass (Tambi et al. 2009; Tanaka et al. 2009) and function as net sinks for inorganic N and P (Kirchman 1994) while remineralizing organic C (Cole et al. 1988).

Many studies have found high nutrient content and low C:P, and N:P ratios in bacterial biomass (Bratbak 1985; Fagerbakke et al. 1996). Several strains of heterotrophic bacteria from the class γ-Proteobacteria (*Escherichia, Pseudomonas, and Vibrio*) have low cellular C:P with little or modest flexibility in their phosphorus content (Bratbak 1985; Løvdal et al. 2008; Makino et al. 2003). In contrast, assemblages of bacteria from lakes adjust their biomass C:P ratios ($C:P_{biomass}$) in kind with their resources and often have higher $C:P_{biomass}$ than single strains (Makino and Cotner 2004; Tezuka 1990; chapter 2; chapter 3). Recent work with environmental samples and axenic cultures demonstrates that some bacteria have lower and more variable nutrient content than previously assumed (Cotner et al. 2010) and that strains differ in how they regulate their C:N:P stoichiometry (Phillips et al. in preparation; Scott et al. 2012; chapter 3).

The physiological basis for bacterial nutrient content and stoichiometry can be traced to cellular constituents, which have variable C:N:P stoichiometry (Elser et al. 1996). Differences in the quantities of protein, nucleic acids, lipids, storage compounds, and structural molecules affect the gross chemical composition of organisms (Loladze and Elser 2011; Sterner and Elser 2002). For example, biomass P content is positively correlated with growth rate for many organisms (Elser et al. 2003), including populations and assemblages of heterotrophic bacteria (Makino and Cotner 2004; Makino et al. 2003). This correlation is due to the increased requirement for P-rich ribosomes at higher growth rates (Elser et al. 2000b).

Responses to P stress can be assigned to three categories: mechanisms to increase acquisition and minimize loss of P, mechanisms to reduce the P content of the cell, and responses involving a reduction in realized growth rate or dormancy. A combination of these strategies can be exhibited by a single bacterium. Bacteria possess multiple

mechanisms to acquire P when it is scarce in the environment. Many bacteria employ high-affinity transporters to acquire inorganic phosphate at low concentrations (Chan and Torriani 1996; Rosenberg et al. 1979) or produce extracellular enzymes to liberate organic P in the environment (Cotner and Wetzel 1991). Additionally, some bacteria exhibit chemotaxis along phosphate gradients (Hutz et al. 2011) or increase the cell surface area in order to facilitate diffusive P uptake (Thingstad et al. 2005).

Strategies for minimizing P content under P limitation (i.e. non-homeostasis) include replacing phospholipids with P-free lipids (Benning et al. 1995; Minnikin et al. 1974; Zavaleta-Pastor et al. 2010) and remodeling cell wall composition (Lahooti and Harwood 1999). Although it has not been studied in the context of ecological stoichiometry, non-homeostatic bacteria could potentially alter their P content by allocating P to either inorganic polyphosphate (Harold 1962; Jahid et al. 2006; Kornberg 1995) or other P-rich molecules (RNA, ATP, and cell walls) (Sterner and Elser 2002). In contrast, homeostatic organisms must respond to P limitation by increasing their nutrient acquisition rate or reducing their growth rate. The dependence of realized growth rate upon resource availability (Monod 1949) implies that all microbes will exhibit reduced growth rates at some level of P limitation. However, bacteria differ in their uptake and growth kinetics for P (Vadstein 1998) and therefore the level of P availability that they require in order to maintain non-zero net growth. Each of these strategies and mechanisms has different impacts on cell function and this could lead to tradeoffs in energy and resource allocation.

In a reciprocal interaction similar to that proposed by Redfield for marine phytoplankton (Redfield 1958), bacterial biomass composition also affects the regeneration and availability of dissolved C, N, and P pools. It is well established in ecological stoichiometry that the ratio of elements regenerated by consumers is controlled by the ratio of those elements in food resources and the demand and efficiency of use within the consumer biomass (Frost et al. 2005; Sterner and Elser 2002; Touratier et al. 2001). The effect of resource imbalance on regeneration has been demonstrated empirically in several classes of consumers (Elser and Urabe 1999; Nakano 1994) and in consumer-resource models (Sterner 1990; Sterner et al. 1992). The majority of these

studies and models are suited to phagotrophic consumers such as zooplankton and macroinvertebrates that consume C, N, and P in discrete packages rather than independently. In contrast, heterotrophic bacteria can consume organic carbon and inorganic nutrients independently and thus alter the stoichiometry of dissolved C, N, and P through both uptake and assimilation of inorganic forms and remineralization of organic material. Since flexible stoichiometry is competitive under low P availability (chapter 2), assemblages in low P environments could decouple C and P cycling by storing surplus C and minimizing their P demands.

There remains a need to understand how stoichiometric flexibility (i.e. non-homeostasis) affects the relationship between bacteria and their resources in ecosystems. Our understanding of the elemental content of bacteria is changing: we have underestimated their flexibility and this has implications for understanding their role in carbon and nutrient cycling, particularly when resources are unbalanced. I sought to answer two questions in this chapter: 1) What is the range of cellular phosphorus content attainable by aquatic heterotrophic bacteria? And 2) How do bacteria minimize their phosphorus content in response to phosphorus stress? I addressed these questions by culturing assemblages of bacteria under variable P concentrations and measuring their cellular elemental content. I found that bacteria were able to alter their P content from more than 3% to less than 0.01% of dry mass ($C:P_{biomass}$ of < 30:1 to > 10,000:1) and that they did this by altering allocation to multiple P pools within the cell.

Methods

Source Lake and Bacterial Inocula. The bacterial-sized fraction of lake water was collected from Christmas Lake, a small lake in southeastern Minnesota (Biddanda et al. 2001; Stets and Cotner 2008). Samples of water were collected from the surface of the lake on July 17, 2011 (Experiment 1, water temperature 25ºC) and on June 07, 2012 (Experiment 2, water temperature 21ºC) using acid-washed sterile bottles. Within one hour of collection, the water samples were filtered through sterilized Whatman GF/A filters (nominal pore size 1.6 μm) to exclude flagellate grazers and phytoplankton.

Growth Media. Basal Microbiological Medium was prepared following Tanner (2002) using 18.2 mΩ deionized water (Milli-Q Nanopure System). All glassware was soaked in 10% hydrochloric acid and rinsed with deionized water. All chemical stocks were ACS grade or equivalent. Glucose was supplied at 23.88 mmoles-C L^{-1} as the sole source of carbon and energy, and ammonium chloride was supplied at 18.69 mmoles-N L^{-1} to ensure nitrogen sufficiency. Additional minerals, vitamins, and trace metals were supplied at concentrations described in Tanner (2002). To alter the C:P supplied to the cultures ($C:P_{supply}$), potassium phosphate was added at eight levels from 755 µmoles-P L^{-1} ($C:P_{supply}$ = 31.6) to 0.239 µmoles-P L^{-1} ($C:P_{supply}$ = 100,000). In Experiment 2, 0.108 µmoles L^{-1} phosphate was added to the medium to provide a $C:P_{supply}$ ratio of 221,000:1 and a second medium treatment included no added phosphate. The medium was buffered at pH 7.2 to 7.4 using 11 mmoles L^{-1} 3-(N-Morpholino)propanesulfonic acid (MOPS). The medium was filter-sterilized using 0.22 µm pore-size filters (Fisher SteriCup).

The total phosphorus content of the medium components without added phosphate was determined separately for concentrated stocks of the glucose, MOPS buffer, and solutions of vitamins, minerals, and trace metals using the ascorbic acid-molybdenum method, following digestion with 25 g L^{-1} potassium persulfate at 121ºC for 30 minutes (APHA 1995). The soluble reactive phosphorus content of the medium was measured directly using the ascorbic acid-molybdenum method (APHA 1995). The detection limit for the total phosphorus measurements was 0.50 µmoles-P L^{-1} in concentrated stocks. Concentrations below detection were accepted as no greater than the detection limit. The background phosphorus content of the finished medium was less than 0.131 µmoles-P L^{-1} as total P and less than 0.06 µmoles-P L^{-1} as soluble reactive P.

Chemostat Cultures - Experiment 1. Triplicate 100 mL batch cultures for each level of $C:P_{supply}$ were inoculated with 20 mL of the bacterial-sized fraction of lake water. Cultures were incubated at 22ºC on a gyratory shaker for 48 hours and then 5 mL from each of the batch cultures was used to inoculate chemostats at the same $C:P_{supply}$. Chemostats, medium reservoirs, and tubing were acid-soaked, rinsed with deionized water, and sterilized prior to use. Continuous cultures were maintained in 100 mL polypropylene chemostats, diluted with sterile medium at a rate of 0.33 d^{-1}, supplied by a

multi-channel peristaltic pump (Watson Marlow Bredel). The dilution rate is equivalent to a doubling time of 2.1 days, which is likely faster than the realized growth rate of many bacteria in natural systems, but is similar to growth rates observed for communities in mesocosm experiments (Cotner et al. 2001). The chemostats were continually aerated and mixed with 0.2 µm filtered air and maintained in the dark at 24 ºC. Triplicate chemostat cultures were run at each level of phosphorus supply for 21 days prior to harvesting samples for analyses. Due to insufficient biomass at the highest $C:P_{supply}$, phosphorus allocation into various cellular pools was measured only between $C:P_{supply}$ of 31.6:1 to 3162:1 (10,000:1 for nucleic acids).

Chemostat Cultures - Experiment 2. Triplicate 100 mL batch cultures were inoculated with 20 mL of the bacteria-sized fraction of lake water at each level of $C:P_{supply}$. The batch cultures were incubated at 22ºC on a gyratory shaker for 72 hours, and then 20 mL from each of the batch cultures were used to inoculate each chemostat. Continuous cultures were maintained in 1 L polypropylene chemostats and diluted with medium at a rate of 0.33 d^{-1} and were continually aerated and mixed with 0.2 µm filtered air and maintained in the dark at 22ºC. Three replicate chemostat cultures were run at both levels of phosphorus supply and the cultures were maintained for 29 days prior to harvesting samples for analyses.

Dry Mass and Cellular Element Content. I collected replicate samples (3 for Experiment 1, 5 for Experiment 2) of the cultures for measuring dry mass and cellular C, N, and P. Aliquots of the cultures were filtered onto pre-combusted acid-rinsed Whatman GF/F filters using low vacuum pressure (< 100 mm Hg). The filters were rinsed with deionized water to remove excess medium and stored at -20ºC until analysis. Dry mass was determined from samples that were collected on filters that had been ashed, dried at 60ºC for three days, and weighed to the nearest microgram. After filtration, the filters were dried at 60ºC for seven days, weighed again, and the difference was used as dry mass biomass. Filter samples for C and N content were dried at 60ºC for five days and analyzed using a CHN analyzer (Perkin-Elmer 2400CHN) with acetanilide (Elemental Microanalysis ltd.) as a reference standard and an internal zooplankton recovery standard. The detection limits were 20 µg C and 2.5 µg N per filter. Filter samples for phosphorus

were digested with 25 g L^{-1} potassium persulfate at 121ºC for 30 minutes (APHA 1995). Following digestion, the phosphorus content was determined using the ascorbic acid molybdenum method. Spinach leaf reference material (NIST) was used as a recovery standard for all phosphorus analyses. The detection limit for phosphorus was 1.2 nmoles P per filter in Experiment 1 and 7.6 nmoles P in Experiment 2, after subtraction of the blank filter content.

Cell Abundance And Morphometry. Aliquots of the chemostat cultures were preserved with 0.2 µm-filtered formaldehyde (3.7 % by volume) and stored at 4ºC. Samples were prepared for microscopic enumeration using sodium pyrophosphate and sonication (Velji and Albright 1993). Duplicate samples from each chemostat were stained with acridine orange, filtered onto black polycarbonate membrane filters (Nucleopore, 0.2 µm pore size), and mounted to slides for microscopy (Hobbie et al. 1977). Cell counts and morphometry measurements were performed at 1000x magnification using an Olympus BX40 epifluorescence microscope. For cell counts, at least 10 fields and 300 cells on each filter were enumerated manually. Photomicrographs were obtained using a digital camera (Spot 2, Diagnostic Instruments) at 1000x magnification. Cell dimensions (length, width, planar area, and planar perimeter) were measured for at least 600 cells from each chemostat using image analysis software (Image Pro Plus, Media Cybernetics). Cell shape was measured as cylinders capped with two hemispheres (Hillebrand et al. 1999). Due to the high proportion of curved cells, cell dimensions were calculated using the planar area and perimeter, rather than the box (feret) length and width. The equations used for estimating, cell length, width, surface area, and volume are given in Appendix D.

Lipid Phosphorus Content. Samples for lipid phosphorus content were collected onto ashed and acid-rinsed filters (Whatman GF/F), flash frozen in liquid nitrogen, and stored at -70ºC until analysis. Lipid phosphorus content (lipid-P) of cells in Experiment 1 was determined using the chloroform extraction method described by Bligh and Dyer (1959) and modified by White et al. (1979). The filters were suspended in 1.5 mL of buffer (50 mmoles L^{-1} tris(hydroxymethyl)aminomethane at pH 7.4) and mixed by vortex. Chloroform (1.88 mL) and methanol (3.75) were added to the samples, followed

by mixing. The mixture was extracted overnight at room temperature. The phases were separated by the addition of deionized water (1.88 mL) and chloroform (1.88 mL), followed by centrifugation at 600x g for 15 minutes. A portion of the chloroform phase was re-extracted with water and methanol and the final chloroform phase was transferred to an acid-soaked borosilicate glass tube and then the solvent was evaporated under a stream of 0.2 μm filtered air. The tubes were heated to 550 ºC for 4 hours to combust the carbon and liberate the phosphorus (Suzumura 2008). Filter blanks were included in each run. The phosphorus residue in the tubes was dissolved by adding 10N sulfuric acid (0.4 mL) and mixing the contents by vortex. Deionized water (5.0 mL) was added to each sample and the tubes were boiled 15 minutes in a water bath. Once cooled, the phosphorus content was measured using the ascorbic acid molybdenum method with potassium phosphate as a primary standard. The detection limit for lipid-P was 6.3 nmoles P per filter.

Protein Phosphorus Content. Phosphorus in the protein fraction (protein-P) in Experiment 1 was quantified in extracts prepared following the phenol extraction method of Carpentier et al. (2005). Samples of the cultures were flash-frozen in liquid nitrogen and stored at -70ºC until analysis. The samples were thawed and 4.9 mL of the suspension was added to 2.62 mL of sucrose solution (2.52 moles L^{-1}) and 7.52 mL water-saturated phenol. All solutions were maintained at 4ºC. The mixtures were vortexed for 3 minutes, followed by centrifugation at 600x g for 3 minutes to separate the phases. A portion of the phenol phase was re-extracted in an equal volume of extraction buffer (0.875 moles L^{-1} sucrose, 100 mmoles L^{-1} potassium chloride, 50 mmoles L^{-1} tris(hydroxymethyl)aminomethane, and 5 mmoles L^{-1} ethylene(diamine)tetraacetic acid, pH 8.5), followed by centrifugation at 600x g for 3 minutes. A portion of the final phenol phase was mixed with 7 volumes of ammonium acetate in methanol (100 mmoles L^{-1}) and allowed to precipitate proteins overnight at -20 ºC. Following centrifugation, the protein pellets were suspended in acetone and transferred to acid-soaked borosilicate glass tubes. The protein extracts were dried, combusted, and analyzed for phosphorus content following the procedure for lipid phosphorus. The detection limit for protein-P was 7.8 nmoles P per filter.

Polyphosphate Content. Polyphosphate content of the chemostat cultures was measured using a method developed by Aschar-Sobbi and others (2008) and subsequently implemented in marine systems (Diaz and Ingall 2010; Martin and Van Mooy 2013) with modifications to ensure specificity for polyphosphate (Phillips et al. in preparation). The method uses DAPI (4',6-diamidino-2-phenylindole), which forms a fluorescent complex with polyphosphate and nucleic acids. Using an excitation wavelength of 415 nm and an emission wavelength of 550 nm distinguishes the fluorescence from DAPI-polyphosphate from that of DAPI-DNA, which has a fluorescence excitation peak at 360 nm and emission at 475 nm (Aschar-Sobbi et al. 2008).

Samples for polyphosphate content were rapidly frozen in liquid nitrogen and stored at -70ºC until analysis. Sodium polyphosphate with 45-monomer chain length (Sigma Aldrich) was used as a standard. Polyphosphate content of the standards was verified by digesting the material in 1 mole L^{-1} hydrochloric acid for 15 minutes at 100ºC (Harold 1966) and measuring the hydrolyzed phosphate. Fresh cell-free medium was used as a blank for the analysis. The sample aliquots were thawed and then heated to 105ºC for 20 minutes in an autoclave to extract the polyphosphate from the cells (Eixler et al. 2005). The hot extracts were filtered through a Whatman GF/F filter to remove cell debris and were subsequently digested with a non-specific nuclease (Benzonase, Merck) to eliminate fluorescence from DNA and RNA. Aliquots (2.4 mL) of the extract were mixed with 200 µL of digestion buffer (150 units mL^{-1} Benzonase, 750 mmoles L^{-1} tris(hydroxymethyl)aminomethane, and 6.5 mmoles L^{-1} magnesium chloride at pH 8.5) and incubated on a gyratory shaker for one hour. Paired samples for each chemostat were analyzed to isolate the fluorescence due to polyphosphate from the background fluorescence. Magnesium chloride (final concentration 12.37 mmoles L^{-1}) was added to one of the paired samples (quenched sample) to inhibit fluorescence of the DAPI-polyphosphate complex (Aschar-Sobbi et al. 2008).

After incubating for 10 minutes, 500 µL of sample buffer (58.8 mmoles L^{-1} DAPI, 2.6 mmoles L^{-1} ethylene(diamine)tetraacetic acid, 120 mmoles L^{-1} 4-(2-hydroxyethyl)-1-piperazineethanesulfonic acid, and 900 mmoles L^{-1} potassium chloride at pH 7.00) was

added to each sample. The final concentration of magnesium in the quenched sample (10 mmoles L^{-1}) was sufficient to quench the fluorescence of polyphosphate at the range of the sample concentrations measured. The samples were mixed and incubated in the dark for one hour. The fluorescence was measured at 415 nm excitation (5 nm slit widths) and 500 nm emission (5 nm slit widths) using a Fluoromax 3 fluorometer (Horbia Jobin Yvon) with a quartz cuvette (1 cm path length). Sample fluorescence was integrated over 0.5 seconds at 10 second intervals for one minute. The difference in maximum fluorescence of the raw and quenched standards and samples was used to determine the polyphosphate content of the samples. The detection limit for the assay was 62 nmoles-P L^{-1} in the original volume.

Nucleic Acid Content. Nucleic acid content of the cultures was determined using Ribogreen (Invitrogen) and specific digestion of RNA (Gorokhova and Kyle 2002; Makino et al. 2003). Triplicate samples for nucleic acids were filtered onto 0.2 μm polycarbonate filters (Nucleopore), flash-frozen in liquid nitrogen, and stored at -70ºC until analysis. DNA (from *E. coli* strain B, Type VIII, Sigma) and RNA (from *S. cerevisiae*, Sigma) were used as standards and the concentrations in stocks were verified by absorbance at 260 nm (Makino et al. 2003). The filters were suspended in 2.5 mL of extraction buffer (5.67 mmoles L^{-1} sodium lauryl sarcosine, 8.35 mmoles L^{-1} tris(hydroxymethyl) aminomethane, and 0.84 mmoles L^{-1} ethylene(diamine)tetraacetic acid at pH 8.0 in sterile nuclease-free water). Following sonication in an ultrasonic bath filled with ice water for 30 minutes, the filters were extracted for 2 hours on a gyratory shaker at room temperature. Samples and standards (75 μL) were added in triplicate to paired black 96-well microtiter plates. One set of plates was treated with 20 μL of RNase type A solution (10 μg/mL, Promega) to remove fluorescence due to RNA and the other set of plates was treated with 20 μL of nuclease-free water. Following incubation at room temperature for one hour, 75 μL of RiboGreen solution (RiboGreen stock diluted 1:200 in TE buffer) was added to each well and the plates were incubated for 10 minutes at room temperature in the dark. The fluorescence was measured at excitation of 485 nm (5 nm slit width) and emission at 518 nm (5 nm slit width) using a Fluoromax 3 fluorometer and MicroMax 384 plate reader (Horbia Jobin Yvon). The fluorescence of the RNase-

treated samples and standards was used to determine the DNA content. The difference in fluorescence between the control and RNase plates was used to determine the RNA content of the samples. The detection limit for DNA was 178 ng per filter and the detection limit for RNA was 473 ng per filter. The phosphorus content of both RNA and DNA was assumed to be 9% by mass (Sterner and Elser 2002).

Statistical Analyses. All biomass ratios ($C:P_{biomass}$, $C:N_{biomass}$, and $N:P_{biomass}$) are molar ratios. The effect of $C:P_{supply}$ on biomass composition was evaluated using a one-way analysis of variance (ANOVA) with $C:P_{supply}$ as a fixed effect. ANOVA tests on $C:P_{biomass}$ and $N:P_{biomass}$ stoichiometry were performed on $\log_{10}$-transformed values. Differences among $C:P_{supply}$ levels were evaluated using post-hoc Tukey's Honest Significant Difference tests. Morphometry measurements for Experiment 1 were $\log_{10}$ transformed to improve normality and homogenize variances. Morphometry data were analyzed with a one-way ANOVA with $C:P_{supply}$ as a fixed effect and a random effect of replicate, nested in level of $C:P_{supply}$. Correlations reported for morphological measurements are Pearson's product-moment correlations. Due to the low biomass of the chemostat cultures, detection limits were calculated and applied to each chemical assay (APHA 1995). The detection limits are the 99% confidence limits of the mean for method blanks.

Literature Dataset And Synthesis. To provide context for the measurements of bacterial element content presented in this chapter, I collected observations from similar studies previously published in the literature. The data included measurements of bacteria cellular C, N, and P and culture conditions. I assembled data from journals in microbiology, aquatic ecology, and microbial ecology. Data from the original publications were converted to common units and simple calculations were performed where applicable. Data were extracted from tables and supplementary materials where possible; otherwise image analysis was performed on figures. Unpublished data from mixed assemblage cultures (chapter 2) were included in the synthesis.

Model of Bacterial Stoichiometry and Resource Use. To evaluate the impacts of variable stoichiometry on bacterial assemblage function, I used a cell quota model of bacterial growth on organic C and inorganic N and P (Thingstad 1987; chapter 1). I

performed simulations of bacteria growing in chemostat conditions (dilution rate 0.1 h^{-1}, C supply at 10 μmoles L^{-1}, and $C:P_{supply}$ between 100:1 and 5,000:1) and populated the cell quotas for C and P using data from the literature and this study. Maximum specific uptake rates were increased for each quota range to satisfy the condition that $V_{max} > Q_{min}$. All other parameter values were set as described by Thingstad (1987). Results are analytical equilibriums and were obtained as described in chapter 1. The effluent C and P concentrations were used as indicators of the effect of the bacterial biomass on ambient dissolved C and P.

Results

Dry Mass and Elemental Content - Experiment 1. Dry mass and cell densities decreased with increasing $C:P_{supply}$ (ANOVA $p < 0.005$, $p < 1x10^{-11}$, Figure 4-1). Cell densities ranged from a mean of $6.8\ x10^{8}$ mL^{-1} at $C:P_{supply}$ of 31.6:1 to $5.7x10^{6}$ mL^{-1} at $C:P_{supply}$ of 100,000:1. Carbon content of the cells increased from a mean of 13.3 fmoles $cell^{-1}$ at $C:P_{supply}$ of 100:1 to 69.4 fmoles $cell^{-1}$ at $C:P_{supply}$ above 10,000:1. Relative to median cell volume, carbon content increased from a mean of 37 fmoles μm^{-3} at $C:P_{supply}$ of 100:1 to 170 fmoles μm^{-3} at $C:P_{supply}$ of 100,000:1. The carbon content as a proportion of dry mass showed no apparent response to $C:P_{supply}$, with a mean of 35% ($p > 0.50$). Growth yield for carbon decreased significantly from 43% to 1.7% between $C:P_{supply}$ of 31.6:1 and 100,000:1 ($p < 0.0001$). Nitrogen content of the cells increased from a mean of 4.2 fmoles $cell^{-1}$ at $C:P_{supply}$ of 31.6:1 to more than 9.2 fmoles $cell^{-1}$ at $C:P_{supply}$ above 10,000:1 ($p < 0.04$). The phosphorus content of the bacterial assemblage decreased from a mean of 0.62 fmoles P $cell^{-1}$ at a $C:P_{supply}$ of 31.6:1 to a mean of 0.055 fmoles P $cell^{-1}$ at a $C:P_{supply}$ of 100,000:1 ($p < 0.005$, Figure 4-1). Phosphorus content was below detection for two chemostats at $C:P_{supply}$ of 100,000:1 (≤ 0.052 and ≤ 0.126 fmoles $cell^{-1}$). Similarly, the phosphorus content decreased from a mean of 3.55% of dry mass at $C:P_{supply}$ of 31.6:1 to 0.017% at $C:P_{supply}$ of 100,000:1. Relative to median cell volume, phosphorus content decreased from a mean of 1.31 fmoles μm^{-3} at $C:P_{supply}$ of 100:1 to 0.195 fmoles μm^{-3} at $C:P_{supply}$ of 31,620:1.

Dry Mass and Elemental Content - Experiment 2. Bacterial dry mass and cell densities were low at both levels of $C:P_{supply}$ in Experiment 2 (Figure 4-1). Cell densities ranged from $8.7x10^5$ cells mL^{-1} to $1.7x10^6$ cells mL^{-1} and lacked any significant effect of medium treatment ($p = 0.52$, two-sample t-test, unequal variances). Dry mass in the chemostats ranged from 7.8 to 52.8 µg mL^{-1} and showed no significant effect of medium treatment ($p = 0.45$). Carbon content (range 90-1,146 fmoles $cell^{-1}$) and nitrogen content of the cells (range 89-160 fmoles $cell^{-1}$) did not differ significantly between treatments ($p > 0.50$). Relative to median cell volume, carbon content ranged from 134 fmoles μm^{-3} to 2,147 fmoles μm^{-3} and did not differ between treatments ($p > 0.05$). Nitrogen content ranged from 89 to 160 fmoles $cell^{-1}$, with one replicate of the treatment without added P below detection (< 8.5 fmoles $cell^{-1}$). Phosphorus content of the cells was variable (0.076 to 0.72 fmoles P $cell^{-1}$, and 0.111 to 0.703 fmoles μm^{-3}), but low relative to dry mass (0.006% to 0.050% P in dry mass) and showed no effect of medium treatment.

Biomass Stoichiometry - Experiment 1. The stoichiometry of the bacterial assemblage changed substantially in response to changes in the phosphorus supply (Figure 4-2). Mean $C:P_{biomass}$ increased significantly from 28:1 to 1,451:1, with a maximum of 2,903:1 (ANOVA, $p < 1x10^{-6}$). Over the linear range ($C:P_{supply}$ 100:1 to 3,162:1), the slope of the biomass-resource regression (chapter 1) was 0.56. Mean $N:P_{biomass}$ increased significantly ($p < 1x10^{-5}$) from 6.7 to 181:1, with a maximum of 311:1. The mean $C:N_{biomass}$ increased significantly under phosphorus limitation ($p < 0.0005$) from 4.3:1 to more than 7.5:1, with a maximum of 12.1:1. Variance in all three ratios increased with increasing $C:P_{supply}$. Cellular nitrogen was strongly correlated with cellular carbon ($R^2 = 0.940$). Cellular phosphorus showed a weak negative correlation with cellular carbon ($R^2 = 0.142$) and cellular nitrogen ($R^2 = 0.061$). $C:N_{biomass}$ showed a weak positive correlation with $C:P_{biomass}$ ($R^2 = 0.245$) and $N:P_{biomass}$ was strongly correlated with $C:P_{biomass}$ ($R^2 = 0.988$).

Biomass Stoichiometry - Experiment 2. The $C:P_{biomass}$ of the bacterial assemblage was greater than observed in Experiment 1 (Figure 4-2). The $C:P_{biomass}$ was higher in the $C:P_{supply}$ 221,000:1 medium treatment (6,942:1, 11,140:1, and 7,861:1) compared to the

medium without amended phosphorus (5,016:1, 1,598:1, and 1,182:1). Biomass N:P ranged from 223 to 1,678:1, but $C:N_{biomass}$ varied little (6.6-7.2:1).

Phosphorus Allocation - Experiment 1. As the overall amount of P in the cells decreased, the amount of P in the measured fractions increased (Figure 4-3). Nucleic acids were the largest measured fraction of total P, increasing from 19.3% to 43.9% between $C:P_{supply}$ of 31.6:1 and 3,162:1. DNA per cell decreased from a mean 20 fg $cell^{-1}$ at $C:P_{supply}$ of 31.6 to 3.2 fg $cell^{-1}$ at $C:P_{supply}$ of 3,162:1. The RNA was below detection in one chemostat at $C:P_{supply}$ of 316:1. RNA per cell showed no apparent response to $C:P_{supply}$ and ranged from 3.9 to 36 fg $cell^{-1}$. The ratio of RNA:DNA did not respond significantly in response to $C:P_{supply}$ (regression, $p > 0.5$). Lipid-P was the second largest P pool and increased from 9.5% to 21.8% of total P with increasing $C:P_{supply}$. Lipid-P relative to mean cellular surface area decreased from a mean of 22 amoles-P μm^{-2} at $C:P_{supply}$ of 31.6:1-100:1 to a mean of 5 amoles-P μm^{-2} at higher $C:P_{supply}$ (two-sample t-test $p > 0.08$). Protein-P increased from 0.5% to 12.2% of total P with increasing $C:P_{supply}$. Polyphosphate was low in all of the cultures between $C:P_{supply}$ of 31.6:1 and 1,000:1, with only one chemostat within detection at $C:P_{supply}$ of 3,162:1. The unclassified fraction of cellular P decreased from a mean of 71% at $C:P_{supply}$ of 31.6:1 to a mean of 21% at $C:P_{supply}$ of 3,162:1.

Cellular Morphology. In Experiment 1, mean cell length increased between $C:P_{supply}$ of 31.6:1 and 10,000:1 (ANOVA, $p < 0.025$), while mean cell width varied little ($p > 0.20$), leading to an increase in the length:width ratio ($p < 0.001$) of cells under P limitation (Figure 4-4). The variance in L:W was heterogeneous among levels of $C:P_{supply}$ (Levene test, $p < 1x10^{-10}$). Skewness in L:W was positive and showed no apparent pattern with $C:P_{supply}$. Cell surface area, volume, and surface area:volume ratios did not change significantly in response to increasing $C:P_{supply}$ (all $p > 0.25$), but exhibited heterogeneity of variances among treatments (Levene test $p < 1x10^{-10}$). The cellular morphometry in Experiment 2 was similar to that observed at $C:P_{supply}$ ratios of 10,000-31,620:1 in Experiment 1. In both experiments, cell SA:V showed a weak positive correlation with L:W (log-log, $R^2 = 0.32$, n =18,880). Cell volume was positively correlated with cell

width (log-log, $R^2 = 0.89$) and SA:V was negatively correlated with cell width (log-log, $R^2 > 0.99$).

Literature Data Analysis. Data compiled from published sources indicate substantial variation in the P quotas of cultured bacteria (Appendix F). P quotas ranged from 7.2 amoles cell^{-1} to 1.22 fmoles cell^{-1}, with 90% of the observations between 0.045 and 0.465 fmoles cell^{-1} (n = 122). From the same sources, carbon quotas ranged from 0.81 to 116 fmoles cell^{-1}, with 90% of the observations between 3.66 and 53.4 fmoles cell^{-1} (n = 124). Phosphorus as a proportion of dry mass ranged from 0.011% to 5.53% (n = 87). Cell C:$P_{biomass}$ ranged from 7.7:1 to 1,248:1, with 90% of the observations between 29:1 and 468:1 (n = 225). Cell N:$P_{biomass}$ ranged from 1.6:1 to 90:1, with 90% of the observations between 6.6:1 and 58:1 (n = 160). Bacterial C:$N_{biomass}$ ratios were less variable and ranged from 2.0:1 to 17.2:1, with 90% of the observations between 3.2:1 and 11.0:1 (n = 163).

Model of Bacterial Resource Use. The quota ranges used in the model were: *E. coli* (Q_C 14-18.72 fmoles cell^{-1} and Q_P 0.34-0.47 fmoles cell^{-1}), literature 25-75% quantile range (Q_C 9.99-33.29 fmoles cell^{-1} and Q_P 0.110-0.279 fmoles cell^{-1}), literature 5-95% quantile range (Q_C 3.66-53.42 fmoles cell^{-1} and Q_P 0.045 – 0.465 fmoles cell^{-1}), and Experiment 1 from this study (Q_C 13.3-99 fmoles cell^{-1} and Q_P 0.04-1.010 fmoles cell^{-1}). Increasing the ranges for C and P quotas changed the interaction between biomass stoichiometry and resource stoichiometry (Figure 4-6). The threshold in C:P_{supply} between C- and P limitation increased with increasing quota ranges. This shift is visible as the point of C:P_{supply} at which the effluent P becomes static and the dissolved C increases. The model simulations with narrower ranges for C and P quotas showed reduced variability in C:$P_{biomass}$ than simulations with larger ranges for these quotas. In each scenario, the cells exhibited non-homeostasis across a range of C:P_{supply} (Figure 4-6, panel e). The model runs for *E. coli* and the literature 25-75% range exhibited limited non-homeostasis, but became homeostatic at high C:P_{supply}. Simulations of bacteria with wider quota ranges showed non-homeostasis across a wider range of C:P_{supply}.

The C:P of the dissolved fraction (C:$P_{dissolved}$) increased with increasing C:P_{supply}, but the rate of this increase was dependent upon the range of quotas. When P is abundant

(low $C:P_{supply}$), more P-rich homeostatic bacteria function as sinks for P and increase the C:P of available resources. In contrast, non-homeostatic bacteria decrease the C:P of available resources when P is abundant. At intermediate levels of $C:P_{supply}$, more homeostatic P-rich bacteria continue to enrich the resources in C relative to P, and the impact of non-homeostatic bacteria on $C:P_{dissolved}$ is diminished. Both homeostatic and non-homeostatic bacteria have a similar effect on $C:P_{dissolved}$ at high $C:P_{supply}$, but the non-homeostatic bacteria reduce the ambient concentrations to lower levels than the bacteria with more constrained quotas.

Discussion

The experiments presented in this study demonstrate that assemblages of bacteria are highly flexible in their elemental content and that this plasticity was previously underestimated. A single assemblage of bacteria showed greater range in P content (expressed as $C:P_{biomass}$, $N:P_{biomass}$, and P/dry mass) than nearly all previously published data for bacterial cultures. The P content of the bacterial assemblage was dependent upon $C:P_{resources}$ and the bacteria had lower P content than is commonly assumed.
Bacteria in these experiments achieved this plasticity in biomass stoichiometry by decreasing P quotas and increasing quotas of C and N in response to P limitation. Bacteria reduced their cellular P quotas primarily through minimizing P that was not allocated to nucleic acids, protein, lipids, or polyphosphate (i.e. unaccounted P). Due to the constraint of chemostat conditions, the strategy of reduced realized growth rate was not relevant to the results discussed in this section. I used these new measurements of biomass composition to model the interaction of bacterial assemblages and their resources and evaluate the implications of highly variable P for ecosystem functioning.

Phosphorus Content: How Low Can They Go?

The experiments presented in this chapter demonstrate that assemblages of aquatic heterotrophic bacteria can be highly plastic in their phosphorus content. This plasticity is evident in the 13-fold range for cellular phosphorus quotas (0.055 to 0.72 fmoles $cell^{-1}$) and the 600-fold range as a proportion of dry weight (0.006% to 3.6%). The

range of phosphorus quotas in these experiments was comparable to the range of values presented in the literature, although no other single assemblage or species has demonstrated such flexibility. The range of phosphorus quotas measured in these experiments suggests that the bacteria were strongly P limited at high $C:P_{supply}$. Previous studies have documented phosphorus quotas lower than 0.055 fmoles $cell^{-1}$ (e.g. 7 amoles $cell^{-1}$, Goldman et al. 1987; chapter 3). Many studies showing low P quotas were performed by elemental analysis of single cells whereas the current study was performed with bulk analyses of assemblages (Cotner et al. 2010; Løvdal et al. 2008). Since these measurements integrate the biomass of multiple strains and at least $1x10^7$ cells, there likely exist some strains and cells that attain even lower phosphorus content.

The cultures grown under high $C:P_{supply}$ had extremely low phosphorus content as a proportion of dry mass (Figure 4-1). The values measured in Experiment 2 are lower than those reported for a bacterium grown in the absence of added phosphate and high concentrations of arsenate (0.012% of dry mass as P, Wolfe-Simon et al. 2010). A response to this work noted that bacteria growing in phosphorus-poor aquatic environments and laboratory cultures have comparably low P content (Cotner and Hall 2011). In their response to this evidence, Wolfe-Simon et al. (2011) maintain that their cells were too phosphorus-poor to be utilizing phosphorus alone. The results presented here clearly demonstrate that assemblages of bacteria growing in chemostats at low, but controlled, levels of phosphorus have phosphorus content less than 0.01% of dry mass.

Bacterial Biomass Stoichiometry. The bacterial assemblages examined in these experiments exhibited substantial flexibility in their biomass stoichiometry (Figure 4-2, Figure 4-5). The ranges of $C:P_{biomass}$ (28:1 to 11,140:1) and $N:P_{biomass}$ (6.7:1 to 1,678:1) observed in this study cover the range of measurements recorded in previously published studies for bacterial cultures (Figure 4-5). To my knowledge, no single species or assemblage has a similar range in $C:P_{biomass}$ or $N:P_{biomass}$, including terrestrial and aquatic primary producers and herbivores (Elser et al. 2000a; Frost et al. 2006). The ranges in $C:P_{biomass}$ and $N:P_{biomass}$ are similar to the ranges observed in vascular plant tissues (Cross et al. 2005). The ranges of $C:P_{biomass}$ and $N:P_{biomass}$ described here exceeded those measured in the bacterial-sized fraction of lakes (Cotner et al. 2010; Villar-Argaiz et al.

2002b), stoichiometrically flexible marine cyanobacteria (Bertilsson et al. 2003), and cultures of bacterial isolates from lakes (Scott et al. 2012; chapter 3). In contrast to the flexibility in $C:P_{biomass}$ and $N:P_{biomass,}$ bacterial cultures exhibited considerably less variability in $C:N_{biomass}$. Dampened variability in $C:N_{biomass}$ has been observed in other studies (Cotner et al. 2010) and is likely explained by low $C:N_{supply}$ and a surplus of C and N relative to P in the medium.

Coupled Changes In C, N, And P

The bacterial cultures in these experiments attained high $C:P_{biomass}$ and $N:P_{biomass}$ through coupled increases in cellular C and N quotas while reducing cellular P. The increase in C and N quotas in response to P limitation could be the result of surplus storage of excess C and N. Between $C:P_{supply}$ of 100:1 and 100,000:1, cellular C and N quotas increased in a molar ratio of approximately 11:1. The cultures in Experiment 2 had markedly high C and N quotas, but the strong linear relationship between cellular C and N suggests that the cells did not accumulate large amounts of C-rich glycogen or poly-β-hydroxybutyrate (Thingstad et al. 2005). Similarly, the contribution of C to dry mass did not respond to $C:P_{supply}$. Instead, the proportional increase in cellular C and N under P limitation suggests an increase in other C- and N-containing cellular components. The C:N ratios of other major constituents are approximately: protein (2.7:1), peptidoglycan (2.2:1), gram-positive cell walls (3.3:1), and bacterial membrane (4.6:1) (Sterner and Elser 2002). These ratios are lower than the C:N of the added biomass, meaning that surplus C and N were not allocated to a single pool. Additionally, phospholipids have high P content (C:P = 40:1), but are relatively deplete of N (C:N = 49:1, Van Mooy et al. 2009; Van Mooy et al. 2006), suggesting that phospholipid substitution alone is insufficient to explain the changes in biomass stoichiometry.

Relative to the biomass composition at $C:P_{supply}$ of 31.6:1, C and N accumulation alone could explain increases to $C:P_{biomass}$ of 131:1 and N:P of 14.9:1 when $C:P_{supply}$ exceeds 10,000:1. Phosphorus depletion alone could account for a $C:P_{biomass}$ ratio of 204:1 and $N:P_{biomass}$ of 48:1 under the same scenario. Phosphorus depletion explains a larger proportion of the observed changes in $C:P_{biomass}$ and $N:P_{biomass}$ compared to C and

N accumulation, but both are required for cells to attain a highly unbalanced stoichiometry.

Phosphorus Allocation: Where's The P?

The allocation of P within microbial biomass is a poorly studied aspect of P cycling by bacteria. Previous studies have investigated the allocation of P within bacterial biomass and sediments using multiple extractions and subsequent measurement of extracted P or P-containing macromolecules (Hupfer et al. 2008; Mino et al. 1985; Waara et al. 1993). Phillips et al. (in preparation) showed that allocation of cellular P to nucleic acids, phospholipids and polyphosphate was variable among three strains and was dependent upon phosphate supply.

Compared to other P-containing cellular constituents, more studies have evaluated the allocation of cellular P to nucleic acids. RNA represents 35-80% of total P in *E. coli*, with 6-11% in DNA (Cotner et al. 2006; Makino et al. 2003). The allocation of P to RNA and DNA in *E. coli* was sensitive to dilution rate, but not to the $C:P_{supply}$ (Makino and Cotner 2004). The difference in P allocation between *E. coli* and the cultures presented in this chapter is likely explained by the rapid growth rates of *E. coli* cultures (0.5-1.5 h^{-1}, Makino et al. 2003) compared to the dilution rate used in my experiments (0.0138 h^{-1}). The Growth Rate Hypothesis predicts that the P content of an organism is proportional to its growth rate due to the role of P-rich ribosomes in growth (Elser et al. 2000b). At slower growth rates, RNA of bacterial isolates represents 2-34% of total P (Phillips et al. in preparation). In previously studied strains, the proportional allocation of P to nucleic acids increased at high $C:P_{supply}$ similarly to what was observed in this study. Phillips et al. (in preparation) observed no effect of $C:P_{supply}$ on the absolute nucleic acid content of two strains, whereas a third strain increased its nucleic acid content with increasing P supply. Together, these data do not suggest that reduction of nucleic acids is responsible for much plasticity in $C:P_{biomass}$ of individual strains.

In chemostat cultures grown at a uniform dilution rate, the effect of P availability on nucleic acid content is independent of the effect of growth rate. At a single realized growth rate, the proportional increase in RNA and DNA under P limitation is likely due to a decrease in the total cellular P. The assemblages described in this study decreased

their mean DNA content (per cell) under P limitation. This result might be attributed to selection for strains with smaller genome sizes, which has been suggested as an adaptation to chronic P-stress (Alcaraz et al. 2008; Hessen et al. 2010; Hessen et al. 2008; Newton et al. 2011). The lowest mean DNA content measured in Experiment 1 was 3.2 fg $cell^{-1}$ at $C:P_{supply}$ of 3,162:1. This DNA content would be equivalent to a genome size of 2.9 million base pairs if there were a single double-stranded copy without replication. Although this estimate of genome size is conservative, it does not indicate a dramatically reduced genome size relative to other prokaryotes (Alcaraz et al. 2008; Dufresne et al. 2005). Strains of bacteria that are adapted to rapid growth have more copies of rRNA operons in their genome (Klappenbach et al. 2000), which suggests that the selection for reduced genome size could also favor slowly growing strains.

Under P-replete conditions, the majority of the cellular P in the assemblage cultures was not allocated into nucleic acids, lipid-P, polyphosphates, or protein-bound phosphorus (Figure 4-3). Other possible locations for the additional P include cell wall polymers (Lahooti and Harwood 1999; Neuhaus and Baddiley 2003), ATP (Hamilton and Holm-Hansen 1967), metabolites (Boer et al. 2010), and free phosphate (Vadstein 1998). Hamilton and Holm-Hansen (1967) measured the ATP content of marine isolates in high P medium and showed that ATP content ranges from 0.2-7.8 fg $cell^{-1}$. In the experiments presented here, these ATP quotas would account for up to 7.4% of the P quota at $C:P_{supply}$ of 31.6:1 and up to 32% of the P quota at $C:P_{supply}$ of 3,162:1. Additionally, inorganic cellular P accounted for 6-10% of cellular P in two bacterial isolates from lakes (Vadstein 1998) and could account for a substantial portion of the unaccounted P in this experiment.

Some bacteria are capable of replacing phospholipids in their membranes with P-free lipids (Benning et al. 1995; Minnikin et al. 1974; Van Mooy et al. 2006; Zavaleta-Pastor et al. 2010). At high $C:P_{supply}$, the assemblage cultures presented in this study exhibited reduced lipid-P density relative to cell surface area, although this was not statistically significant. Under P-replete conditions, non-homeostatic bacteria could store surplus cellular P as inorganic polyphosphate (Harold 1962; Jahid et al. 2006; Kornberg 1995). Although the cultures contained detectable polyphosphate, it remained a small

fraction of cellular P even when the $C:P_{supply}$ and $C:P_{biomass}$ were low. This is explained by the dual function of polyphosphate. In addition to their role in phosphorus storage, polyphosphates are energy-rich molecules that accumulate when organic substrates and P are abundant (Kornberg 1995; Kulaev and Kulakovskaya 2000). At low $C:P_{supply}$, the cultures were likely limited by the availability of glucose and thus polyphosphate production would not be expected to occur. Although cells might regulate any of these pools to alter their P content, it is unknown which, if any, of these pools are responsible for the unaccounted cellular P observed at moderate growth rates in the presence of surplus phosphorus.

Cellular Morphology And P Limitation. The cells in Experiment 1 were more elongate under phosphorus stress, but did not dramatically increase their surface area relative to their volume. Cells with the greatest SA:V ratios were typically the smallest in width. Increasing SA:V by elongation has been proposed as a mechanism for facilitating uptake of P under P limitation (Thingstad et al. 2005). However, these data show that SA:V is poorly predicted by L:W in a large number of cells from more than three orders of magnitude in P availability. Although cellular SA:V was weakly correlated with $C:P_{supply}$, L:W increased significantly in response to P stress, suggesting that increasing L:W is not the sole means of changing SA:V. Effective changes in SA:V can also occur by minimizing the internal volume through which solutes can diffuse (Koch 1996). Elongation coupled with intracellular inclusions of carbon-rich high-density material (poly-β-hydroxybutryate or glycogen) would increase the surface area relative to the volume of cytoplasm (Thingstad et al. 2005). However, I found little evidence for C-rich inclusions in these cultures, as evidenced by the low and relatively consistent $C:N_{biomass}$. Since this alteration of morphology was not accompanied by an increase in SA:V, these data provide only weak support for elongation as an adaptation to increase phosphorus uptake.

Implications of Highly Variable C:N:P

These experiments demonstrate that assuming low and invariant $C:P_{biomass}$ (Tambi et al. 2009; Tanaka et al. 2009) and high P quota (Wolfe-Simon et al. 2011) for bacteria can limit our understanding of C and P cycling by bacteria. Traditional models of

heterotroph growth (Frost et al. 2005; Sterner 1990; Sterner and Elser 2002) predict that the ratio of regenerated C and P increases with increasing food C:P. Although consumption, egestion, and regeneration mechanisms in phagotrophic animals differ from the nutritional physiology of osmotrophs, the stoichiometry of consumer-resource interactions behaved similarly. Non-homeostasis in biomass C and P creates a less dynamic relationship between bacterial biomass stoichiometry and the supply of resources in the environment, although the flexible cells consume proportionally more of the resources. This model represents an allochthonous system where the bacteria do not directly affect the supply of resources, but do affect the concentration and ratio available in their environment. However, heterotrophic bacteria in natural systems compete with primary producers for inorganic nutrients (Cotner and Wetzel 1992; Currie 1990) and consume organic C derived from phytoplankton, suggesting a feedback in which depletion of inorganic P could lead to decreased C availability. Non-homeostasis in bacterial C:N:$P_{biomass}$ also has implications for trophic transfer of these elements within the 'microbial loop' (Azam et al. 1983). Grover and Chrzanowski (2006) showed that a flagellate consumer adjusted its biomass stoichiometry in response to the stoichiometry of the bacterial prey. Compared to homeostatic consumers, non-homeostatic assemblages of bacteria and a non-homeostatic protist consumer would allow for increased efficiency in the transfer of C within the microbial loop.

Elemental Content as an Indicator of Nutritional Status

The elemental composition and stoichiometry of organisms are commonly used as indicators of nutrient stress and nutritional status. This principle has been applied extensively to algae and phytoplankton (Healey and Hendzel 1980; Hillebrand and Sommer 1999), but less commonly in heterotrophic bacteria. In this study, the high C:$P_{biomass}$, high N:$P_{biomass}$, and low P/dry mass for the assemblages cultured at low P-availability suggest severe P limitation. The P quotas of these cells were correspondingly low, but were still greater than some observations of P quota in the literature, suggesting that the cells were not severely P-stressed. This discrepancy is due to simultaneous increases in cellular C and N as the P quota decreases. Indeed, while the majority of the change in C:$P_{biomass}$ observed under P limitation was attributable to a reduction in P

quota, minimization of P alone was not sufficient to explain the high $C:P_{biomass}$ ratios that were observed.

Methods to assess the P nutritional status of bacteria can be classified into three categories: absolute measures (cell quotas, P $cell^{-1}$), relative measures ($C:P_{biomass}$, $N:P_{biomass}$, or P/dry mass) and activity measures. Although all three measures are potentially sensitive to P limitation, there is potential for mismatch among diagnoses obtained with these methods. Absolute measures of P content (quotas) efficiently diagnose P limitation within assemblages and populations and are not sensitive to accumulation of surplus resources. However, the growth rate of cells (absolute and relative) is relevant when interpreting these measures of biomass P content. The Growth Rate Hypothesis predicts that slowly growing cells have reduced demand for ribosomes, and therefore a lower P quota, compared to quickly growing cultures (Elser et al. 2000b). Some of the variation in bacterial P content within and among strains is attributable to differences in realized growth rate, which makes comparison among studies with varying culture conditions difficult. Other studies report lower P quotas than described in this chapter, but were performed in static cultures (Goldman et al. 1987) or at very low dilution rates (Løvdal et al. 2008), effectively lowering the minimum P quota required for growth.

Relative measures of the P content of bacteria (C:P, N:P, and P/dry mass) are also effective indicators of P stress in bacteria (Makino and Cotner 2004; Phillips et al. in preparation; Scott et al. 2012). However, as shown in this study, these measures are sensitive to the effects of surplus C and N storage. Relative measures are sensitive to P availability, but in contrast to P quotas, relative measures are particularly sensitive to resource imbalance. Similar to P quotas, relative measures are sensitive to growth rate (absolute and relative). Multiple studies have demonstrated decreases in $C:P_{biomass}$ and $N:P_{biomass}$ at faster chemostat dilution rates (Chrzanowski and Kyle 1996; Makino and Cotner 2004; Makino et al. 2003). Phosphorus content of bacteria has been normalized to cell volume (Chrzanowski and Grover 2008; Makino and Cotner 2004), but this relative measure is sensitive to cell morphometry, which is also dependent upon P availability (chapter 3; Phillips et al. in preparation). Phosphorus deficiency in bacteria is also

assessed as the activity of extracellular enzymes (phosphatases, Cotner and Wetzel 1991; Thingstad et al. 1998). Since these measurements are specific to the culture conditions used, these methods are best suited to relative comparisons and evaluation of treatment conditions. Recently, transcriptional profiling of genes related to P metabolism has been used to infer P stress and this method shows good correspondence with bulk measures of phosphorus content (Chan et al. 2012).

Both absolute and relative measures of P content are informative, but relative measures are more appropriate as indicators of imbalance in resource availability whereas absolute measures are more appropriate as indicators of P limitation. Due to the effects of surplus storage and growth rate, a more nuanced approach is required to interpret the nutritional state of bacteria from their biomass composition. The bacterial-sized fraction of seston exhibits substantial variability in absolute P content (P quotas from 0.001 to 1.0 fmoles $cell^{-1}$) and modest variability in relative P content ($C:P_{biomass}$ from < 50:1 to > 300:1, Cotner et al. 2010). Both of these ranges likely reflect variation in realized growth rates and P availability in natural systems, but the range of biomass stoichiometry also suggests that bacteria experience low to moderate resource imbalance in ecosystems. Integrating both absolute and relative measures allows us to discern the effects of resource concentration, growth rate, and resource imbalance and would improve the comparability of data from multiple studies.

Limitations And Conclusions. The bacterial assemblages examined in this study exhibited substantial flexibility in biomass C and P. However, it is not possible to discern the influence of resource-driven shifts in assemblage composition. Although the relative abundance of strains likely changed during the incubation and across the $C:P_{supply}$ gradient, there is evidence that much of the non-homeostasis was the result of physiological acclimation of multiple strains. A study of the stoichiometry of assemblages showed similar stoichiometric non-homeostasis of assemblages from different environments (chapter 2) and non-homeostasis is characteristic of many pure cultures (chapter 3; Scott et al. 2012).

It appears likely that different bacterial assemblages or strains are capable of attaining lower P content than the cultures described to date and in this study. This study

is not intended as a definitive or absolute answer to the question "how low can they go?" Instead, this work expands the range of P quotas documented in bacterial cultures and highlights the problems associated with the assumption that bacteria have low and invariant $C:P_{biomass}$. As we improve our understanding of bacterial biogeochemistry under variable P conditions it is important that our models reflect the range and flexibility of bacterial biomass composition.

Figures

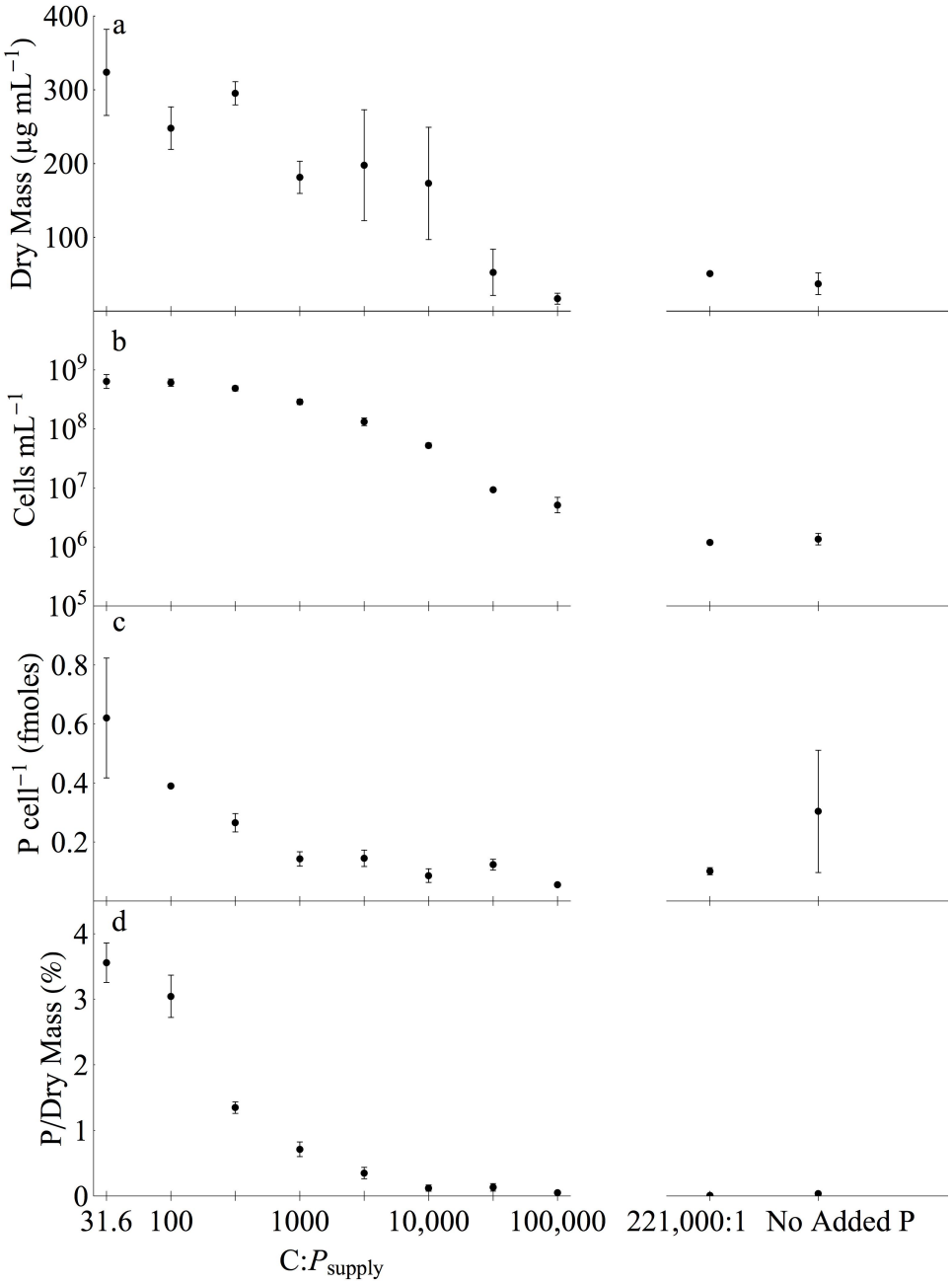

Figure 4-1. Cell dry mass, abundance, phosphorus quota, and phosphorus content of assemblages.

Error bars are standard errors of the mean of 3 chemostats.

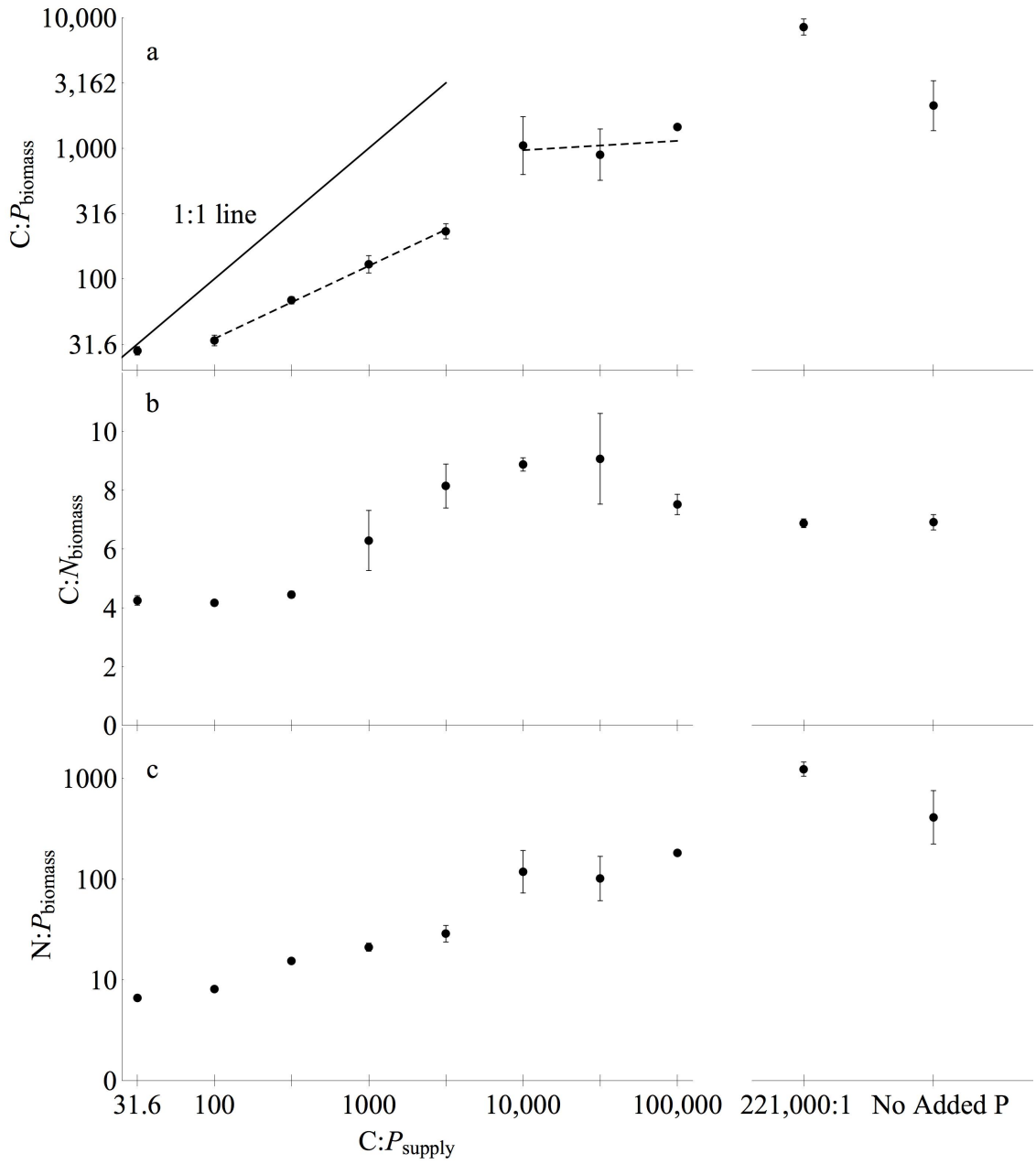

Figure 4-2. Effect of C:P_{supply} ratio on biomass C:P, C:N, and N:P ratios.

Note that C:$N_{biomass}$ is plotted using a linear scale and C:$P_{biomass}$ and N:$P_{biomass}$ are plotted on log-transformed scales. The solid line in panel a represents a 1:1 relationship between C:$P_{biomass}$ and C:P_{supply} and the dashed line is the linear regression in the non-homeostatic and homeostatic regions of C:P_{supply}. Error bars denote standard errors of the mean, n = 3 chemostats.

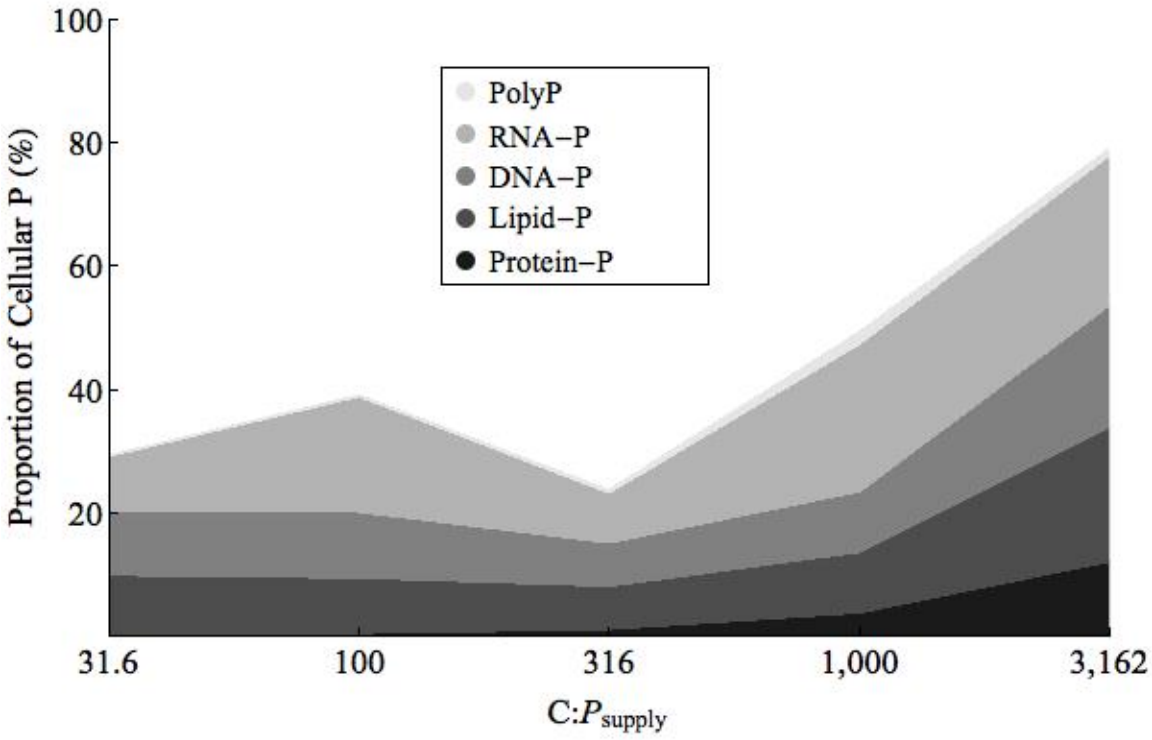

Figure 4-3. Effect of C:P_{supply} on phosphorus allocation within biomass in Experiment 1.

Data are the mean of three chemostats and the non-shaded portion represents unclassified cellular phosphorus.

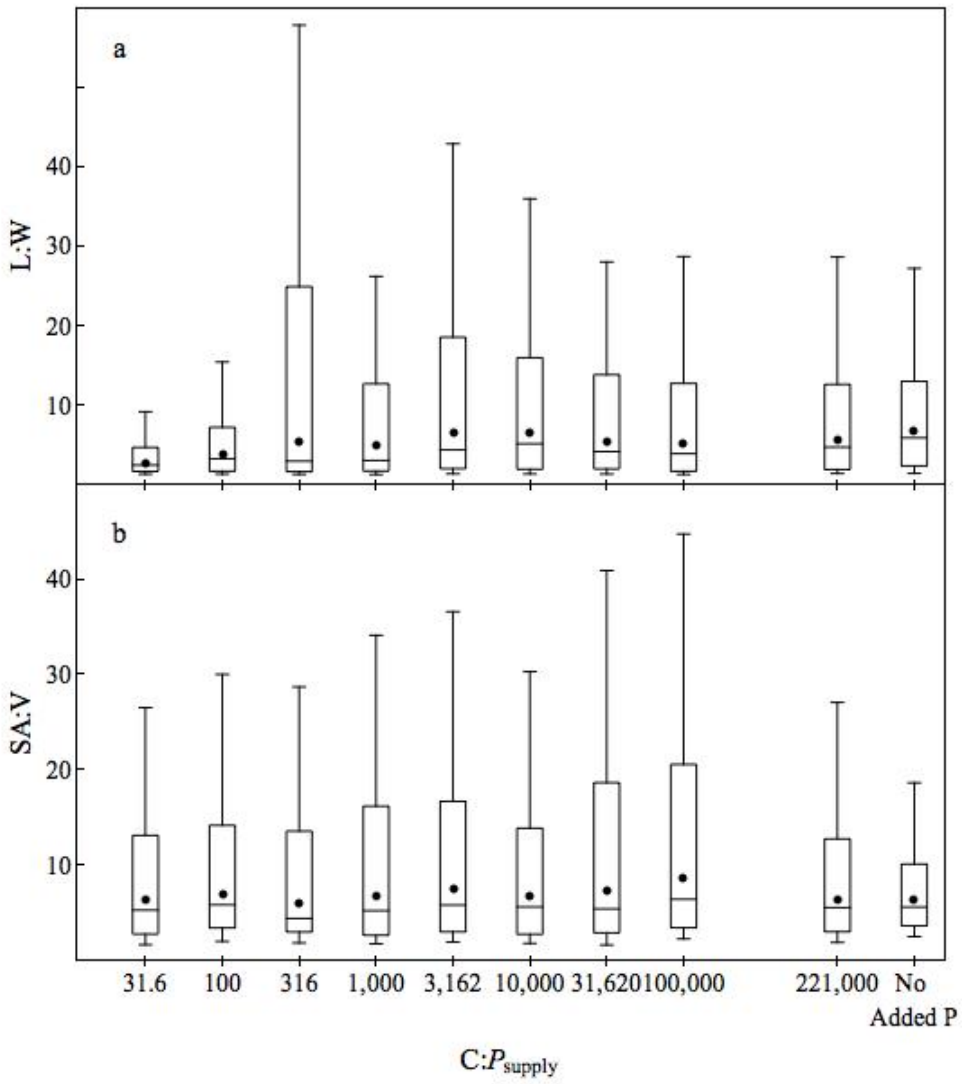

Figure 4-4. Plots of cellular length:width and surface area:volume ratios across C:P_{supply} ratios.

Error bars denote the standard error of the mean. The horizontal line denotes the median and the filled circles represent the mean. The 25th and 75th quantiles are represented by the upper and lower bounds of the box and the whiskers represent the range of data within three times the interquantile range. Outliers outside this range are excluded.

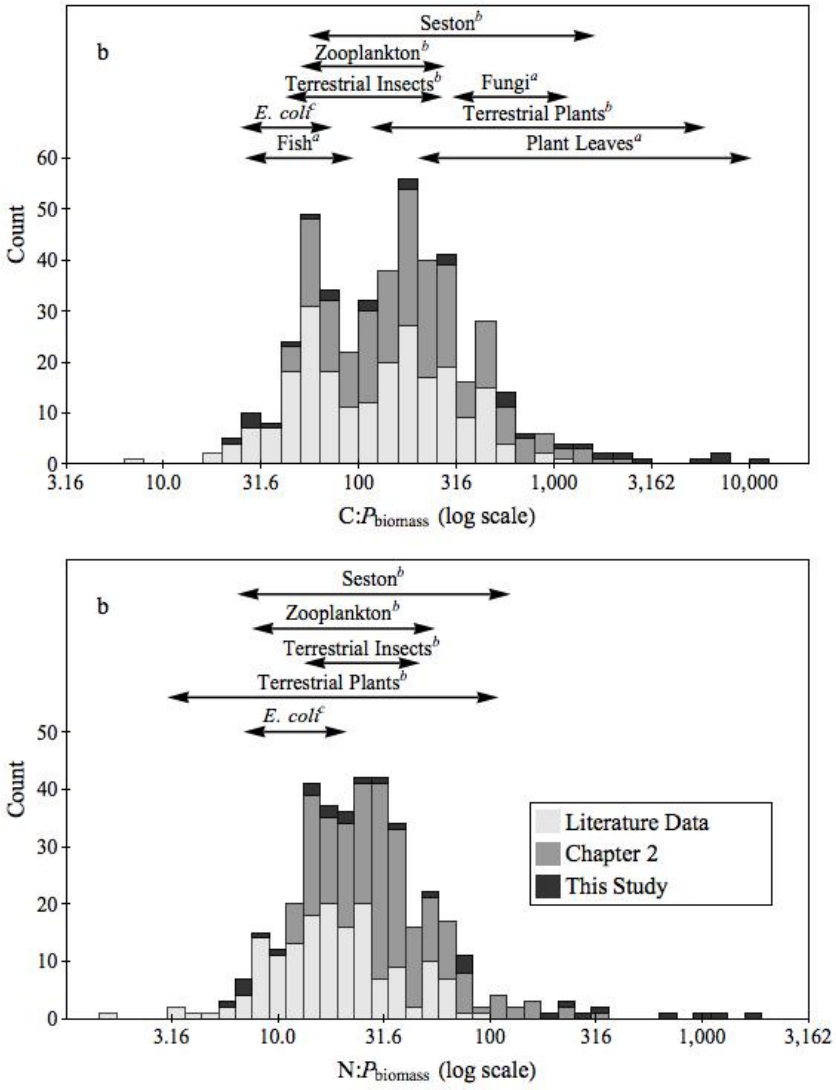

Figure 4-5. Histograms of C:$P_{biomass}$ and N:$P_{biomass}$ for bacteria.

Separate panels for C:$P_{biomass}$ (panel a) and N:$P_{biomass}$ (panel b) for heterotrophic bacteria from published sources, assemblage cultures (chapter 2), and this chapter. Ranges for other organisms were from [a]Cross et al. (Cross et al. 2005) and [b]Elser et al. (Elser et al. 2000a). [c]Ranges for *E. coli* were compiled from multiple studies (Cotner et al. 2006; Fagerbakke et al. 1996; Heldal et al. 1985; Makino et al. 2003; Nakano 1994; Norland et al. 1995). Histogram counts are for single replicate cultures where data are available or treatment means.

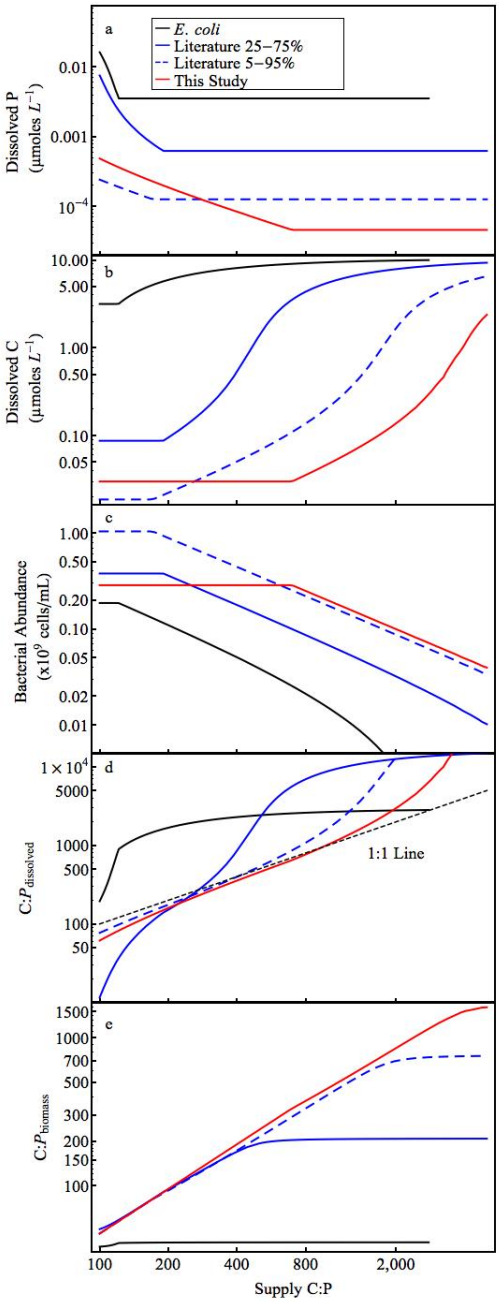

Figure 4-6. Model solutions for heterotrophic bacteria interacting with dissolved P and C.

Separate panels for (a), dissolved C (b), bacterial abundance (c), $C:P_{dissolved}$ (d), and $C:P_{biomass}$ (e) using elemental content ranges from the literature and from this study. Dissolved C, dissolved P, and $C:P_{dissolved}$ are for unutilized supply (i.e. dissolved organic carbon and phosphate in the chemostat effluent).

Bibliography

Acharya, K., M. Kyle, and J. J. Elser. 2004. Biological stoichiometry of *Daphnia* growth: An ecophysiological test of the growth rate hypothesis. Limnology and Oceanography **49:** 656-665.

Aerts, R. 1999. Interspecific competition in natural plant communities: Mechanisms, trade-offs and plant-soil feedbacks. Journal of Experimental Botany **50:** 29-37.

Aerts, R., and F. S. Chapin. 2000. The mineral nutrition of wild plants revisited: A re-evaluation of processes and patterns. Advances in Ecological Research **30:** 1-67.

Ågren, G. I. 2004. The C : N : P stoichiometry of autotrophs - theory and observations. Ecology Letters **7:** 185-191.

Alcaraz, L. D., G. Olmedo, G. Bonilla, R. Cerritos, G. Hernandez, A. Cruz, E. Ramirez, C. Putonti, B. Jimenez, E. Martinez, V. Lopez, J. L. Arvizu, F. Ayala, F. Razo, J. Caballero, J. Siefert, L. Eguiarte, J. P. Vielle, O. Martinez, V. Souza, A. Herrera-Estrella, and L. Herrera-Estrella. 2008. The genome of *Bacillus coahuilensis* reveals adaptations essential for survival in the relic of an ancient marine environment. Proceedings of the National Academy of Sciences of the United States of America **105:** 5803-5808.

Allen, A. P., and J. F. Gillooly. 2009. Towards an integration of ecological stoichiometry and the metabolic theory of ecology to better understand nutrient cycling. Ecology Letters **12:** 369-384.

Allison, S. D., and J. B. H. Martiny. 2008. Resistance, resilience, and redundancy in microbial communities. Proceedings of the National Academy of Sciences of the United States of America **105:** 11512-11519.

Anderson, T. R., M. Boersma, and D. Raubenheimer. 2004. Stoichiometry: Linking elements to biochemicals. Ecology **85:** 1193-1202.

APHA. 1995. Standard methods for the examination of water and wastewater: Including bottom sediments and sludges, 20th ed. American Public Health Association.

Aschar-Sobbi, R., A. Y. Abramov, C. Diao, M. E. Kargacin, G. J. Kargacin, R. J. French, and E. Pavlov. 2008. High sensitivity, quantitative measurements of polyphosphate using a new DAPI-based approach. Journal of Fluorescence **18:** 859-866.

Azam, F. 1998. Microbial control of oceanic carbon flux: The plot thickens. Science **280:** 694-696.

Azam, F., T. Fenchel, J. G. Field, J. S. Gray, L. A. Meyer-Reil, and F. Thingstad. 1983. The ecological role of water-column microbes in the sea. Marine Ecology-Progress Series **10:** 257-263.

Barer, M. R., and C. R. Harwood. 1999. Bacterial viability and culturability. Advances in microbial physiology **41:** 93-137.

Begg, K. J., and W. D. Donachie. 1978. Changes in cell size and shape in thymine-requiring *Escherichia coli* associated with growth in low concentrations of thymine. Journal of Bacteriology **133:** 452-458.

Benning, C., Z. H. Huang, and D. A. Gage. 1995. Accumulation of a novel glycolipid and a betaine lipid in cells of *Rhodobacter sphaeroides* grown under phosphate limitation. Archives of biochemistry and biophysics **317:** 103-111.

Bertilsson, S., O. Berglund, D. M. Karl, and S. W. Chisholm. 2003. Elemental composition of marine *Prochlorococcus* and *Synechococcus*: Implications for the ecological stoichiometry of the sea. Limnology and Oceanography **48:** 1721-1731.

Biddanda, B., M. Ogdahl, and J. Cotner. 2001. Dominance of bacterial metabolism in oligotrophic relative to eutrophic waters. Limnology and oceanography **46:** 730-739.

Bligh, E. G., and W. J. Dyer. 1959. A rapid method of total lipid extraction and purification. Canadian journal of biochemistry and physiology **37:** 911-917.

Boer, V. M., C. A. Crutchfield, P. H. Bradley, D. Botstein, and J. D. Rabinowitz. 2010. Growth-limiting intracellular metabolites in yeast growing under diverse nutrient limitations. Molecular biology of the cell **21:** 198-211.

Box, G. E. P., and D. R. Cox. 1964. An analysis of transformations. Journal of the Royal Statistical Society. Series B (Methodological)**:** 211-252.

Bradshaw, C., U. Kautsky, and L. Kumblad. 2012. Ecological stoichiometry and multi-element transfer in a coastal ecosystem. Ecosystems **15:** 591-603.

Branco, P., M. Stomp, M. Egas, and J. Huisman. 2010. Evolution of nutrient uptake reveals a trade-off in the ecological stoichiometry of plant-herbivore interactions. American Naturalist **176:** E162-E176.

Bratbak, G. 1985. Bacterial biovolume and biomass estimations. Applied and Environmental Microbiology **49:** 1488-1493.

Brutemark, A., E. Lindehoff, E. Granéli, and W. Granéli. 2009. Carbon isotope signature variability among cultured microalgae: Influence of species, nutrients and growth. J. Exp. Mar. Biol. Ecol. **372:** 98-105.

Butler, N. M., C. A. Suttle, and W. E. Neill. 1989. Discrimination by freshwater zooplankton between single algal cells differing in nutritional status. Oecologia **78:** 368-372.

Cardinale, M., L. Brusetti, P. Quatrini, S. Borin, A. M. Puglia, A. Rizzi, E. Zanardini, C. Sorlini, C. Corselli, and D. Daffonchio. 2004. Comparison of different primer sets for use in automated ribosomal intergenic spacer analysis of complex bacterial communities. Applied and Environmental Microbiology **70:** 6147-6156.

Carpentier, S. C., E. Witters, K. Laukens, P. Deckers, R. Swennen, and B. Panis. 2005. Preparation of protein extracts from recalcitrant plant tissues: An evaluation of different methods for two-dimensional gel electrophoresis analysis. PROTEOMICS **5:** 2497-2507.

Chan, F. Y., and A. Torriani. 1996. Pstb protein of the phosphate-specific transport system of *Escherichia coli* is an ATPase. Journal of Bacteriology **178:** 3974-3977.

Chan, L.-K., R. J. Newton, S. Sharma, C. B. Smith, P. Rayapati, A. J. Limardo, C. Meile, and M. A. Moran. 2012. Transcriptional changes underlying elemental stoichiometry shifts in a marine heterotrophic bacterium. Frontiers in Microbiology **3:** 1-24.

Cherif, M., and M. Loreau. 2010. Towards a more biologically realistic use of Droop's equations to model growth under multiple nutrient limitation. Oikos **119:** 897-907.
Chrzanowski, T. H., and J. P. Grover. 2008. Element content of *Pseudomonas fluorescens* varies with growth rate and temperature: A replicated chemostat study addressing ecological stoichiometry. Limnology and Oceanography **53:** 1242-1251.
Chrzanowski, T. H., and M. Kyle. 1996. Ratios of carbon, nitrogen and phosphorus in *Pseudomonas fluorescens* as a model for bacterial element ratios and nutrient regeneration. Aquatic Microbial Ecology **10:** 115-122.
Chrzanowski, T. H., N. C. Lukomski, and J. P. Grover. 2010. Element stoichiometry of a mixotrophic protist grown under varying resource conditions. Journal of Eukaryotic Microbiology **57:** 322-327.
Cole, J. J. 1999. Aquatic microbiology for ecosystem scientists: New and recycled paradigms in ecological microbiology. Ecosystems **2:** 215-225.
Cole, J. J., S. Findlay, and M. L. Pace. 1988. Bacterial production in fresh and saltwater ecosystems: A cross-system overview. Marine Ecology-Progress Series **43:** 1-10.
Colwell, R. R., and D. J. Grimes. 2000. Nonculturable microorganisms in the environment. ASM press.
Cotner, J. B., J. W. Ammerman, E. R. Peele, and E. Bentzen. 1997. Phosphorus-limited bacterioplankton growth in the Sargasso Sea. Aquatic Microbial Ecology **13:** 141-149.
Cotner, J. B., and B. A. Biddanda. 2002. Small players, large role: Microbial influence on biogeochemical processes in pelagic aquatic ecosystems. Ecosystems **5:** 105-121.
Cotner, J. B., and E. K. Hall. 2011. Comment on “a bacterium that can grow by using arsenic instead of phosphorus”. Science Express **332:** 1149.
Cotner, J. B., E. K. Hall, J. T. Scott, and M. Heldal. 2010. Freshwater bacteria are stoichiometrically flexible with a nutrient composition similar to seston. Frontiers in Microbiology **1:** 1-11.
Cotner, J. B., W. Makino, and B. A. Biddanda. 2006. Temperature affects stoichiometry and biochemical composition of *Escherichia coli*. Microbial Ecology **52:** 26-33.
Cotner, J. B., M. L. Ogdahl, and B. A. Biddanda. 2001. Double-stranded DNA measurement in lakes with the fluorescent stain Picogreen and the application to bacterial bioassays. Aquatic Microbial Ecology **25:** 65-74.
Cotner, J. B., and R. G. Wetzel. 1991. 5'-nucleotidase activity in a eutrophic lake and an oligotrophic lake. Applied and Environmental Microbiology **57:** 1306-1312.
---. 1992. Uptake of dissolved inorganic and organic phosphorus compounds by phytoplankton and bacterioplankton. Limnology and Oceanography **37:** 232-243.
Cowles, T. J., R. J. Olson, and S. W. Chisholm. 1988. Food selection by copepods: Discrimination on the basis of food quality. Mar. Biol. **100:** 41-49.
Cross, W. F., J. P. Benstead, P. C. Frost, and S. A. Thomas. 2005. Ecological stoichiometry in freshwater benthic systems: Recent progress and perspectives. Freshwater Biology **50:** 1895-1912.
Crowley, P. H. 1975. Natural selection and the Michaelis constant. J. Theor. Biol. **50:** 461-475.

---. 1992. Resampling methods for computation-intensive data analysis in ecology and evolution. Annu. Rev. Ecol. Syst. **23:** 405-447.
Currie, D. J. 1990. Large-scale variability and interactions among phytoplankton, bacterioplankton, and phosphorus. Limnology and Oceanography **35:** 1437-1455.
Danger, M., T. Daufresne, F. Lucas, S. Pissard, and G. Lacroix. 2008. Does Liebig's law of the minimum scale up from species to communities? Oikos **117:** 1741-1751.
Danger, M., C. Oumarou, D. Benest, and G. Lacroix. 2007. Bacteria can control stoichiometry and nutrient limitation of phytoplankton. Functional Ecology **21:** 202-210.
DeMott, W. R., R. D. Gulati, and K. Siewertsen. 1998. Effects of phosphorus-deficient diets on the carbon and phosphorus balance of *Daphnia magna*. Limnology and Oceanography **43:** 1147 - 1161.
Diaz, J. M., and E. D. Ingall. 2010. Fluorometric quantification of natural inorganic polyphosphate. Environmental Science & Technology **44:** 4665-4671.
Diehl, S., S. Berger, and R. Wöhrl. 2005. Flexible nutrient stoichiometry mediates environmental influences on phytoplankton and its resources. Ecology **86:** 2931-2945.
Droop, M. R. 1973a. Nutrient limitation in osmotrophic protista. American Zoologist **13:** 209-214.
---. 1973b. Some thoughts on nutrient limitation in algae. Journal of Phycology **9:** 264-272.
---. 1974. The nutrient status of algal cells in continuous culture. Journal of the Marine Biological Association of the United Kingdom **54:** 825-855.
---. 2003. In defence of the cell quota model of micro-algal growth. Journal of Plankton Research **25:** 103-107.
Dufresne, A., L. Garczarek, and F. Partensky. 2005. Accelerated evolution associated with genome reduction in a free-living prokaryote. Genome Biol. **6:** 10.
Eccleston-Parry, J. D., and B. S. C. Leadbeater. 1995. Regeneration of phosphorus and nitrogen by four species of heterotrophic nanoflagellates feeding on three nutritional states of a single bacterial strain. Applied and Environmental Microbiology **61:** 1033-1038.
Eilers, H., J. Pernthaler, F. O. Glockner, and R. Amann. 2000. Culturability and in situ abundance of pelagic bacteria from the North Sea. Applied and Environmental Microbiology **66:** 3044-3051.
Eixler, S., U. Selig, and U. Karsten. 2005. Extraction and detection methods for polyphosphate storage in autotrophic planktonic organisms. Hydrobiologia **533:** 135-143.
Eker-Develi, E., A. E. Kideys, and S. Tugrul. 2006. Effect of nutrients on culture dynamics of marine phytoplankton. Aquatic Sciences **68:** 28-39.
Elser, J. J., K. Acharya, M. Kyle, J. Cotner, W. Makino, T. Markow, T. Watts, S. Hobbie, W. Fagan, J. Schade, J. Hood, and R. W. Sterner. 2003. Growth rate-stoichiometry couplings in diverse biota. Ecology Letters **6:** 936-943.
Elser, J. J., T. H. Chrzanowski, R. W. Sterner, and K. H. Mills. 1998. Stoichiometric constraints on food-web dynamics: A whole-lake experiment on the Canadian Shield. Ecosystems **1:** 120-136.

Elser, J. J., D. R. Dobberfuhl, N. A. MacKay, and J. H. Schampel. 1996. Organism size, life history, and N:P stoichiometry. Bioscience **46:** 674-684.

Elser, J. J., W. F. Fagan, R. F. Denno, D. R. Dobberfuhl, A. Folarin, A. Huberty, S. Interlandi, S. S. Kilham, E. McCauley, K. L. Schulz, E. H. Siemann, and R. W. Sterner. 2000a. Nutritional constraints in terrestrial and freshwater food webs. Nature **408:** 578-580.

Elser, J. J., and R. P. Hassett. 1994. A stoichiometric analysis of the zooplankton-phytoplankton interaction in marine and fresh-water ecosystems. Nature **370:** 211-213.

Elser, J. J., R. W. Sterner, E. Gorokhova, W. F. Fagan, T. A. Markow, J. B. Cotner, J. F. Harrison, S. E. Hobbie, G. M. Odell, and L. J. Weider. 2000b. Biological stoichiometry from genes to ecosystems. Ecology Letters **3:** 540-550.

Elser, J. J., and J. Urabe. 1999. The stoichiometry of consumer-driven nutrient recycling: Theory, observations, and consequences. Ecology **80:** 735-751.

Færøvig, P. J., and D. O. Hessen. 2003. Allocation strategies in crustacean stoichiometry: The potential role of phosphorus in the limitation of reproduction. Freshwater Biology **48:** 1782-1792.

Fagerbakke, K. M., M. Heldal, and S. Norland. 1996. Content of carbon, nitrogen, oxygen, sulfur and phosphorus in native aquatic and cultured bacteria. Aquatic Microbial Ecology **10:** 15-27.

Fanin, N., N. Fromin, B. Buatois, and S. Hättenschwiler. 2013. An experimental test of the hypothesis of non-homeostatic consumer stoichiometry in a plant litter–microbe system. Ecology Letters **16:** 764-772.

Fisher, M. M., and E. W. Triplett. 1999. Automated approach for ribosomal intergenic spacer analysis of microbial diversity and its application to freshwater bacterial communities. Applied and Environmental Microbiology **65:** 4630-4636.

Frost, P. C., J. P. Benstead, W. F. Cross, H. Hillebrand, J. H. Larson, M. A. Xenopoulos, and T. Yoshida. 2006. Threshold elemental ratios of carbon and phosphorus in aquatic consumers. Ecology Letters **9:** 774-779.

Frost, P. C., J. J. Elser, and M. A. Turner. 2002. Effects of caddisfly grazers on the elemental composition of epilithon in a boreal lake. Journal of the North American Benthological Society **21:** 54-63.

Frost, P. C., M. A. Evans-White, Z. V. Finkel, T. C. Jensen, and V. Matzek. 2005. Are you what you eat? Physiological constraints on organismal stoichiometry in an elementally imbalanced world. Oikos **109:** 18-28.

Geider, R. J., and J. La Roche. 2002. Redfield revisited: Variability of C:N:P in marine microalgae and its biochemical basis. Eur. J. Phycol. **37:** 1-17.

Ghosh, S., and T. M. LaPara. 2007. The effects of subtherapeutic antibiotic use in farm animals on the proliferation and persistence of antibiotic resistance among soil bacteria. Isme Journal **1:** 191-203.

Glibert, P. M., T. M. Kana, and K. Brown. 2013. From limitation to excess: The consequences of substrate excess and stoichiometry for phytoplankton physiology, trophodynamics and biogeochemistry, and the implications for modeling. Journal of Marine Systems **in press**.

Goldman, J. C., D. A. Caron, and M. R. Dennett. 1987. Regulation of gross growth efficiency and ammonium regeneration in bacteria by substrate C: N ratio. Limnol. Oceanogr **32:** 1239-1252.

Gorokhova, E., and M. Kyle. 2002. Analysis of nucleic acids in daphnia: Development of methods and ontogenetic variations in RNA-DNA content. Journal of Plankton Research **24:** 511-522.

Gough, L., C. W. Osenberg, K. L. Gross, and S. L. Collins. 2000. Fertilization effects on species density and primary productivity in herbaceous plant communities. Oikos **89:** 428-439.

Grime, J. P. 1977. Evidence for the existence of three primary strategies in plants and its relevance to ecological and evolutionary theory. The American Naturalist **111:** 1169-1194.

---. 1979. Plant strategies and vegetation processes. John Wiley & Sons.

Grover, J. 1989. Effects of Si: P supply ratio, supply variability, and selective grazing in the plankton: An experiment with a natural algal and protistan assemblage. Limnology and Oceanography **34:** 349-367.

Grover, J. P. 1991a. Dynamics of competition among microalgae in variable environments: Experimental tests of alternative models. Oikos **62:** 231-243.

---. 1991b. Resource competition in a variable environment: Phytoplankton growing according to the variable-internal-stores model. American Naturalist **138:** 811-835.

Grover, J. P., and T. H. Chrzanowski. 2006. Stoichiometry and growth kinetics in the "smallest zooplankton" - phagotrophic flagellates. Archiv Fur Hydrobiologie **167:** 467-487.

Grover, N. B., E. Eidelstein, and L. J. H. Koppes. 2004. Bacterial shape maintenance: An evaluation of various models. J. Theor. Biol. **227:** 547-559.

Güsewell, S. 2004. N:P ratios in terrestrial plants: Variation and functional significance. New Phytol. **164:** 243-266.

Güsewell, S., U. Bollens, P. Ryser, and F. Klötzli. 2003. Contrasting effects of nitrogen, phosphorus and water regime on first-and second-year growth of 16 wetland plant species. Functional Ecology **17:** 754-765.

Haines, J. R., B. A. Wrenn, E. L. Holder, K. L. Strohmeier, R. T. Herrington, and A. D. Venosa. 1996. Measurement of hydrocarbon-degrading microbial populations by a 96-well plate most-probable-number procedure. Journal of Industrial Microbiology **16:** 36-41.

Hall, E. K., A. R. Dzialowski, S. M. Stoxen, and J. B. Cotner. 2009. The effect of temperature on the coupling between phosphorus and growth in lacustrine bacterioplankton communities. Limnology and Oceanography **54:** 880-889.

Hall, E. K., F. Maixner, O. Franklin, H. Daims, A. Richter, and T. Battin. 2011. Linking microbial and ecosystem ecology using ecological stoichiometry: A synthesis of conceptual and empirical approaches. Ecosystems **14:** 261-273.

Hall, S. R., V. H. Smith, D. A. Lytle, and M. A. Leibold. 2005. Constraints on primary producer N:P stoichiometry along N:P supply ratio gradients. Ecology **86:** 1894-1904.

Hamilton, R. D., and O. Holm-Hansen. 1967. Adenosine triphosphate content of marine bacteria. Limnology and Oceanography **12:** 319-324.
Harold, F. M. 1962. Depletion and replenishment of the inorganic polyphosphate pool in *Neurospora crassa*. J. Bacteriol. **83:** 1047-1057.
Harold, F. M. 1966. Inorganic polyphosphates in biology: Structure, metabolism, and function. Bacteriological Reviews **30:** 772-794.
Haukka, K., E. Kolmonen, R. Hyder, J. Hietala, K. Vakkilainen, T. Kairesalo, H. Haario, and K. Sivonen. 2006. Effect of nutrient loading on bacterioplankton community composition in lake mesocosms. Microbial Ecology **51:** 137-146.
Healey, F. P. 1985. Interacting effects of light and nutrient limitation on the growth rate of *Synechococcus linearis* (cyanophyceae). Journal of Phycology **21:** 134-146.
Healey, F. P., and L. L. Hendzel. 1980. Physiological indicators of nutrient deficiency in lake phytoplankton. Can. J. Fish. Aquat. Sci. **37:** 442-453.
Hecky, R. E., P. Campbell, and L. L. Hendzel. 1993. The stoichiometry of carbon, nitrogen, and phosphorus in particulate matter of lakes and oceans. Limnology and Oceanography **38:** 709-724.
Heldal, M., S. Norland, and O. Tumyr. 1985. X-ray microanalytic method for measurement of dry matter and elemental content of individual bacteria. Applied and Environmental Microbiology **50:** 1251-1257.
Hendrixson, H. A., R. W. Sterner, and A. D. Kay. 2007. Elemental stoichiometry of freshwater fishes in relation to phylogeny, allometry and ecology. Journal of Fish Biology **70:** 121-140.
Hessen, D. O., P. J. Færøvig, and T. Andersen. 2002. Light, nutrients, and P : C ratios in algae: Grazer performance related to food quality and quantity. Ecology **83:** 1886-1898.
Hessen, D. O., P. D. Jeyasingh, M. Neiman, and L. J. Weider. 2010. Genome streamlining and the elemental costs of growth. Trends in Ecology & Evolution **25:** 75-80.
Hessen, D. O., M. Ventura, and J. J. Elser. 2008. Do phosphorus requirements for rna limit genome size in crustacean zooplankton? Genome **51:** 685-691.
Hillebrand, H., E. T. Borer, M. E. S. Bracken, B. J. Cardinale, J. Cebrian, E. E. Cleland, J. J. Elser, D. S. Gruner, W. Stanley Harpole, J. T. Ngai, S. Sandin, E. W. Seabloom, J. B. Shurin, J. E. Smith, and M. D. Smith. 2009. Herbivore metabolism and stoichiometry each constrain herbivory at different organizational scales across ecosystems. Ecology Letters **12:** 516-527.
Hillebrand, H., C.-D. Dürselen, D. Kirschtel, U. Pollingher, and T. Zohary. 1999. Biovolume calculation for pelagic and benthic microalgae. Journal of Phycology **35:** 403-424.
Hillebrand, H., D. S. Gruner, E. T. Borer, M. E. S. Bracken, E. E. Cleland, J. J. Elser, W. S. Harpole, J. T. Ngai, E. W. Seabloom, J. B. Shurin, and J. E. Smith. 2007. Consumer versus resource control of producer diversity depends on ecosystem type and producer community structure. Proceedings of the National Academy of Sciences **104:** 10904-10909.

Hillebrand, H., and M. Kahlert. 2001. Effect of grazing and nutrient supply on periphyton biomass and nutrient stoichiometry in habitats of different productivity. Limnology and Oceanography **46:** 1881-1898.

Hillebrand, H., and U. Sommer. 1999. The nutrient stoichiometry of benthic microalgal growth: Redfield proportions are optimal. Limnology and Oceanography **44:** 440-446.

Hobbie, J. E., R. J. Daley, and S. Jasper. 1977. Use of Nuclepore filters for counting bacteria by fluorescence microscopy. Applied and Environmental Microbiology **33:** 1225-1228.

Holmquist, L., and S. Kjelleberg. 1993. Changes in viability, respiratory activity and morphology of the marine *Vibrio* sp. Strain s14 during starvation of individual nutrients and subsequent recovery. Fems Microbiology Ecology **12:** 215-223.

Hood, J. M., and R. W. Sterner. 2010. Diet mixing: Do animals integrate growth or resources across temporal heterogeneity? American Naturalist **176:** 651-663.

Huisman, J., and F. J. Weissing. 1999. Biodiversity of plankton by species oscillations and chaos. Nature **402:** 407-410.

Hupfer, M., S. Glöss, P. Schmieder, and H. P. Grossart. 2008. Methods for detection and quantification of polyphosphate and polyphosphate accumulating microorganisms in aquatic sediments. Int. Rev. Hydrobiol. **93:** 1-30.

Hutz, A., K. Schubert, and J. Overmann. 2011. Thalassospira sp isolated from the oligotrophic Eastern Mediterranean sea exhibits chemotaxis toward inorganic phosphate during starvation. Applied and Environmental Microbiology **77:** 4412-4421.

Jahid, I. K., A. J. Silva, and J. A. Benitez. 2006. Polyphosphate stores enhance the ability of *Vibrio cholerae* to overcome environmental stresses in a low-phosphate environment. Applied and Environmental Microbiology **72:** 7043-7049.

Jannasch, H. W. 1974. Steady state and the chemostat in ecology. Limnology and Oceanography **19:** 716-720.

Jarvis, B., C. Wilrich, and P. T. Wilrich. 2010. Reconsideration of the derivation of most probable numbers, their standard deviations, confidence bounds and rarity values. J. Appl. Microbiol. **109:** 1660-1667.

Jensen, T. C., T. R. Anderson, M. Daufresne, and D. O. Hessen. 2006. Does excess carbon affect respiration of the rotifer *Brachionus calyciflorus* pallas? Freshwater Biology **51:** 2320-2333.

Jeyasingh, P. D., L. J. Weider, and R. W. Sterner. 2009. Genetically-based trade-offs in response to stoichiometric food quality influence competition in a keystone aquatic herbivore. Ecology Letters **12:** 1229-1237.

Johansson, N., and E. Granéli. 1999a. Cell density, chemical composition and toxicity of *Chrysochromulina polylepis* (haptophyta) in relation to different N:P supply ratios. Mar. Biol. **135:** 209-217.

---. 1999b. Influence of different nutrient conditions on cell density, chemical composition and toxicity of *Prymnesium parvum* (haptophyta) in semi-continuous cultures. J. Exp. Mar. Biol. Ecol. **239:** 243-258.

Jürgens, K., and H. Güde. 1990. Incorporation and release of phosphorus by planktonic bacteria and phagotrophic flagellates. Marine Ecology-Progress Series **59:** 271-284.
Kaprelyants, A. S., J. C. Gottschal, and D. B. Kell. 1993. Dormancy in non-sporulating bacteria. Fems Microbiology Reviews **104:** 271-286.
Kilham, P., and R. Hecky. 1988. Comparative ecology of marine and freshwater phytoplankton. Limnology and Oceanography **33:** 776-795.
Kim, H. J., M. P. Fay, B. Yu, M. J. Barrett, and E. J. Feuer. 2004. Comparability of segmented line regression models. Biometrics **60:** 1005-1014.
Kirchman, D. L. 1994. The uptake of inorganic nutrients by heterotrophic bacteria. Microbial Ecology **28:** 255-271.
Klappenbach, J. A., J. M. Dunbar, and T. M. Schmidt. 2000. rRNA operon copy number reflects ecological strategies of bacteria. Applied and Environmental Microbiology **66:** 1328-1333.
Klausmeier, C. A., E. Litchman, T. Daufresne, and S. A. Levin. 2004a. Optimal nitrogen-to-phosphorus stoichiometry of phytoplankton. Nature **429:** 171-174.
---. 2008. Phytoplankton stoichiometry. Ecological Research **23:** 479-485.
Klausmeier, C. A., E. Litchman, and S. A. Levin. 2004b. Phytoplankton growth and stoichiometry under multiple nutrient limitation. Limnology and Oceanography **49:** 1463-1470.
Koch, A. L. 1996. What size should a bacterium be? A question of scale. Annual Review of Microbiology **50:** 317-348.
Kornberg, A. 1995. Inorganic polyphosphate: Toward making a forgotten polymer unforgettable. Journal of Bacteriology **177:** 491-496.
Kulaev, I., and T. Kulakovskaya. 2000. Polyphosphate and phosphate pump. Annual Review of Microbiology **54:** 709-734.
Lahooti, M., and C. R. Harwood. 1999. Transcriptional analysis of the *Bacillus subtilis* teichuronic acid operon. Microbiology **145:** 3409-3417.
Laspoumaderes, C., B. Modenutti, and E. Balseiro. 2010. Herbivory versus omnivory: Linking homeostasis and elemental imbalance in copepod development. Journal of Plankton Research **32:** 1573-1582.
Leonardos, N., and R. J. Geider. 2004a. Effects of nitrate: Phosphate supply ratio and irradiance on the C : N : P stoichiometry of chaetoceros muelleri. Eur. J. Phycol. **39:** 173-180.
---. 2004b. Responses of elemental and biochemical composition of *Chaetoceros muelleri* to growth under varying light and nitrate: Phosphate supply ratios and their influence on critical N : P. Limnology and Oceanography **49:** 2105-2114.
---. 2005. Elemental and biochemical composition of *Rhinomonas reticulata* (cryptophyta) in relation to light and nitrate-to-phosphate supply ratios. Journal of Phycology **41:** 567-576.
Lindehoff, E., E. Granéli, and W. Granéli. 2009. Effect of tertiary sewage effluent additions on *Prymnesium parvum* cell toxicity and stable isotope ratios. Harmful Algae **8:** 247-253.
Loladze, I., and J. J. Elser. 2011. The origins of the redfield nitrogen-to-phosphorus ratio are in a homoeostatic protein-to-rRNA ratio. Ecology Letters **14:** 244-250.

Løvdal, T., E. F. Skjoldal, M. Heldal, S. Norland, and T. F. Thingstad. 2008. Changes in morphology and elemental composition of *Vibrio splendidus* along a gradient from carbon-limited to phosphate-limited growth. Microbial Ecology **55:** 152-161.

Lynn, S. G., S. S. Kilham, D. A. Kreeger, and S. J. Interlandi. 2000. Effect of nutrient availability on the biochemical and elemental stoichiometry in the freshwater diatom *Stephanodiscus minutulus* (bacillariophyceae). Journal of Phycology **36:** 510-522.

MacArthur, R. H., and E. O. Wilson. 1967. The theory of island biogeography. Princeton University Press.

Makino, W., and J. B. Cotner. 2004. Elemental stoichiometry of a heterotrophic bacterial community in a freshwater lake: Implications for growth- and resource-dependent variations. Aquatic Microbial Ecology **34:** 33-41.

Makino, W., J. B. Cotner, R. W. Sterner, and J. J. Elser. 2003. Are bacteria more like plants or animals? Growth rate and resource dependence of bacterial C : N : P stoichiometry. Functional Ecology **17:** 121-130.

Malzahn, A. M., N. Aberle, C. Clemmesen, and M. Boersma. 2007. Nutrient limitation of primary producers affects planktivorous fish condition. Limnology and Oceanography **52:** 2062-2071.

Mamolos, A. P., D. S. Veresoglou, and N. Barbayiannis. 1995. Plant species abundance and tissue concentrations of limiting nutrients in low-nutrient grasslands: A test of competition theory. Journal of Ecology **83:** 485-495.

Marinho, M. M., and S. M. F. de Oliveira E Azevedo. 2007. Influence of N/P ratio on competitive abilities for nitrogen and phosphorus by *Microcystis aeruginosa* and *Aulacoseira distans*. Aquatic Ecology **41:** 525-533.

Martin, P., and B. A. S. Van Mooy. 2013. Fluorometric quantification of polyphosphate in environmental plankton samples: Extraction protocols, matrix effects, and nucleic acid interference. Applied and Environmental Microbiology **79:** 273-281.

Minnikin, D. E., H. Abdolrahimzadeh, and J. Baddiley. 1974. Replacement of acidic phospholipids by acidic glycolipids in *Pseudomonas diminuta*. Nature **249:** 268-269.

Mino, T., T. Kawakami, and T. Matsuo. 1985. Location of phosphorus in activated sludge and function of intracellular polyphosphates in biological phosphorus removal process. Water Science and Technology **17:** 93-106.

Moe, S. J., R. S. Stelzer, M. R. Forman, W. S. Harpole, T. Daufresne, and T. Yoshida. 2005. Recent advances in ecological stoichiometry: Insights for population and community ecology. Oikos **109:** 29-39.

Monod, J. 1949. The growth of bacterial cultures. Annual Reviews in Microbiology **3:** 371-394.

Morita, R. Y. 1997. Bacteria in oligotrophic environments. Chapman & Hall New York.

Morrison, D. A. 1977. Transformation in *Escherichia coli*: Cryogenic preservation of competent cells. Journal of Bacteriology **132:** 349-351.

Nakano, S. 1994. Carbon: Nitrogen: Phosphorus ratios and nutrient regeneration of a heterotrophic flagellate fed on bacteria with different elemental ratios. Archiv Fur Hydrobiologie **129:** 257-271.

Nelson, D. K., T. M. LaPara, and P. J. Novak. 2010. Effects of ethanol-based fuel contamination: Microbial community changes, production of regulated compounds, and methane generation. Environmental Science & Technology **44:** 4525-4530.

Neuhaus, F. C., and J. Baddiley. 2003. A continuum of anionic charge: Structures and functions of d-alanyl-teichoic acids in gram-positive bacteria. Microbiology and Molecular Biology Reviews **67:** 686-723.

Newton, R. J., S. E. Jones, A. Eiler, K. D. McMahon, and S. Bertilsson. 2011. A guide to the natural history of freshwater lake bacteria. Microbiology and Molecular Biology Reviews **75:** 14-49.

Nix, P. G., and M. M. Daykin. 1992. Resazurin reduction tests as an estimate of coliform and heterotrophic bacterial numbers in environmental samples. Bulletin of Environmental Contamination and Toxicology **49:** 354-360.

Norland, S., K. M. Fagerbakke, and M. Heldal. 1995. Light element analysis of individual bacteria by x-ray microanalysis. Applied and Environmental Microbiology **61:** 1357-1362.

Okie, J. G. 2013. General models for the spectra of surface area scaling strategies of cells and organisms: Fractality, geometric dissimilitude, and internalization. American Naturalist **181:** 421-439.

Oksanen, J. F., G. Blanchet, R. Kindt, P. Legendre, P. R. Minchin, R. B. O'Hara, G. L. Simpson, P. Solymos, M. H. H. Stevens, and H. Wagner. 2011. Vegan: Community ecology package. R package version 2.0-0.

Page, K. A., S. A. Connon, and S. J. Giovannoni. 2004. Representative freshwater bacterioplankton isolated from Crater Lake, Oregon. Applied and Environmental Microbiology **70:** 6542-6550.

Persson, J., P. Fink, A. Goto, J. M. Hood, J. Jonas, and S. Kato. 2010. To be or not to be what you eat: Regulation of stoichiometric homeostasis among autotrophs and heterotrophs. Oikos **119:** 741-751.

Phillips, K. N., C. M. Godwin, and J. B. Cotner. Submitted.

Pilati, A., and M. J. Vanni. 2007. Ontogeny, diet shifts, and nutrient stoichiometry in fish. Oikos **116:** 1663-1674.

Plath, K., and M. Boersma. 2001. Mineral limitation of zooplankton: Stoichiometric constraints and optimal foraging. Ecology **82:** 1260-1269.

Preiss, J. 1984. Bacterial glycogen synthesis and its regulation. Annual Reviews in Microbiology **38:** 419-458.

Price, H. J. 1988. Feeding mechanisms in marine and freshwater zooplankton. Bulletin of Marine Science **43:** 327-343.

Quigg, A., A. J. Irwin, and Z. V. Finkel. 2011. Evolutionary inheritance of elemental stoichiometry in phytoplankton. Proceedings of the Royal Society B-Biological Sciences **278:** 526-534.

Ramette, A. 2009. Quantitative community fingerprinting methods for estimating the abundance of operational taxonomic units in natural microbial communities. Applied and Environmental Microbiology **75:** 2495-2505.

Raven, J. A., L. L. Handley, and M. Andrews. 2004. Global aspects of C/N interactions determining plant-environment interactions. Journal of Experimental Botany **55:** 11-25.
Redfield, A. C. 1958. The biological control of chemical factors in the environment. American Scientist **46:** 205-221.
Rhee, G.-Y. 1973. A continuous culture study of phosphate uptake, growth rate and polyphosphate in *Scenedesmus* sp. Journal of Phycology **9:** 95-506.
---. 1978. Effects of N:P atomic ratios and nitrate limitation on algal growth, cell composition, and nitrate uptake. Limnology and Oceanography **23:** 10-25.
Ribalet, F., C. Vidoudez, D. Cassin, G. Pohnert, A. Ianora, A. Miralto, and R. Casotti. 2009. High plasticity in the production of diatom-derived polyunsaturated aldehydes under nutrient limitation: Physiological and ecological implications. Protist **160:** 444-451.
Rosenberg, H., R. G. Gerdes, and F. M. Harold. 1979. Energy coupling to the transport of inorganic phosphate in *Escherichia coli* k12. Biochemical Journal **178:** 133-137.
Sakshaug, E., K. Andresen, S. Myklestad, and Y. Olsen. 1983. Nutrient status of phytoplankton communities in Norwegian waters (marine, brackish, and fresh) as revealed by their chemical composition. Journal of Plankton Research **5:** 175-196.
Schatz, G. S., and E. McCauley. 2007. Foraging behavior by *Daphnia* in stoichiometric gradients of food quality. Oecologia **153:** 1021-1030.
Schlesinger, W. H., J. J. Cole, A. C. Finzi, and E. A. Holland. 2011. Introduction to coupled biogeochemical cycles. Frontiers in Ecology and the Environment **9:** 5-8.
Schut, F., E. J. De Vries, J. C. Gottschal, B. R. Robertson, W. Harder, R. A. Prins, and D. K. Button. 1993. Isolation of typical marine bacteria by dilution culture: Growth, maintenance, and characteristics of isolates under laboratory conditions. Appl. Environ. Microbiol. **59:** 2150-2160.
Scott, J. T., J. B. Cotner, and T. M. LaPara. 2012. Variable stoichiometry and homeostatic regulation of bacterial biomass elemental composition. Frontiers in Microbiology **3:** 1-8.
Shafik, H. M., S. Herodek, M. Présing, L. Vörös, and K. V. Balogh. 1997. Growth of *Cyclotella meneghiniana* kutz. Ii. Growth and cell composition under different growth rates with different limiting nutrient. Annales De Limnologie-International Journal of Limnology **33:** 223-233.
Smalley, G. W., D. W. Coats, and D. K. Stoecker. 2003. Feeding in the mixotrophic dinoflagellate *Ceratium furca* is influenced by intracellular nutrient concentrations. Marine Ecology-Progress Series **262:** 137-151.
Sokal, R., and F. Rohlf. 1995. Biometry. Freeman.
Sommer, U. 1984. The paradox of the plankton: Fluctuations of phosphorus availability maintain diversity of phytoplankton in flow-through cultures. Limnology and Oceanography **29:** 633-636.
---. 1985. Comparison between steady-state and non-steady state competition: Experiments with natural phytoplankton. Limnology and Oceanography **30:** 335-346.

Staley, J. T., and A. Konopka. 1985. Measurement of in situ activities of nonphotosynthetic microorganisms in aquatic and terrestrial habitats. Annual Review of Microbiology **39:** 321-346.
Sterner, R. W. 1990. The ratio of nitrogen to phosphorus resupplied by herbivores: Zooplankton and the algal competitive arena. American Naturalist **136:** 209-229.
---. 1997. Modelling interactions of food quality and quantity in homeostatic consumers. Freshwater Biology **38:** 473-481.
Sterner, R. W. 2011. C: N: P stoichiometry in lake superior: Freshwater sea as end member. Inland Waters **1:** 29-46.
Sterner, R. W., T. Andersen, J. J. Elser, D. O. Hessen, J. M. Hood, E. McCauley, and J. Urabe. 2008. Scale-dependent carbon: Nitrogen: Phosphorus seston stoichiometry in marine and freshwaters. Limnology and Oceanography **53:** 1169-1180.
Sterner, R. W., and J. J. Elser. 2002. Ecological stoichiometry: The biology of elements from molecules to the biosphere. Princeton University Press.
Sterner, R. W., J. J. Elser, E. J. Fee, S. J. Guildford, and T. H. Chrzanowski. 1997. The light: Nutrient ratio in lakes: The balance of energy and materials affects ecosystem structure and process. The American Naturalist **150:** 663-684.
Sterner, R. W., J. J. Elser, and D. O. Hessen. 1992. Stoichiometric relationships among producers, consumers and nutrient cycling in pelagic ecosystems. Biogeochemistry **17:** 49-67.
Sterner, R. W., D. D. Hagemeier, W. L. Smith, and R. F. Smith. 1993. Phytoplankton nutrient limitation and food quality for *Daphnia*. Limnology and Oceanography **38:** 857-871.
Sterner, R. W., and D. O. Hessen. 1994. Algal nutrient limitation and the nutrition of aquatic herbivores. Annu. Rev. Ecol. Syst. **25:** 1-29.
Sterner, R. W., T. M. Smutka, R. M. L. McKay, X. M. Qin, E. T. Brown, and R. M. Sherrell. 2004. Phosphorus and trace metal limitation of algae and bacteria in lake superior. Limnology and Oceanography **49:** 495-507.
Stets, E. G., and J. B. Cotner. 2008. The influence of dissolved organic carbon on bacterial phosphorus uptake and bacteria-phytoplankton dynamics in two minnesota lakes. Limnology and Oceanography **53:** 137-147.
Sunda, W. G., and D. R. Hardison. 2010. Evolutionary tradeoffs among nutrient acquisition, cell size, and grazing defense in marine phytoplankton promote ecosystem stability. Marine Ecology Progress Series **401:** 63-76.
Suzumura, M. 2008. Persulfate chemical wet oxidation method for the determination of particulate phosphorus in comparison with a high-temperature dry combustion method. Limnology and Oceanography: Methods **6:** 619-629.
Tambi, H., G. A. F. Flaten, J. K. Egge, G. Bødtker, A. Jacobsen, and T. F. Thingstad. 2009. Relationship between phosphate affinities and cell size and shape in various bacteria and phytoplankton. Aquat Microb Ecol **57:** 311-320.
Tan, Q. G., and W. X. Wang. 2009. Calcium influence on phosphorus regulation in *Daphnia magna*: Implications for phosphorus cycling. Aquatic Biology **5:** 1-11.
Tanaka, T., T. F. Thingstad, J. M. Gasol, C. Cardelús, J. Jezbera, M. M. Sala, K. Šimek, and F. Unrein. 2009. Determining the availability of phosphate and glucose for

bacteria in p-limited mesocosms of nw mediterranean surface waters. Aquatic Microbial Ecology **56:** 81-91.
Tanaka, T., T. F. Thingstad, T. Løvdal, H. P. Grossart, A. Larsen, M. Allgaier, M. Meyerhöfer, K. G. Schulz, J. Wohlers, E. Zöllner, and U. Riebesell. 2008. Availability of phosphate for phytoplankton and bacteria and of glucose for bacteria at different pCO2 levels in a mesocosm study. Biogeosciences **5:** 669-678.
Tanner, R. 2002. Cultivation of bacteria and fungi. *In* C. Hurst, G. Knudsen, M. McInerney, L. Stetzenbach and M. Walter [eds.], Manual of environmental microbiology, 2nd edition. ASM Press
Tett, P., S. I. Heaney, and M. R. Droop. 1985. The Redfield ratio and phytoplankton growth rate. Journal of the Marine Biological Association of the United Kingdom **65:** 487-504.
Tezuka, Y. 1990. Bacterial regeneration of ammonium and phosphate as affected by the Carbon: Nitrogen: Phosphorus ratio of organic substrates. Microbial Ecology **19:** 227-238.
Theissen, K. M., W. O. Hobbs, J. M. R. Hobbs, K. D. Zimmer, L. M. Domine, J. B. Cotner, and S. Sugita. 2012. The altered ecology of lake christina: A record of regime shifts, land-use change, and management from a temperate shallow lake. Science of the Total Environment **433:** 336-346.
Thingstad, T. F. 1987. Utilization of N, P, and organic C by heterotrophic bacteria. I. Outline of a chemostat theory with a consistent concept of 'maintenance' metabolism. Marine Ecology-Progress Series **35:** 99-109.
Thingstad, T. F., L. Øvreas, J. K. Egge, T. Løvdal, and M. Heldal. 2005. Use of non-limiting substrates to increase size; a generic strategy to simultaneously optimize uptake and minimize predation in pelagic osmotrophs? Ecology Letters **8:** 675-682.
Thingstad, T. F., U. L. Zweifel, and F. Rassoulzadegan. 1998. P limitation of heterotrophic bacteria and phytoplankton in the northwest mediterranean. Limnology and Oceanography **43:** 88-94.
Tilman, D. 1977. Resource competition between planktonic algae: An experimental and theoretical approach. Ecology **58:** 338-348.
---. 1980. Resources: A graphical-mechanistic approach to competition and predation. American Naturalist **116:** 362-393.
---. 1982. Resource competition and community structure. Princeton University Press.
---. 1988. Plant strategies and the dynamics and structure of plant communities. Princeton University Press.
---. 1990. Constraints and tradeoffs: Toward a predictive theory of competition and succession. Oikos **58:** 3-15.
---. 1994. Competition and biodiversity in spatially structured habitats. Ecology **75:** 2-16.
Tilman, D., and S. S. Kilham. 1976. Phosphate and silicate growth and uptake kinetics of the diatoms *Asterionella formosa* and *Cyclotella meneghiniana* in batch and semicontinuous culture. Journal of Phycology **12:** 375-383.
Tilman, D., S. S. Kilham, and P. Kilham. 1982. Phytoplankton community ecology: The role of limiting nutrients. Annu. Rev. Ecol. Syst. **13:** 349-372.

Tilman, D., and D. Wedin. 1991. Plant traits and resource reduction for five grasses growing on a nitrogen gradient. Ecology **72:** 685-700.
Touratier, F., J. G. Field, and C. L. Moloney. 2001. A stoichiometric model relating growth substrate quality (C:N:P ratios) to N:P ratios in the products of heterotrophic release and excretion. Ecological Modelling **139:** 265-291.
Uronen, P., S. Lehtinen, C. Legrand, P. Kuuppo, and T. Tamminen. 2005. Haemolytic activity and allelopathy of the haptophyte *Prymnesium parvum* in nutrient-limited and balanced growth conditions. Marine Ecology-Progress Series **299:** 137-148.
Vadstein, O. 1998. Evaluation of competitive ability of two heterotrophic planktonic bacteria under phosphorus limitation. Aquatic Microbial Ecology **14:** 119-127.
van den Berg, H. A. 2001. How microbes can achieve balanced growth in a fluctuating environment. Acta Biotheoretica **49:** 1-21.
Van Mooy, B. A. S., H. F. Fredricks, B. E. Pedler, S. T. Dyhrman, D. M. Karl, M. Koblížek, M. W. Lomas, T. J. Mincer, L. R. Moore, T. Moutin, M. S. Rappé, and E. A. Webb. 2009. Phytoplankton in the ocean use non-phosphorus lipids in response to phosphorus scarcity. Nature **458:** 69-72.
Van Mooy, B. A. S., G. Rocap, H. F. Fredricks, C. T. Evans, and A. H. Devol. 2006. Sulfolipids dramatically decrease phosphorus demand by picocyanobacteria in oligotrophic marine environments. Proceedings of the National Academy of Sciences of the United States of America **103:** 8607-8612.
Velji, M. I., and L. J. Albright. 1993. Improved sample preparation for enumeration of aggregated aquatic substrate bacteria, p. 139-142. *In* P. F. Kemp, B. F. Sherr, E. B. Sherr and J. J. Cole [eds.], Handbook of methods in aquatic microbial ecology. Lewis Publishers.
Ventura, M., and J. Catalan. 2005. Reproduction as one of the main causes of temporal variability in the elemental composition of zooplankton. Limnology and Oceanography **50:** 2043-2056.
Villar-Argaiz, M., J. M. Medina-Sánchez, and P. Carrillo. 2002a. Linking life history strategies and ontogeny in crustacean zooplankton: Implications for homeostasis. Ecology **83:** 1899-1914.
Villar-Argaiz, M., J. M. Medina-Sánchez, and P. Carrillo. 2002b. Microbial plankton response to contrasting climatic conditions: Insights from community structure, productivity and fraction stoichiometry. Aquatic Microbial Ecology **29:** 253-266.
Vrede, K., M. Heldal, S. Norland, and G. Bratbak. 2002. Elemental composition (C, N, P) and cell volume of exponentially growing and nutrient-limited bacterioplankton. Applied and Environmental Microbiology **68:** 2965-2971.
Vrede, T., D. R. Dobberfuhl, S. A. L. M. Kooijman, and J. J. Elser. 2004. Fundamental connections among organism C:N:P stoichiometry, macromolecular composition, and growth. Ecology **85:** 1217-1229.
Waara, T., M. Jansson, and K. Pettersson. 1993. Phosphorus composition and release in sediment bacteria of the genus *Pseudomonas* during aerobic and anaerobic conditions. Hydrobiologia **253:** 131-140.
Warton, D. I., I. J. Wright, D. S. Falster, and M. Westoby. 2006. Bivariate line-fitting methods for allometry. Biol. Rev. **81:** 259-291.

White, D. C., W. M. Davis, J. S. Nickels, J. D. King, and R. J. Bobbie. 1979. Determination of the sedimentary microbial biomass by extractible lipid phosphate. Oecologia **40:** 51-62.

Wilkinson, J. F. 1963. Carbon and energy storage in bacteria. Journal of General Microbiology **32:** 171-176.

Wolfe-Simon, F., J. S. Blum, T. R. Kulp, G. W. Gordon, S. E. Hoeft, J. Pett-Ridge, J. F. Stolz, S. M. Webb, P. K. Weber, and P. C. W. Davies. 2011. Response to comments on ,"a bacterium that can grow using arsenic instead of phosphorus". Science **332:** 1149-1149.

Wolfe-Simon, F., J. S. Blum, T. R. Kulp, G. W. Gordon, S. E. Hoeft, J. Pett-Ridge, J. F. Stolz, S. M. Webb, P. K. Weber, P. C. W. Davies, A. D. Anbar, and R. S. Oremland. 2010. A bacterium that can grow by using arsenic instead of phosphorus. Science **332:** 1163-1166.

Yu, Q., J. J. Elser, N. He, H. Wu, Q. Chen, G. Zhang, and X. Han. 2011. Stoichiometric homeostasis of vascular plants in the inner mongolia grassland. Oecologia **166:** 1-10.

Zavaleta-Pastor, M., C. Sohlenkamp, J. L. Gao, Z. Guan, R. Zaheer, T. M. Finan, C. R. H. Raetz, I. M. López-Lara, and O. Geiger. 2010. *Sinorhizobium meliloti* phospholipase c required for lipid remodeling during phosphorus limitation. Proceedings of the National Academy of Sciences of the United States of America **107:** 302-307.

Appendix A: Homeostasis and Stoichiometry Datasets

Zooplankton Homeostasis Datasets Summary

For each element ratio, there are at least three discrete resource ratios used for the log-log biomass-resource regressions. The slope of the biomass-resource regressions is β and the elevation of the regressions is α. [1]Dilution rates 0.12 to 1 d^{-1}, [2] Control, [3] HUFA supplement, [4]Dilution rates 0.2 to 1.2 d^{-1}.

Predator Species	Prey Species	$C:P_{resources}$ Levels, β, α, R^2	$N:P_{resources}$ Levels, β, α, R^2	$C:N_{resources}$ Levels, β, α, R^2	Source
Acartia tonsa	*Rhodomonas alina*	4, 0.38, 1.42, 0.51	4, -0.02, 1.63, 0.00	3, 0.15, 0.59, 0.06	(Malzahn et al. 2007)
Brachionus calyciflorus	*Selenastrum capricornutum*	3, 0.08, 1.80, 0.11	3, -0.12, 1.33, 0.22	3, 0.07, 0.70, 0.05	(Jensen et al. 2006)
Daphnia galeta [1]	*Scenedesmus acutus*	6, -0.21, 2.51, 0.86	6, -0.02, 1.27, 0.06	7, -0.27, 1.01, 0.71	(Acharya et al. 2004)
Daphnia magna	*Chlamydomonas reinhardtii*	4, 0.21, 1.18, 0.99	-	-	(Tan and Wang 2009)
Daphnia magna	*Scenedesmus acutus* and *Synechococcus elongatus*	5, 0.19, 1.50, 0.99	-	-	(DeMott et al. 1998)
Daphnia magna	*Scenedesmus obliquus*	6, 0.11, 1.28, 0.13	-	-	(Hood and Sterner 2010)
Daphnia magna [1]	*Scenedesmus acutus*	-	-	6, 0.32, 0.41, 0.77	(Acharya et al. 2004)
Daphnia magna [2]	*Scenedesmus obliquus*	6, 0.13, 1.81, 0.59	-	-	(Plath and Boersma 2001)
Daphnia magna[3]	*Scenedesmus obliquus*	6, 0.13, 1.76, 0.76	-	-	(Plath and Boersma 2001)
Daphnia obtusa	*Scenedesmus acutus*	-	3, -0.05, 1.40, 0.86	-	(Sterner et al. 1993)
Daphnia pulicaria [1]	*Scenedesmus acutus*	6, -0.07, 2.09, 0.07	6, 0.01, 1.21, 0.01	10, -0.18, 0.87, 0.38	(Acharya et al. 2004)

Ochromonas danica	*Pseudomonas fluorescens*	4, 1.67, -0.86, 0.62	4, 0.73, 0.44, 0.21	4, 1.26, 0.09, 0.31	(Chrzanowski et al. 2010)
Paraphysomonas imperforata [4]	*Dunaliella tertiolecta*	6, 0.80, 0.12, 0.92	6, 0.76, 0.16, 0.82	6, 0.39, 0.43, 0.43	(Goldman et al. 1987)
Paraphysomonas imperforata [4]	*Phaeodactylum tricornutum*	6, 0.80, 0.17, 0.91	6, 0.68, 0.26, 0.84	6, 0.32, 0.53, 0.89	(Goldman et al. 1987)

Phytoplankton Homeostasis Datasets Summary

For each dataset, there are at least three discrete resource ratios used for the log-log biomass-resource regressions. The slope of the biomass-resource regressions is β and the elevation of the regressions is α. [1] Dilution rate 0.3 d^{-1}, [2] Dilution rate 0.6 d^{-1}, [3] Dilution rate 0.125 d^{-1}, [4] Dilution rate 0.25 d^{-1}, [5] Dilution rate 0.5 d^{-1}, [6] Dilution rate 0.75 d^{-1}, [7] Low Light, [8] High Light, [9] Dilution rate 0.9 d^{-1}, [10] Dilution rate 0.28 d^{-1}

Species	$N:P_{resources}$ Levels, β, α, R^2	Source
Amphidinium carterae	3, 0.08, 1.29, 0.94	(Sakshaug et al. 1983)
Aulacoseira distans	3, 1.49, -0.62, 0.99	(Marinho and de Oliveira E Azevedo 2007)
Ceratium furca	5, 0.59, -0.14, 0.99	(Smalley et al. 2003)
Chaetoceros muelleri [1]	5, 0.55, 0.79, 0.76	(Leonardos and Geider 2004a)
Chaetoceros muelleri [2]	5, 0.82, 0.25, 0.91	(Leonardos and Geider 2004a)
Chrysochromulina polylepis	5, 0.23, 0.93, 0.98	(Johansson and Granéli 1999a)
Cyclotella meneghiniana [3]	3, 0.51, 0.02, 0.99	(Shafik et al. 1997)
Cyclotella meneghiniana [4]	3, 0.18, 0.38, 0.99	(Shafik et al. 1997)
Cyclotella meneghiniana [5]	3, 0.14, 0.92, 0.09	(Shafik et al. 1997)
Cyclotella meneghiniana [6]	3, 0.31, 0.25, 0.33	(Shafik et al. 1997)
Dunaliella tertiolecta	3, 0.82, -0.44, 0.99	(Brutemark et al. 2009)
Emiliania huxleyi	5, 0.08, 1.15, 0.99	(Sakshaug et al. 1983)
Heterocapsa triquetra	3, 0.71, -0.35, 0.99	(Brutemark et al. 2009)
Microcystis aeruginosa	3, 1.54, -0.75, 0.98	(Marinho and de Oliveira E Azevedo 2007)
Prorocentrum micans	4, 0.30, 0.61, 0.91	(Eker-Develi et al. 2006)
Pyrmnesium parvum	3, 0.35, 0.82, 0.96	(Uronen et al. 2005)
Pyrmnesium parvum [7]	3, 0.42, 0.77, 0.99	(Lindehoff et al. 2009)
Pyrmnesium parvum [8]	3, 0.28, 0.79, 0.99	(Johansson and Granéli 1999b)
Rhinomonas reticulata [7]	5, 0.63, 0.78, 0.72	(Leonardos and Geider 2005)
Rhinomonas reticulata [8]	5, 0.66, 0.69, 0.86	(Leonardos and Geider 2005)
Rhodomonas sp.	3, 0.70, -0.09, 0.99	(Brutemark et al. 2009)
Scenedesmus sp.	16, 1.03, -0.05, 0.99	(Rhee 1978)
Selenastrum capricornutum	3, 0.33, 0.64, 0.95	(Jensen et al. 2006)

Selenastrum capricornutum [7]	6, 0.39, 0.58, 0.70	(Hessen et al. 2002)
Selenastrum capricornutum [8]	6, 0.52, 0.47, 0.84	(Hessen et al. 2002)
Skeletonema costatum	4, 0.42, 0.35, 0.98	(Eker-Develi et al. 2006)
Skeletonema marinoi [9]	3, 0.02, 1.04, 0.29	(Ribalet et al. 2009)
Skeletonema marinoi [10]	3, 0.36, 0.50, 0.88	(Ribalet et al. 2009)
Stephanodiscus minutulus	3, 0.25, 0.49, 0.77	(Lynn et al. 2000)

Heterotrophic Bacteria Homeostasis Datasets Summary

For each element ratio, there are at least three discrete resource ratios used for the log-log biomass-resource regressions. The slope of the biomass-resource regressions is β and the elevation of the regressions is α. [1] Temperature 20 ºC, [2] Dilution rate 0.5 h^{-1}, [3] Dilution rate 1.0 h^{-1}, [4] Dilution rate 1.5 h^{-1}, [5] Dilution rate 0.03 h^{-1}, [6] Dilution rate 0.06 h^{-1}, [7] Dilution rate 0.09 h^{-1}, [8] Dilution rate 0.25 h^{-1}, [9] Dilution rate 0.5 h^{-1}, [10] Dilution rate 0.7 h^{-1}

Culture	$C:P_{resources}$ Levels, β, α, R^2	$N:P_{resources}$ Levels, β, α, R^2	$C:N_{resources}$ Levels, β, α, R^2	Source
Aeromonas sp.	10, 0.35, 1.34, 0.83	-	-	(Scott et al. 2012)
Agrobacterium sp. [1]	3, 0.55, 0.89, 0.99	3, 0.46, 0.42, 0.96	-	(Philips et al. in prep.)
Arthrobacter sp.	10, 0.29, 1.68, 0.45	-	-	(Scott et al. 2012)
Arthrobacter sp. [1]	3, 0.52, 1.00, 0.90	3, 0.65, -0.05, 0.94	-	(Philips et al. in prep.)
Cellulomonas sp.	10, 0.34, 1.39, 0.95	-	-	(Scott et al. 2012)
Cellvibrio sp.	10, 0.25, 1.81, 0.99	-	-	(Scott et al. 2012)
Escherichia coli	3, -0.06, 1.85, 0.88	3, 0.04, 1.23, 0.21	-	(Nakano 1994)
Escherichia coli [2]	5, 0.04, 1.71, 0.57	5, 0.03, 1.15, 0.53	-	(Makino et al. 2003)
Escherichia coli [3]	5, 0.05, 1.65, 0.64	5, 0.04, 1.08, 0.36	-	(Makino et al. 2003)

Escherichia coli [4]	5, 0.04, 1.61, 0.29	5, 0.03, 1.03, 0.26	-	(Makino et al. 2003)
Flavobacterium sp.	10, 0.57, 1.03, 0.99	-	-	(Scott et al. 2012)
Flavobacterium sp.	10, 0.50, 1.08, 0.91	-	-	(Scott et al. 2012)
Flavobacterium sp. [1]	3, 0.64, 0.57, 0.96	3, 0.37, 0.38, 0.87	-	(Philips et al. in prep.)
Lake Biwa Strain	6, 0.17, 1.54, 0.95	5, 0.17, 1.08, 0.82	5, 0.16, 0.47, 0.97	(Nakano 1994)
Marine Isolate 2	3, 0.43, 0.64, 0.99	3, 0.23, 0.64, 0.69	3, 0.21, 0.57, 0.98	(Vrede et al. 2002)
Marine Isolate 3	3, 0.20, 1.41, 0.56	3, 0.13, 0.99, 0.46	3, 0.13, 0.63, 0.24	(Vrede et al. 2002)
Pseudomonas fluorescens	3, 0.08, 1.69, 0.93	3, 0.13, 0.95, 0.96	3, 0.18, 0.61, 0.99	(Chrzanowski et al. 2010)
Pseudomonas fluorescens [5]	9, 0.94, -0.92, 0.34	9, 0.32, 0.78, 0.70	9, 0.09, 0.71, 0.06	(Chrzanowski and Kyle 1996)
Pseudomonas fluorescens [6]	8, -0.24, 2.96, 0.12	8, 0.01, 1.30, 0.01	8, -0.05, 0.94, 0.21	(Chrzanowski and Kyle 1996)
Pseudomonas fluorescens [7]	5, -0.13, 2.47, 0.01	5, -0.18, 1.55, 0.85	5, -0.06, 0.91, 0.08	(Chrzanowski and Kyle 1996)
Pseudomonas putida	3, 0.43, 0.28, 0.99	3, 0.23, 0.28, 0.38	3, 0.07, 0.68, 0.89	(Bratbak 1985)
Ruegeria pomeroyi	3, 0.32, 1.44, 0.77	3, 0.15, 0.63, 0.69	3, 0.24, 0.59, 0.66	(Chan et al. 2012)
Vibrio splendidus	8, 0.09, 2.18, 0.21	-	8, 0.05, 0.62, 0.16	(Løvdal et al. 2008)
Assemblage (Christmas Lake, MN)	4, 0.70, 0.58, 0.89	4, 0.52, 0.31, 0.85	-	chapter 2

Assemblage (Christmas Lake, MN)	8, 0.56, 0.49, 0.89	8, 0.44, 0.13, 0.84	-	chapter 4
Assemblage (Lake Biwa, Japan)	8, 0.91, -0.09, 0.95	6, 0.71, 0.29, 0.85	5, 0.73, 0.13, 0.79	(Tezuka 1990)
Assemblage (Lake Leverson, MN)	4, 0.39, 1.19, 0.46	4, 0.25, 0.85, 0.44	-	chapter 2
Assemblage (Lake Owasso, MN)	4, 0.50, 0.81, 0.92	4, 0.29, 0.62, 0.90	-	chapter 2
Assemblage (Lake Owasso, MN)	3, 0.34, 1.33, 0.85	3, 0.16, 1.02, 0.66	-	chapter 2
Assemblage (Lake Owasso, MN)	3, 0.58, 0.83, 0.78	3, 0.49, 0.30, 0.76	-	chapter 2
Assemblage (Lake Owasso, MN) [8]	3, 0.39, 1.12, 0.73	3, 0.39, 0.40, 0.71	-	(Makino and Cotner 2004)
Assemblage (Lake Owasso, MN) [9]	3, 0.13, 1.63, 0.42	3, 0.07, 1.07, 0.12	-	(Makino and Cotner 2004)
Assemblage (Lake Owasso, MN) [10]	3, 0.07, 1.73, 0.41	3, 0.01, 1.21, 0.00	-	(Makino and Cotner 2004)
Assemblage (Lake Superior, MN)	4, 0.53, 0.65, 0.79	4, 0.42, 0.30, 0.78	-	chapter 2
Assemblage (Marine)	4, -0.48, 2.78, 0.84	-	4, 0.15, 0.58, 0.79	(Goldman et al. 1987)
Assemblage (Seawater)	3, 0.75, -0.06, 0.79	3, 0.69, 0.21, 0.74	3, 0.03, 0.67, 0.50	(Bratbak 1985)

Appendix B: Bootstrap Parameterization of Fulcrum Stoichiometry

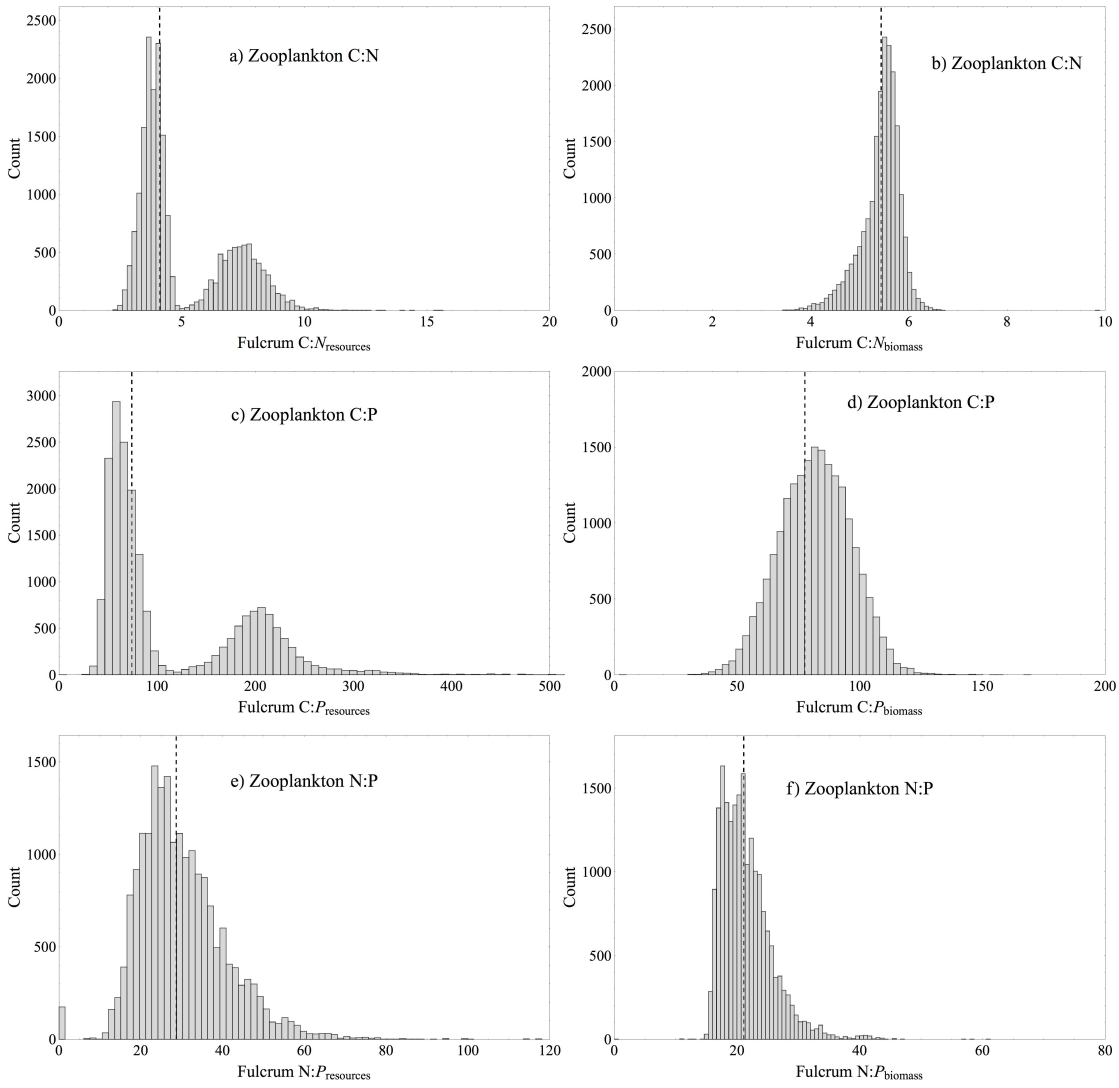

Appendix Figure B-1. Bootstrap distributions of resource and biomass stoichiometry for zooplankton C:N (a and b), C:P (c and d), and N:P (e and f). The vertical dashed line in each panel represents the parametric fulcrum estimate obtained using the complete dataset.

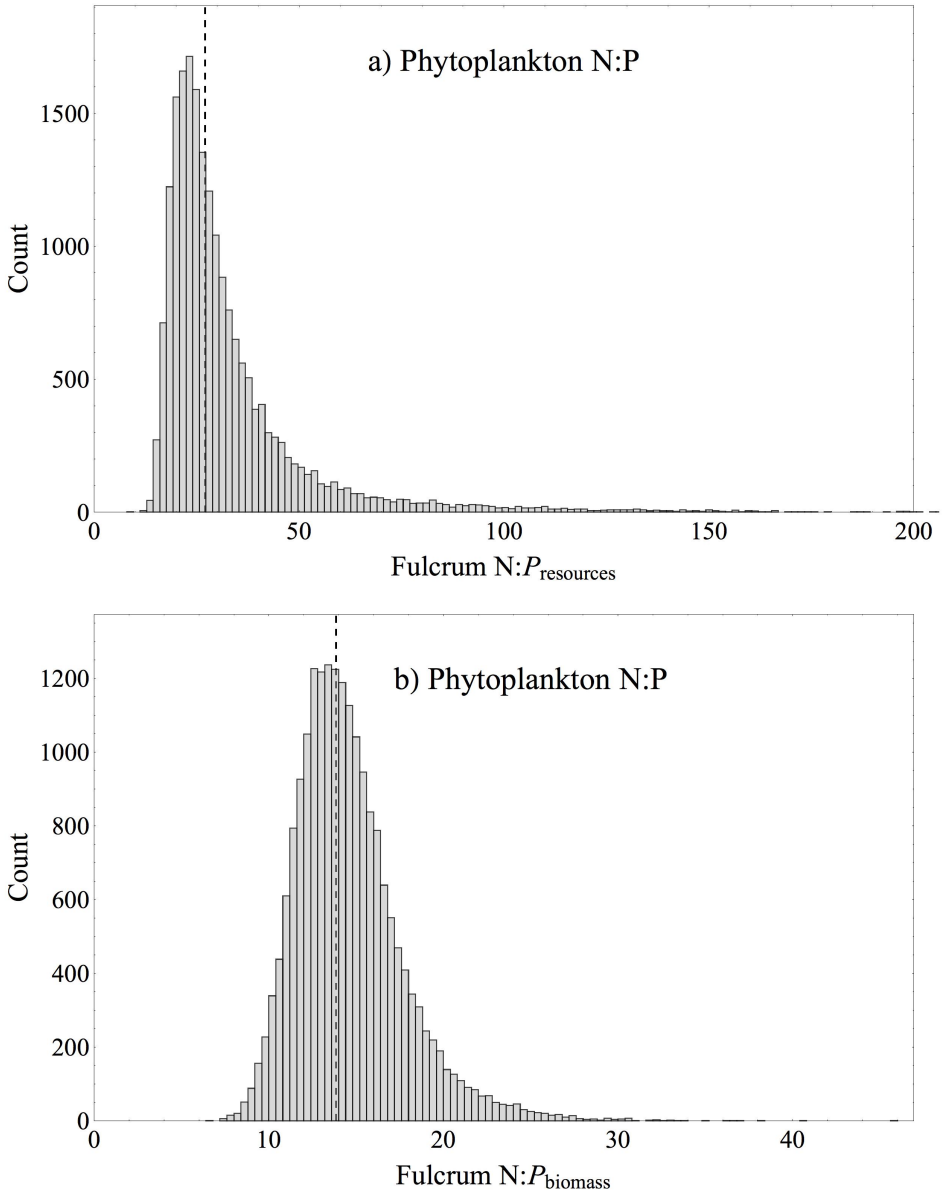

Appendix Figure B-2. Bootstrap distributions of fulcrum resource (a) and biomass (b) stoichiometry for phytoplankton N:P. The vertical dashed line in each panel represents the parametric fulcrum estimate obtained using the complete dataset.

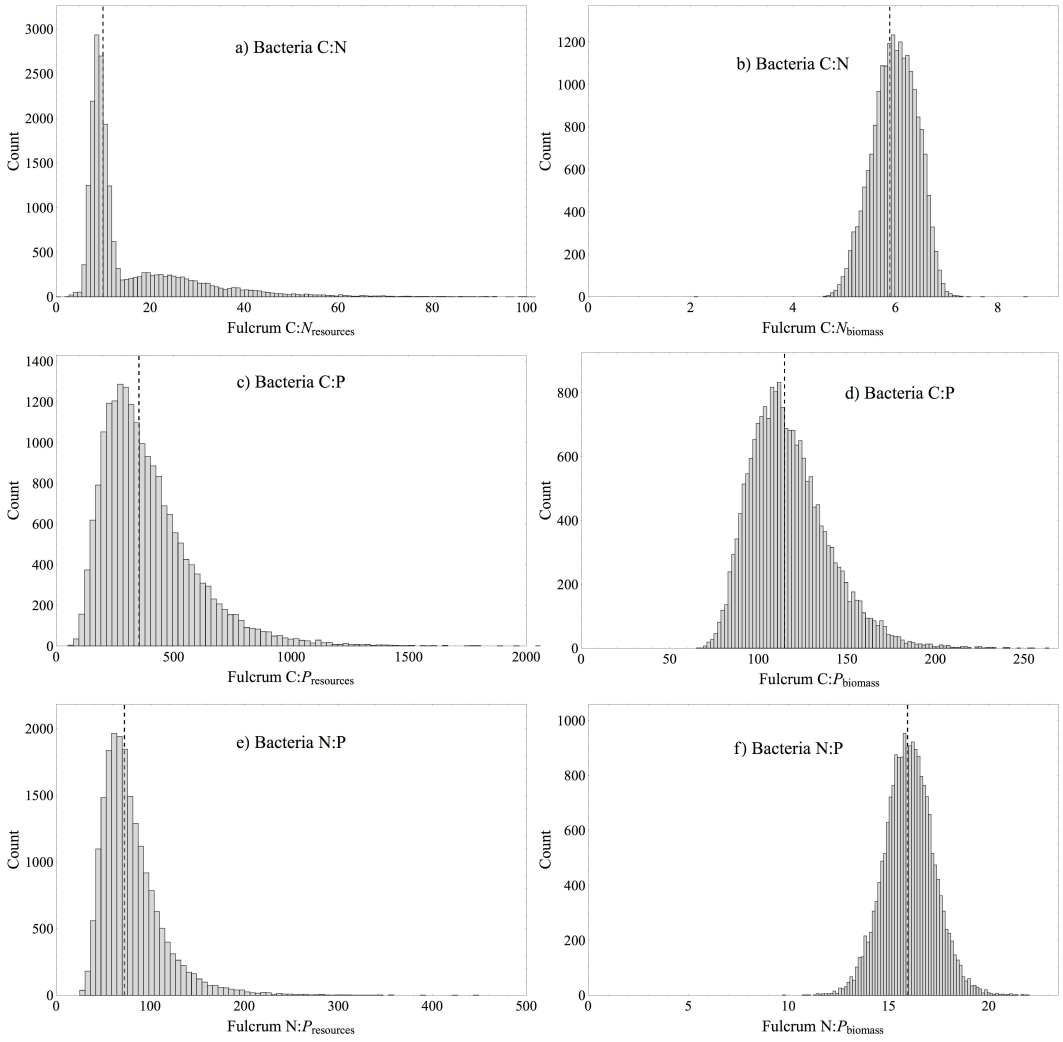

Appendix Figure B-3. Bootstrap distributions of fulcrum resource and biomass stoichiometry for bacteria C:N (a and b), C:P (c and d), and N:P (e and f). The vertical dashed line in each panel represents the parametric fulcrum estimate obtained using the complete dataset.

Appendix Table B-1. Comparison of parametric and bootstrap estimates of the fulcrum resource stoichiometry and fulcrum biomass stoichiometry for each dataset. Values in parentheses are the 95% confidence intervals for the estimates.

Taxa	Ratio	Parametric		Bootstrap	
		Fulcrum Resource Ratio	Fulcrum Biomass Ratio	Fulcrum Resource Ratio	Fulcrum Biomass Ratio
Zooplankton	C:N	4.10 (2.89, 6.54)	5.43 (4.46, 6.62)	4.10 (2.93, 8.94)	5.50 (4.42, 6.04)
Zooplankton	C:P	74.21 (36.30, 174.94)	77.61 (48.84, 123.33)	75.13 (44.60, 308.19)	82.03 (53.48, 109.67)
Zooplankton	N:P	28.67 (13.42, 76.44)	21.08 (14.55, 30.54)	28.35 (14.42, 55.88)	20.74 (16.17, 31.60)
Phytoplankton	N:P	27.08 (14.16, 60.67)	13.85 (8.75, 21.91)	27.10 (16.52, 92.16)	14.13 (9.90, 22.16)
Bacteria	C:N	9.97 (6.07, 18.78)	5.89 (5.15, 6.74)	10.20 (6.38, 49.73)	6.00 (5.13, 6.75)
Bacteria	C:P	352.17 (176.81, 768.85)	114.83 (82.69, 159.47)	348.41 (140.48, 897.09)	114.33 (83.44, 169.15)
Bacteria	N:P	72.60 (37.98, 155.75)	15.94 (12.50, 20.31)	72.93 (39.82, 166.81)	16.01 (13.57, 18.51)

Appendix C: Cell Quota Model and Equations

This cell quota model was adapted from Thingstad (1987) without substantial modification.

Realized Growth Rate:

$$\mu = \mu_{max} \cdot \left(1 - Max\left[\frac{Q_{C\,min}}{Q_C}, \frac{Q_{N\,min}}{Q_N}, \frac{Q_{P\,min}}{Q_P}\right]\right)$$

Cell Quotas:

$$Q_C = \frac{B_C}{B}, Q_N = \frac{B_N}{B}, Q_P = \frac{B_P}{B}$$

Specific Uptake Rates of C, N, and P:

$$V_C = V_{C\,max} \cdot \left(\frac{Q_{C\,max} - Q_C}{Q_{C\,max} - Q_{C\,min}}\right) \cdot \frac{C}{K_C + C}$$

$$V_N = V_{N\,max} \cdot \left(\frac{Q_{N\,max} - Q_N}{Q_{N\,max} - Q_{N\,min}}\right) \cdot \frac{N}{K_N + N}$$

$$V_P = V_{P\,max} \cdot \left(\frac{Q_{P\,max} - Q_P}{Q_{P\,max} - Q_{P\,min}}\right) \cdot \frac{P}{K_P + P}$$

Specific Respiration Rate:

$$R = \rho_g \cdot Q_C \cdot \mu + \rho_R \cdot (Q_C - Q_{C\,min})$$

Differential Equations:

$$\frac{dB}{dt} = \mu \cdot B - d \cdot B$$

$$\frac{dB_C}{dt} = (V_C - R) \cdot B - d \cdot B_C$$

$$\frac{dB_N}{dt} = V_N \cdot B - d \cdot B_N$$

$$\frac{dB_P}{dt} = V_P \cdot B - d \cdot B_P$$

$$\frac{dC}{dt} = -V_C \cdot B + d \cdot \left(C_{Supply} - C_t\right)$$
$$\frac{dN}{dt} = -V_N \cdot B + d \cdot \left(N_{Supply} - N_t\right)$$
$$\frac{dP}{dt} = -V_P \cdot B + d \cdot \left(P_{Supply} - P_t\right)$$

Equilibrium Solutions for C*, N*, and P*:

$$C^* = \frac{-d \cdot K_C \cdot (Q_{C\,max} - Q_{C\,min}) \cdot Q_{C\,min} \cdot \left(\rho_R + \mu_{max} + \rho_g \cdot \mu_{max}\right)}{d \cdot Q_{C\,max} \cdot V_{C\,max} + d \cdot (Q_{C\,max} - Q_{C\,min}) \cdot Q_{C\,min} \cdot \rho_R + (Q_{C\,max} - Q_{C\,min}) \cdot \left(-V_{C\,max} + d \cdot Q_{C\,min} \cdot \left(1 + \rho_g\right) \cdot \mu_{max}\right)}$$

$$N^* = \frac{d \cdot K_N \cdot Q_{N\,min}(Q_{N\,min} - Q_{N\,max}) \cdot \mu_{max}}{d \cdot Q_{N\,max} \cdot V_{C\,max} + (Q_{N\,max} - Q_{N\,min}) \cdot (d \cdot Q_{N\,min} - V_{N\,max}) \cdot \mu_{max}}$$

$$P^* = \frac{d \cdot K_P \cdot Q_{P\,min}(Q_{P\,min} - Q_{P\,max}) \cdot \mu_{max}}{d \times Q_{P\,max} \cdot V_{P\,max} + (Q_{P\,max} - Q_{P\,min}) \cdot (d \cdot Q_{P\,min} - V_{P\,max}) \cdot \mu_{max}}$$

Table C-1. Model parameters and physiological constants for the cell quota model.

Symbol	Parameter	Default Value
B	Bacterial density (10^9 cells/L)	-
B_C	Biomass carbon (μM C)	-
B_N	Biomass nitrogen (μM N)	-
B_P	Biomass phosphorus (μM P)	-
C	Ambient carbon (μM C)	-
N	Ambient nitrogen (μM N)	-
P	Ambient phosphorus (μM P)	-
μ_{max}	Maximum growth rate (h^{-1})	0.5
d	Volumetric dilution rate (h^{-1})	1.0
ρ_g	Carbon incorporated/carbon respired	1.0
ρ_r	Proportion of surplus carbon respired	0.05
$V_{C\ max}$	Maximum uptake rate of carbon (fmol L^{-1} h^{-1} $cell^{-1}$)	2.12
$V_{N\ max}$	Maximum uptake rate of nitrogen (fmol L^{-1} h^{-1} $cell^{-1}$)	0.32
$V_{P\ max}$	Maximum uptake rate of phosphorus (fmol L^{-1} h^{-1} $cell^{-1}$)	0.02
K_C	Half-saturation constant for uptake of carbon (μM)	1.0
K_N	Half-saturation constant for uptake of nitrogen (μM)	0.1
K_P	Half-saturation constant for uptake of phosphorus (μM)	0.01
$Q_{C\ min}$	Minimum cell quota for carbon (fmol $cell^{-1}$)	1.06
$Q_{C\ max}$	Maximum cell quota for carbon (fmol $cell^{-1}$)	2.12
$Q_{N\ min}$	Minimum cell quota for nitrogen (fmol $cell^{-1}$)	0.16
$Q_{N\ max}$	Maximum cell quota for nitrogen (fmol $cell^{-1}$)	0.32
$Q_{P\ min}$	Minimum cell quota for phosphorus (fmol $cell^{-1}$)	0.01
$Q_{P\ max}$	Maximum cell quota for phosphorus (fmol $cell^{-1}$)	0.02

Appendix D: Cell Morphometry Equations and Figures

Equations for a cylinder capped with two hemispheres were adapted from Hillebrand et al (1999).

Surface area given length (l) and width (w):

$$SA = l \cdot w \cdot \pi$$

Volume (V) given length and width:

$$V = \frac{1}{12}(3 \cdot l - w) \cdot w^2 \cdot \pi$$

Surface area : volume ($SA{:}V$) given length and width:

$$SA{:}V = \frac{12 \cdot l}{3 \cdot l \cdot w - w^2}$$

Length given planar area (s) and perimeter (p):

$$\frac{2 \cdot p + (\pi - 2) \cdot \sqrt{p^2 - 4 \cdot \pi \cdot s}}{2 \cdot \pi}$$

Width given planar area and perimeter:

$$w = \frac{p - \sqrt{p^2 - 4 \cdot \pi \cdot s}}{\pi}$$

Volume given planar area and perimeter:

$$v = \frac{\left(p - \sqrt{p^2 - 4 \cdot \pi \cdot s}\right)^2 \cdot \left(4 \cdot p + (3 \cdot \pi - 4) \cdot \sqrt{p^2 - 4 \cdot \pi \cdot s}\right)}{24 \cdot \pi^2}$$

Surface area given planar area and perimeter:

$$SA = \frac{-p^2 \cdot (\pi - 4) + 4 \cdot \pi \cdot s \cdot (\pi - 2) + p \cdot (\pi - 4) \cdot \sqrt{p^2 - 4 \cdot \pi \cdot s}}{2 \cdot \pi}$$

Length : width ratio given planar area and perimeter:

$$L{:}W = \frac{-4 \cdot s \cdot (\pi - 2) + p \cdot \left(p + \sqrt{p^2 - 4 \cdot \pi \cdot s}\right)}{8 \cdot s}$$

Surface area : volume ratio given planar area and perimeter:

$$SA{:}V = \frac{12 \cdot \pi \cdot \left(2 \cdot p + (\pi - 2) \cdot \sqrt{p^2 - 4 \cdot \pi \cdot s}\right)}{\left(-p + \sqrt{p^2 - 4 \cdot \pi \cdot s}\right) \cdot \left(4 \cdot p + (3 \cdot \pi - 4) \cdot \sqrt{p^2 - 4 \cdot \pi \cdot s}\right)}$$

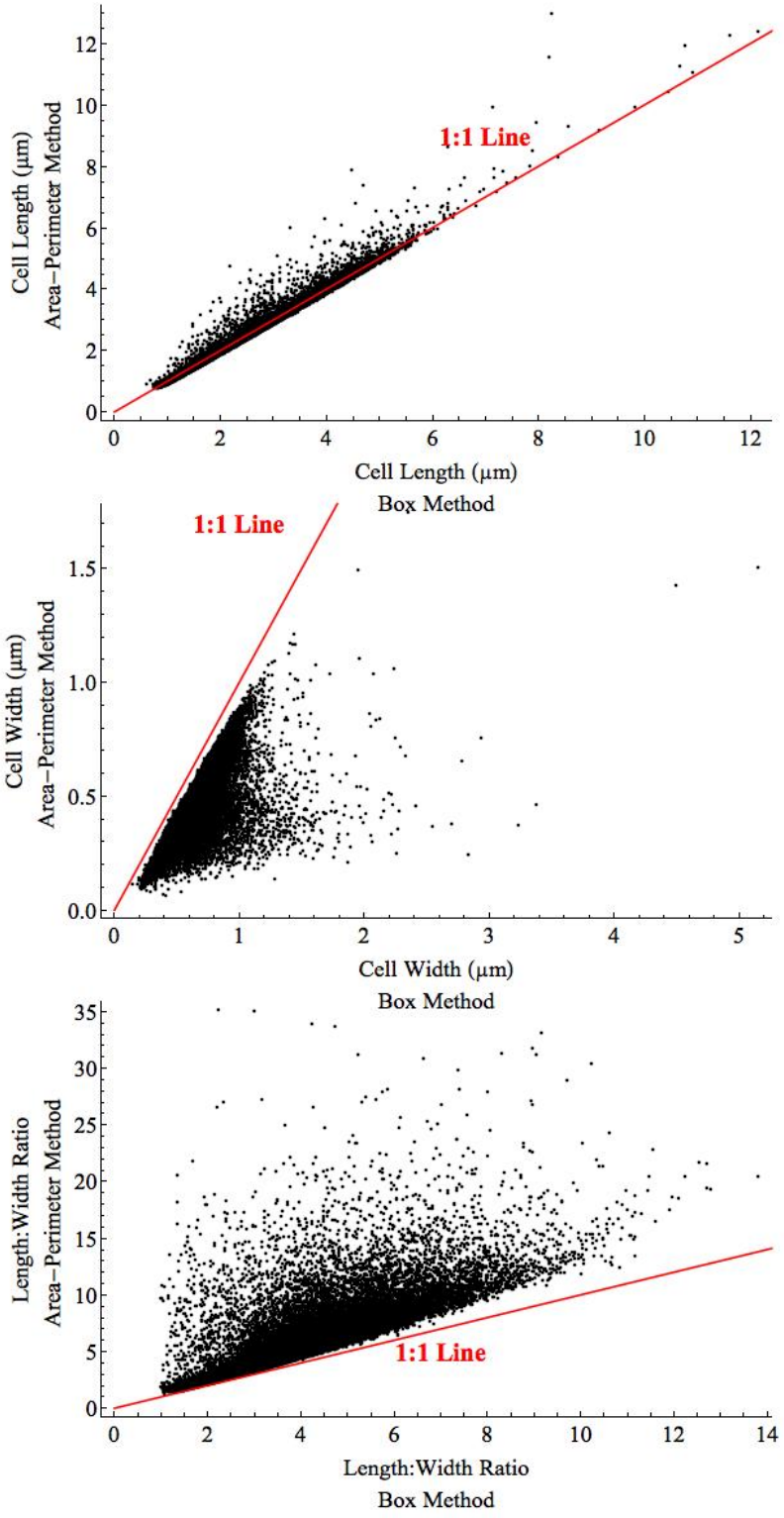

Appendix Figure D-1. Morphometry data from all bacterial isolates, n = 48,453 cells.

Appendix E: Photomicrographs of Bacterial Isolates

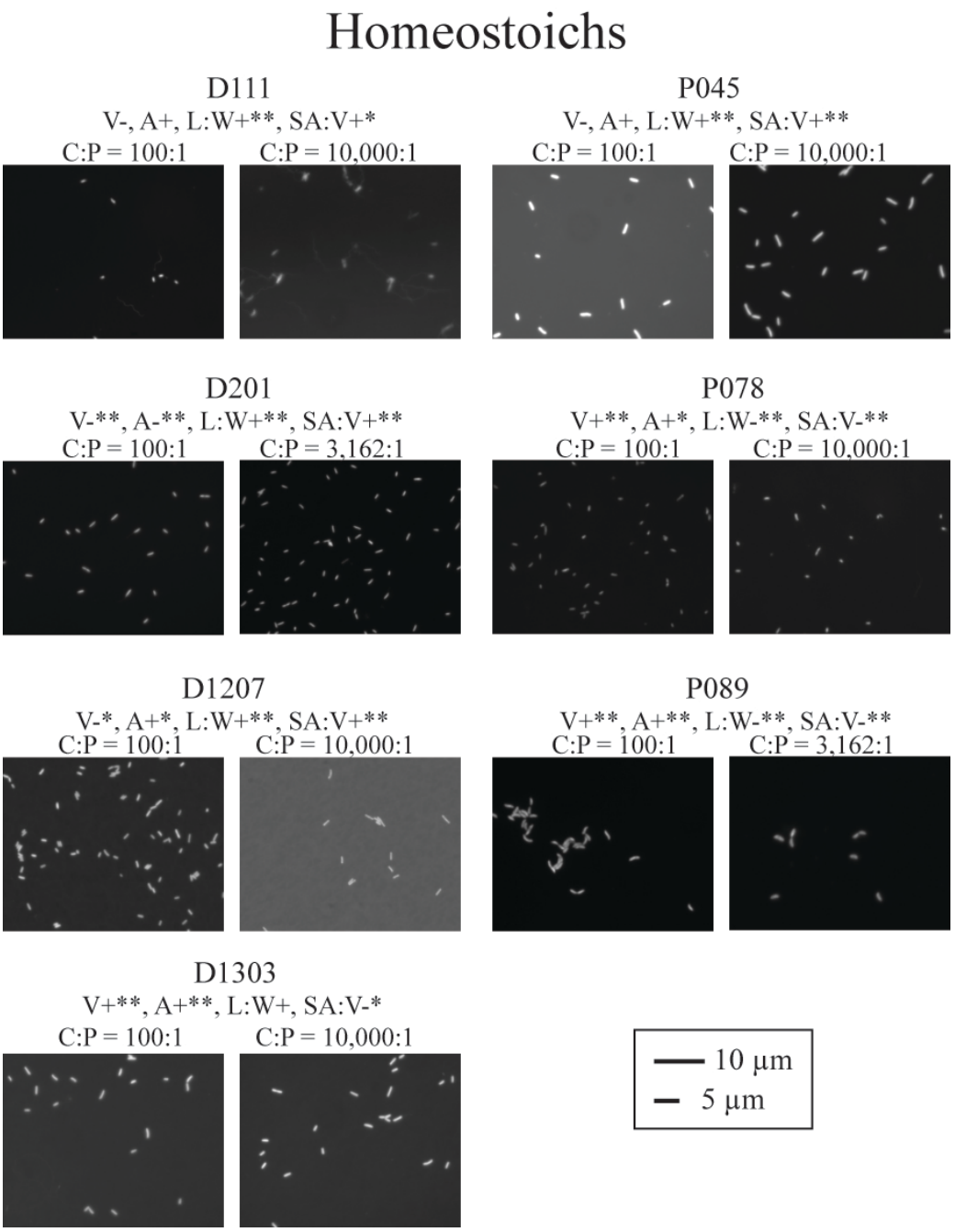

Appendix Figure E-1. Photomicrographs of homeostoich strains from chemostats at high and low $C:P_{supply}$. For each strain, direction of changes in morphometry under P limitation are given for volume (V), area (A), length : width (L:W), and surface area : volume (SA:V), with significance in ANOVA denoted as $p < 0.05$ (*) and $p < 0.0001$ (**). Scale bars are for all images.

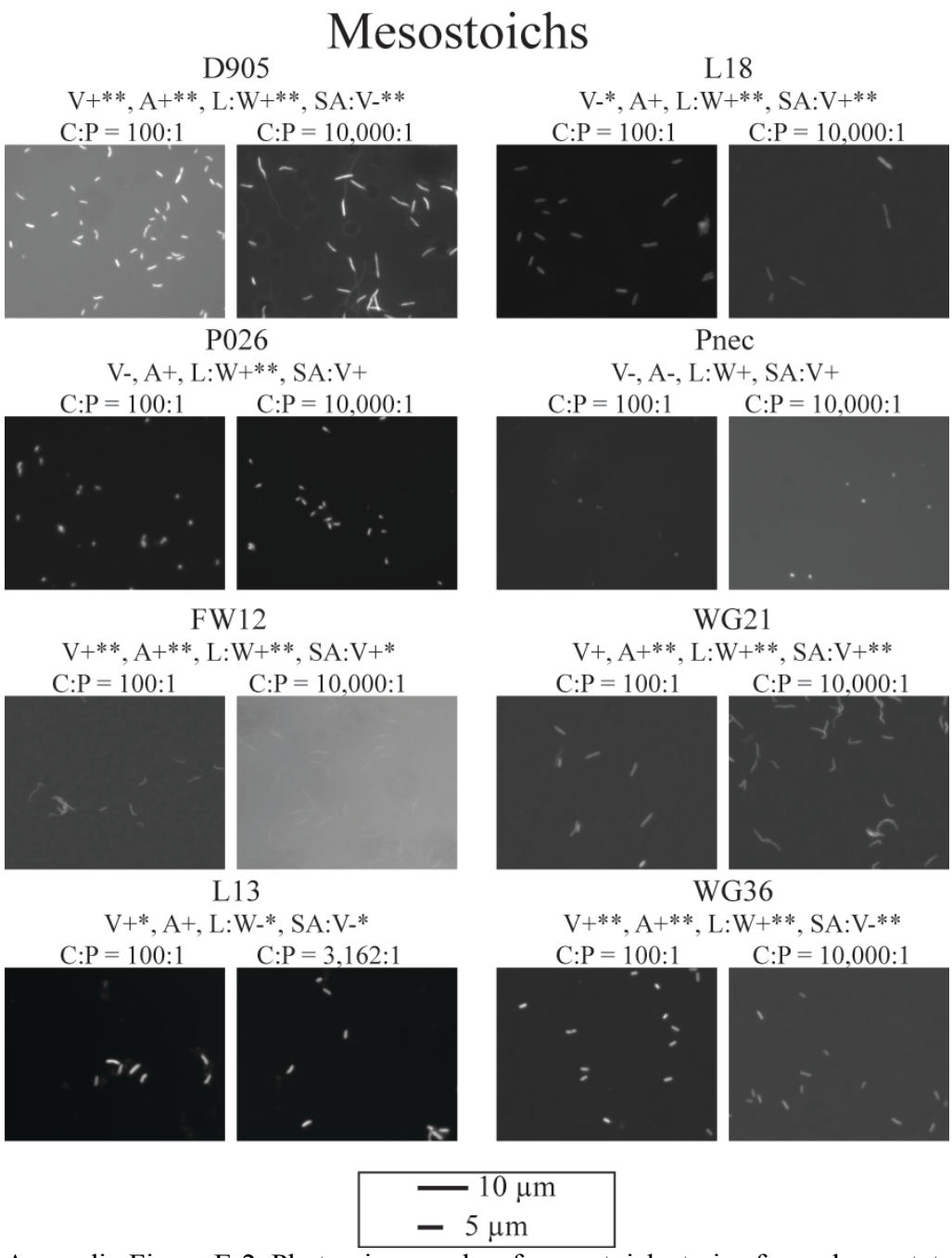

Appendix Figure E-2. Photomicrographs of mesostoich strains from chemostats at high and low $C:P_{supply}$. For each strain, direction of changes in morphometry under P limitation are given for volume (V), area (A), length : width (L:W), and surface area : volume (SA:V), with significance in ANOVA denoted as $p < 0.05$ (*) and $p < 0.0001$ (**). Scale bars are for all images.

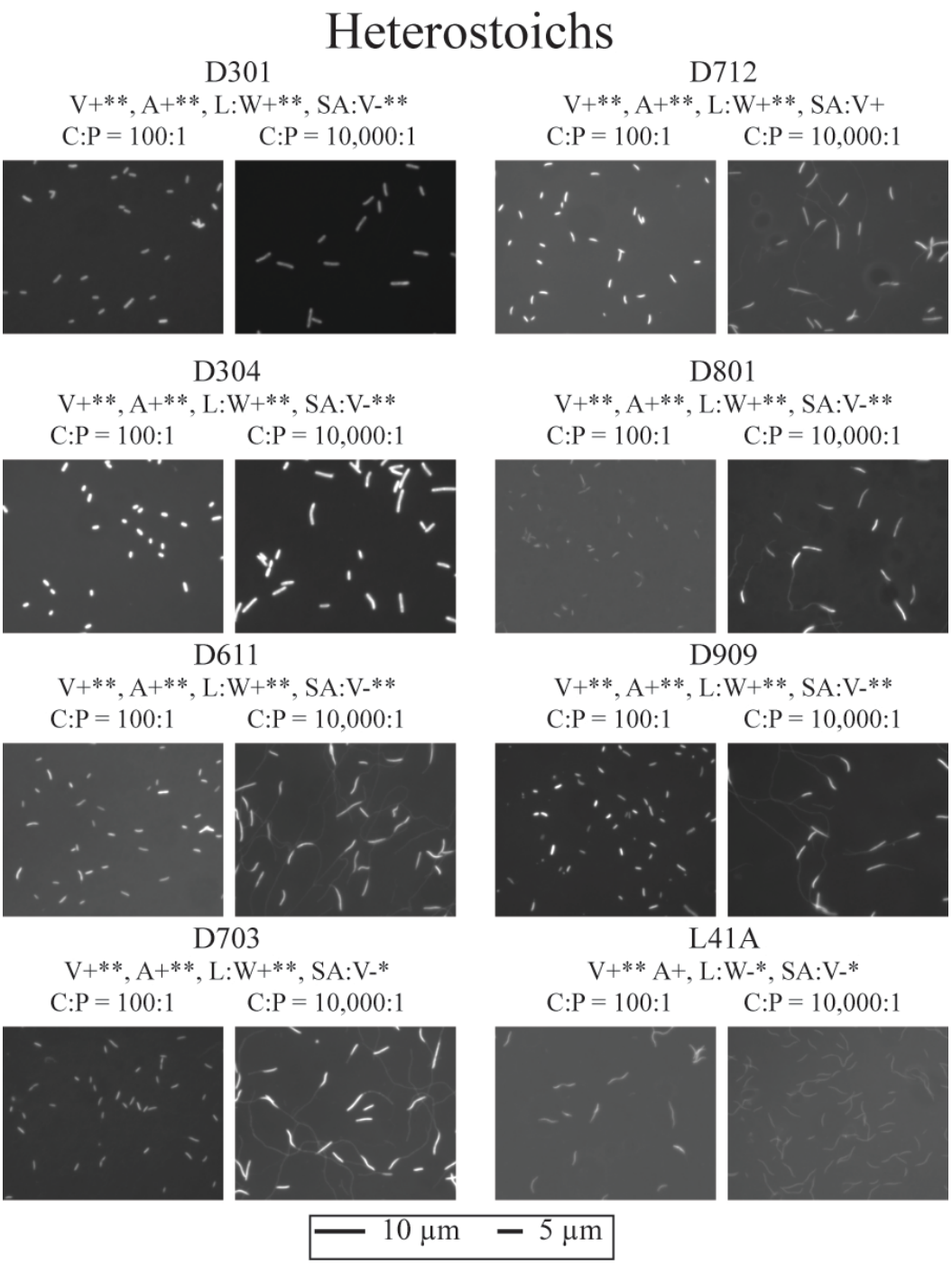

Appendix Figure E-3. Photomicrographs of heterostoich strains from chemostats at high and low $C:P_{supply}$. For each strain, direction of changes in morphometry under P limitation are given for volume (V), area (A), length : width (L:W), and surface area : volume (SA:V), with significance in ANOVA denoted as $p < 0.05$ (*) and $p < 0.0001$ (**). Scale bars are for all image.

Appendix F: Literature Datasets for Bacterial Phosphorus Content

The dilution rate refers to the volumetric replacement rate continuous cultures (chemostats), batch cultures are listed as 'static'. Data for $C:P_{biomass}$, $N:P_{biomass}$, C quota (Q_C), and P quota (Q_P) are ranges of treatment means, or replicate cultures where applicable.

Organism	N (data points/ treatments)	Dilution Rate (h^{-1})	$C:P_{biomass}$	$N:P_{biomass}$	Q_C (fmol $cell^{-1}$)	Q_P (fmol $cell^{-1}$)	Reference
Aeromonas sp.	10 / 10	0.06	31-281	-	-	-	(Scott et al. 2012)
Agrobacterium sp. (#103)	15 / 3	0.011-0.11	42-500	9.7-83	10-52	0.058-0.31	(Phillips et al. in preparation)
Arthrobacter sp. (#23)	15 / 3	0.012-0.109	46-424	8.4-58	6.3-64	0.10-0.28	(Phillips et al. in preparation)
Arthrobacter sp.	10 / 10	0.1	51-857	-	-	-	(Scott et al. 2012)
Cellulomonas sp.	10 / 10	0.06	40-384	-	-	-	(Scott et al. 2012)
Cellvibrio sp.	10 / 10	0.05	111-543	-	-	-	(Scott et al. 2012)
Escherichia coli	15 / 5	0.5-1.5	42-73	11-18	-	-	(Makino et al. 2003)
Escherichia coli	3 / 3	static	54-65	17-21	-	-	(Nakano 1994)
Escherichia coli	6 / 1	0.88	32-51	10-15	15-19	0.34-0.47	(Cotner et al. 2006)
Escherichia coli	2 / 1	static	29-41	7-8	9.2-29	0.22-1.0	(Fagerbakke et al. 1996)
Escherichia coli	2 / 1	static	27-41	7-8	12-30	0.30-1.1	(Norland et al. 1995)
Escherichia coli	1	static	25	-	9.3	0.38	(Heldal et al. 1985)
Flavobacterium ferrugineum	1	static	66	25	-	-	(Nakano 1994)
Flavobacterium sp. (#51)	10 / 10	0.06	27-492	-	-	-	(Scott et al. 2012)
Flavobacterium sp. (#64)	15 / 3	0.016-0.061	41-413	8.4-69	8.7-46	0.12-0.27	(Phillips et al. in preparation)
Flavobacterium sp. (#64)	10 / 10	0.05	37-1,248	-	-	-	(Scott et al. 2012)
Pseudomonas fluorescens	4 / 4	static	62-131	7.9-20	29-116	0.05-0.36	(Chrzanowski et al. 2010)

Pseudomonas fluorescens	1	static	40	20	-	-	(Nakano 1994)
Pseudomonas fluorescens	22 / 5	0.03-0.09	77-216	10-27	6.6-54	0.07-0.47	(Chrzanowski and Kyle 1996)
Pseudomonas putida	3 / 3	static	8-56	2-9	-	-	(Bratbak 1985)
Ruegeria pomeroyi	4 / 4	0.042	56-333	13-35	-	-	(Chan et al. 2012)
Vibrio splendidus	8 / 8	0.02	165-411	30-69	4.6-44	0.03-0.11	(Tanaka et al. 2008)
Vibrio natriegens	2 / 1	static	47-52	10-12	5.2-29	0.11-0.55	(Fagerbakke et al. 1996)
Unidentified strain (marine Isolate 1)	2 / 2	static	29-52	6.2-14	2.7-7.5	0.06-0.27	(Vrede et al. 2002)
Unidentified strain (marine Isolate 2)	3 / 3	static	25-180	6.1-19	2.8-8.7	0.07-0.15	(Vrede et al. 2002)
Unidentified strain (marine Isolate 3)	3 / 3	static	55-176	8.7-21	3.7-8.8	0.07-0.16	(Vrede et al. 2002)
Unidentified strain (marine Isolate 4)	1	static	28	7.9	4.2	0.14	(Vrede et al. 2002)
Unidentified strain B1	3 / 3	0.1	23-133	4.6-54	6.7-7.4	0.06-0.32	(Eccleston-Parry and Leadbeater 1995)
Unidentified isolate (Lake Biwa, Japan)	6 / 6	static	32-130	10-25	-	-	(Nakano 1994)
Assemblage (Lake Owasso, MN, USA)	9 / 3	0.25-0.7	66-114	11-26	26-56	0.15-0.47	(Makino and Cotner 2004)
Assemblage (seawater)	3 / 3	static	16-500	4-90	-	-	(Bratbak 1985)
Assemblage (Lake Biwa, Japan)	8 / 8	static	31-515	7-42	-	-	(Tezuka 1990)
Assemblage (Lake Constance (Germany)	4 / 2	0.042	37-88	-	6.3-22	0.11-0.32	(Jürgens and Güde 1990)
Assemblage (seawater)	4 / 1	static	50-128	9.0-27	0.81-2.9	0.01-0.05	(Goldman et al. 1987)